Quantum Dynamical Studies on Collisions Involving Molecular Ions

A thesis presented to the University College London in partial fulfilment of the requirements for the degree of Doctor of Philosophy

by

Mark Craimer

UCL Chemistry Department
Christopher Ingold Laboratories
20 Gordon Street
London WC1H 0AJ

January 2002

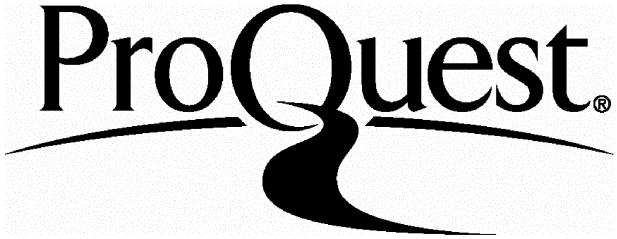

To my parents,
for all their support

ABSTRACT

This thesis describes the application of some of the techniques of quantum dynamics to chemical systems involving molecular ions which have recently been investigated experimentally. Each of the reactions studied requires the development of some aspect of the theory used for such calculations, in order to take into account the specific characteristics of the system involved.

The first part of the thesis concerns the evaluation of the rate constants for the energy transfer between a molecular ion and a neutral atom: the vibrational relaxation of O_2^+ in collision with Kr. The Π electronic state nature of the diatomic molecule is considered, which requires the inclusion of two potential energy surfaces of differing symmetry in the calculations. The results are compared to those obtained by approximating the molecule to be in a Σ state, using a single potential energy surface.

The second part of the thesis investigates the doubly charged triatomic ion O_3^{2+}, created by the double ionisation of ozone, and evaluates the distribution of internal energy states present in the ion fragment, O_2^+, which is produced as a result of its dissociation. The potential surface for this system has a Coulomb term which, to be accommodated in the calculations, requires an adaptation of the existing methods used for such an analysis.

In order to gain insight into some of the effects of the Coulombic potential in collisions between ions, a simpler system is studied initially which involves the elastic scattering between H^+ and Cl^+. This allows an assessment as to the necessity of considering the nature of the Coulombic potential when carrying out quantum dynamical calculations.

Acknowledgements

Firstly, I must thank Professor D. Clary for all his invaluable support and patience throughout my PhD. It was so assuring to have a Supervisor who made himself available more often than I wished him to be!

Thanks also to Dr. Sergei Pogrebnya for allowing me to interrupt him interminably for help and advice and the rest of the Clary Group for much helpful discussion over the years.

I would also like to thank Phil Champkin for so obligingly supplying me with the ozone dication potential and UCL for funding my research.

Contents

List of Figures

List of Tables

INTRODUCTION

The quantum mechanical wavefunction of any system of particles contains within it all the information about the state of the system. The theory of quantum dynamics is directed at extracting some of that information from the wavefunction in order to study interactions which take place between the particles of the system. Quantum dynamics is able to derive the values of a large number of the observable quantities associated with the interactions and is therefore a powerful tool for studying many different types of reactions between particles. It is extremely effective at both explaining and predicting the results of a variety of experiments on atoms and molecules.

A quantum dynamical study of a chemical process generally consists of a method for solving the Schrödinger equation to determine all or part of the wavefunction of the system, followed by a means of deriving the desired observable quantities from the wavefunction. Most quantum dynamical studies involving the collision of particles have many aspects of the method for solving the Schrödinger equation in common, but differ in the choice of observable that is to be extracted from the wavefunction and thus in the method of its extraction.

This thesis describes research performed on some chemical processes which involve the collision of molecular ions, using quantum dynamical methods. The thesis is in two parts, with each part concentrating on a separate process and investigating different observable quantities. Nevertheless, much of the theory used is common to both parts of the thesis, to the extent that the method described in Part 2 is able to refer back to many of the equations derived in Part 1 and build upon some of the formulae previously developed.

The first part of the thesis deals with the vibrational relaxation of the diatomic ion O_2^+, as a consequence of inelastic scattering with a Kr atom. The aim of the investigation is to evaluate the temperature-dependent rate constant of the reaction and compare the results with previous experimental and theoretical studies. This

triatomic system exhibits two types of spatial symmetry and the analysis involves incorporating the potential energy surfaces of both symmetries in the calculations.

The aim of the second part of the thesis is to determine the distribution of internal energy states of O_2^+ formed as the product of the dissociation of doubly ionised ozone in the process:

$$O_3 \xrightarrow{e^-} O_3^{2+} \longrightarrow O_2^+ + O^+ \quad .$$

Other observable quantities which are evaluated in Part 2 relate to the properties of weakly bound states of doubly charged molecules.

Due to the special nature of the systems chosen to be studied, some elements of the theory used in each of the parts of the thesis have never previously been implemented in a quantum dynamics calculation. Part 1 undertakes, for the first time, a fully quantum dynamical study of the vibrational relaxation of a diatom in a Π electronic ground state, whilst Part 2 develops existing theoretical methods to analyse a system involving a Coulombic interaction.

PART 1

1 Introduction

1.1 Vibrational Relaxation of O_2^+ with Kr

Vibrational relaxation through inelastic scattering involves the collision of a vibrationally excited molecule with a "quencher", an atom or small molecule, such that some or all of the internal vibrational energy of the target molecule is transferred to translational energy (of the quencher or the target molecule) or to rotational energy of the target molecule or, if the quencher is a molecule, to the internal energy of the quencher.

1.1.1 Background

Experimental Studies

Experimental observation of the inelastic scattering of diatomic molecules reveals two major differences between the vibrational relaxation of diatomic molecular ions and that of most neutral diatomic molecules. As Ferguson [1, 2] notes, in the case of the vibrational relaxation of many neutral molecules the temperature dependence of experimentally measured rate constants, k_q, is consistent with the famous Landau-Teller [3] model which predicts that:

$$\ln (k_q) \propto -(1/T)^{1/3}$$

where T is the temperature. Thus, for example, in systems such as $CO(v)$ + He and $CO(v)$ + H_2 it has been found [4] that, even at quite low temperatures, an increase in temperature (or collision energy) will yield an increase in the rate constant for vibrational relaxation.

In contrast, the quenching of diatomic molecular ions appears to exhibit negative temperature dependence of the rate constant at low temperatures [5, 6], with positive dependence at higher temperatures. For example, a minimum in the plot of the rate coefficient versus collision energy or temperature has been detected in drift tube experiments on the vibrational

relaxation of O_2^+ with Kr [7]. Such behaviour had previously been observed in the case of neutrals for systems with strongly attractive electrostatic potentials such as HF-HF [8], HCl-HCl, HBr-HBr [9] and NO-NO [10].

This has led Ferguson [1] to suggest a qualitative interpretation of the experimental data which has subsequently been supported through the use of classical trajectory calculations and related graphical studies by Tosi *et al* [11] and by Ramachandran & Ezra [12]. The suggestion is that, whereas in the case of the majority of neutral molecules it is the dominant repulsive interaction which leads to vibrational energy transfer, the attractive electrostatic forces present in the interactions of highly polar molecules and ions result in an alternative mechanism for relaxation. First, an ion molecule "long-lived" complex is formed:

$$AB^+(v) + Q \leftrightarrow (AB^+(v) - Q)^*$$

then vibrational predissociation occurs, i.e. the energy in the vibrating AB^+ bond transfers into the $AB^+ - Q$ coordinate:

$$(AB^+(v) - Q)^* \rightarrow AB^+(v' < v) + Q + \text{K.E.}$$

Since, the longer the complex stays together the more likely it is to vibrationally predissociate and the lifetime of the complex decreases with increase in collision energy (or temperature), the negative dependence of the rate coefficient at low energies would be expected.

For higher energies, the direct mechanism due to the short-range repulsion dominates so that, the more collision energy, the closer the atom can get to the molecule and hence the greater the likelihood of vibrational relaxation. The existence of these two mechanisms thus qualitatively explains the change in behaviour over the collision energy range, although it has been shown [11] that both mechanisms are always present and it is just the relative dominance of the one over the other which causes the observed results.

The other characteristic of the vibrational relaxation of diatomic molecular ions which distinguishes it from that of neutral diatoms is the efficiency of the energy transfer. The rate constant for vibrational relaxation of neutral diatoms is generally in the range $10^{-15} > k_q > 10^{-19}$ $cm^3 s^{-1}$ at room temperature [13]. The much stronger attractive electrostatic interaction present in ion-neutral collisions results in the rate of vibrational energy transfer observed in such systems being significantly higher [6, 7].

However, experiments performed on $O_2^+(v)$ [5, 7] and $NO^+(v)$ [6] reveal that the vibrational quenching of O_2^+ with Kr is exceptionally efficient. Even though the electrostatic attraction of the O_2^+ / Kr system is approximately the same as that for the NO^+ / Kr system, the former shows a rate constant of $k_q \approx 10^{-11}$ $cm^3 s^{-1}$ at room temperature for the process:

$$O_2^+(v \geq 1) + Kr \rightarrow O_2^+(v=0) + Kr$$

as compared to $k_q \approx 10^{-13}$ $cm^3 s^{-1}$ for the equivalent NO^+ / Kr process. This difference has been attributed to the influence of the unfilled orbital present in the O_2^+ molecule [6].

Theoretical Studies

Theoretical analysis of the process:

$$O_2^+(v=1) + Kr \rightarrow O_2^+(v=0) + Kr \qquad (1)$$

has been carried out using classical, semi-classical and quantum methods. Tosi, Ronchetti and Lagana [14, 11] (TRL) have performed classical trajectory calculations based on a semi-empirical potential energy surface, created by adding the O_2^+ diatomic potential to terms representing the Kr-O_2^+ interaction, and found good agreement with the experimental data [7]. The same potential surface has been used to calculate cross sections as a function of the collision energy by means of a semi-classical approach [15].

Goldfield [16] has applied a time-dependent wave packet technique to study the process (1) but only at two values of collision energy, 0.1 and 0.5 eV, and with the total angular momentum, J, equal to zero. These results were obtained using a slightly different potential surface developed by Ramachandran and Ezra (RE), who also used it to carry out classical trajectory calculations [12].

As Gianturco *et al* [17] point out, a fully exact time-independent quantum mechanical study of the rate constants of a system such as process (1), involving, as it does, a large number of rotational and vibrational quantum levels, would require enormous computational power and time. It is therefore necessary to find an appropriate approximate method if meaningful results of time-independent quantum mechanical calculations are to be obtained.

Gianturco *et al* [17] found that the rotational infinite order sudden (RIOS) approximation [18], used on the TRL surface, fails dramatically when applied to the reaction (1) and could only be used for a qualitative study of pure rotational excitations. Also, the results [17] of restricted calculations ($J = 0$ and $J = 60$, only) made within an exact fully close coupling treatment suggest that the correct results will lie a factor of about 10^4 above RIOS values.

Potential Energy Surface

More recently, Ramiro-Diaz, Wahnon and Sidis (RDWS) have carried out *ab initio* calculations of the O_2^+ / Kr potential energy surface [19, 20]. Projected valence bond configuration interaction calculations were carried out to produce the seven lowest adiabatic potential energy surfaces of the $O_2^+(^2\Pi)$/Kr system in each of ^{2}A" and ^{2}A' symmetries and for a large number of geometries. They found the well depth of the lowest surface, 1 ^{2}A", to be $V_m = -0.173$ eV. The well depth used in the semi-empirical potentials of TRL and RE [11, 12], deduced from photodissociation data [21], was much larger, with $V_m = -0.33 \pm 0.1$ eV. Given the fact that one vibrational quantum of O_2 is 0.196 eV, it is suggested [19] that this discrepancy could be explained by a shift of one unit in the assignment of the vibrational states of the photodissociation data in Ref. [21].

1.1.2 This Research

The discovery that the *ab initio* potential energy surface differs considerably from the semi-empirical surfaces used for all previous theoretical studies of process (1) prompts further interest in the calculation of the rate constants for the scattering reaction, based on this new energy surface.

The centrifugal sudden or coupled states approximation (CSA) [22, 23] is a quantum mechanical method which recently has been proven to be highly accurate in studying vibrational relaxation of diatomic ions, such as NO^+ in collision with He [24] and N_2^+ with He [25]. This method allows the application of a quantum mechanical analysis to process (1) without incurring the computational expense of a fully close coupled calculation.

In addition to which, the existence of *ab initio* adiabatic potential energy surfaces of both forms of symmetry present in the O_2^+/Kr system [20] presents the opportunity of incorporating two potential surfaces into the calculations. Until now, almost all quantum scattering calculations on vibrational relaxation have been made on a single potential energy surface, but to do so here would involve approximating the ground electronic state of the diatom to be $^1\Sigma$ instead of $^2\Pi$. It is now possible to check whether such an approximation would be justified. The aim of this part of my research was, therefore, to perform quantum dynamical calculations for process (1) using the centrifugal sudden approximation on the two lowest adiabatic potential energy surfaces of Ref. [20].

Confidence in the accuracy of the rate constants found will depend on an assurance of the applicability of the CSA to the O_2^+ / Kr system. Therefore, results of CSA calculations using the TRL surface are presented first, in order that comparisons can be made between the CSA method and all previous theoretical studies.

Subsequently, the quantum dynamical calculations have been carried out on the *ab initio* RDWS potential surface and the results obtained compared with those observed in experiment [5, 7]. The calculations are first done using the lowest potential energy surface of the system [19] and then developed to take

into account the lowest surface of the alternative symmetry [20] as well. Thus, an assessment of the legitimacy of approximating a system which shows two different symmetries through the use of just one potential energy surface can be made. This is the first time that vibrational relaxation calculations have been done on more than one potential energy surface.

The description of this first part of the thesis will initially set up the Schrödinger equation in a form suitable to the problem. This section is valid for all formulations of the O_2^+ / Kr system and will also be required for the second part of the thesis, as will be outlined in Part 2. Then, in Chapter 3, the effects of the various potential surfaces on the calculations are discussed, followed by the solution of the resultant equations in Chapter 4. Chapter 5 deals with the derivation of the observable quantities from the solutions of the equations. The final three chapters present and discuss the results and submit the conclusions of this part of the thesis.

The results of the calculations using the semi-empirical, TRL potential energy surface and those on the single *ab initio* potential were carried out by Dr. S. K. Pogrebnya, with whom I collaborated for the first part of this thesis. My principal task, in this part of the thesis, has thus been the extension and application of the theory to the Π-state description of the diatom, which uses the combination of both adiabatic *ab initio* potential surfaces of the system together.

2 Method: Setting up the Schrödinger Equation

The calculation of cross sections, and thus rate constants, for a scattering interaction using quantum dynamics is based on an evaluation of the probability that the interaction will occur. According to the Copenhagen Interpretation of the Schrödinger equation, the wavefunction of a system at any given moment can be expressed as a sum of all possible outcomes of a measurement on the system, with each outcome weighted (i.e. multiplied) by the square root of the probability of that outcome being the one recorded in the measurement.

Therefore, one way to determine the probability of any given outcome of a measurement being the one observed is to calculate the wavefunction at any moment (i.e. independent of time), expressed as a linear combination of all possible outcomes, and ascertain the value of the square of the coefficient of the desired outcome at the position in space at which the measurement will take place. The measurement of a scattering interaction can be considered as occurring at an infinite distance from the position of the collision.

Hence, for this research, the method by which theoretical values of the observables are calculated is through the solution of the time-independent Schrödinger equation to obtain the wavefunction for the system in the region corresponding to infinite separation of the quencher and the target molecule. Since the aim is to find the probability of the diatom changing from one internal energy state (or 'channel') to another, the wavefunction is then expressed as a linear combination of all possible internal energy states of the diatom at infinite separation so that the desired coefficients and consequently the probabilities can be found.

2.1 The Hamiltonian

The time-independent Schrödinger equation for an atom colliding with a diatom can be written in operator form as:

$$\hat{H}\Psi_{vjm_j} = E\Psi_{vjm_j} \tag{2.1}$$

where Ψ_{vjm_j} is the nuclear scattering wavefunction for the system with the diatom initially in a vibrational state v and rotational state j, with m_j the projection of j on the laboratory frame z-axis. E is the total energy of the system.

The Hamiltonian in space-fixed Cartesian coordinates is

$$\hat{H} = -\left[\frac{\hbar^2}{2m_A}\nabla_A^2 + \frac{\hbar^2}{2m_B}\nabla_B^2 + \frac{\hbar^2}{2m_C}\nabla_C^2\right] + \hat{V}(x_A, x_B, x_C, y_A, y_B, y_C, z_A, z_B, z_C) \tag{2.2}$$

where the Laplacian, ∇^2, is given by:

$$\nabla_i^2 = \frac{\partial^2}{\partial x_i^2} + \frac{\partial^2}{\partial y_i^2} + \frac{\partial^2}{\partial z_i^2} \quad ,$$

x_i , y_i , z_i being the Cartesian coordinates of atom i and m_i being its mass. $\hat{V}$ is the potential energy surface (PES) on which the atom and molecule move.

This is much easier to handle when transferred to centre-of-mass coordinates, where the motion of the centre of mass of the system is factorised out of the Hamiltonian. To derive this transformation, consider the Hamiltonian for a two-particle system:

$$\hat{H} = \hat{T} + \hat{V} = \frac{\hat{\underline{P}}_1^2}{2m_1} + \frac{\hat{\underline{P}}_2^2}{2m_2} + \hat{V}$$

where $\hat{\underline{P}}_i$ is the momentum operator for particle i. Then,

$$\hat{T} = \frac{1}{2m_1 m_2}\left(m_2\hat{\underline{P}}_1^2 + m_1\hat{\underline{P}}_2^2\right)$$

$$= \frac{1}{2m_1 m_2(m_1+m_2)}\left[m_2^2\hat{\underline{P}}_1^2 + m_1^2\hat{\underline{P}}_2^2 + m_1 m_2\left(\hat{\underline{P}}_1^2 + \hat{\underline{P}}_2^2\right)\right]$$

$$= \frac{m_1 m_2}{2(m_1+m_2)}\left(\frac{\hat{\underline{P}}_1}{m_1} - \frac{\hat{\underline{P}}_2}{m_2}\right)^2 + \frac{\left(\hat{\underline{P}}_1 + \hat{\underline{P}}_2\right)^2}{2(m_1+m_2)} \quad .$$

The right-hand term is the kinetic energy term for the composite system of (particle 1 + particle 2). For a three-particle system, therefore, the above can simply be repeated, treating the two-particle composite as a single particle. Hence:

$$\hat{H} = \hat{T} + \hat{V} = \frac{\hat{\underline{P}}_1^2}{2m_1} + \frac{\hat{\underline{P}}_2^2}{2m_2} + \frac{\hat{\underline{P}}_3^2}{2m_3} + \hat{V}$$

$$\hat{T} = \frac{m_1 m_2}{2(m_1+m_2)}\left(\frac{\hat{\underline{P}}_1}{m_1} - \frac{\hat{\underline{P}}_2}{m_2}\right)^2 + \frac{\left(\hat{\underline{P}}_1 + \hat{\underline{P}}_2\right)^2}{2(m_1+m_2)} + \frac{\hat{\underline{P}}_3^2}{2m_3}$$

$$= \frac{m_1 m_2}{2(m_1+m_2)}\left(\frac{\hat{\underline{P}}_1}{m_1} - \frac{\hat{\underline{P}}_2}{m_2}\right)^2 + \frac{(m_1+m_2)m_3}{2(m_1+m_2+m_3)}\left(\frac{\hat{\underline{P}}_3}{m_3} - \frac{\left(\hat{\underline{P}}_1 + \hat{\underline{P}}_2\right)}{(m_1+m_2)}\right)^2 + \frac{\left(\hat{\underline{P}}_1 + \hat{\underline{P}}_2 + \hat{\underline{P}}_3\right)^2}{2(m_1+m_2+m_3)} \quad .(2.3)$$

The centre-of-mass (CM) coordinate system is defined as that in which the centre of mass of the total composite system (particle 1 + particle 2 + particle 3) is at rest. Therefore,

$$\hat{\underline{P}}_1 + \hat{\underline{P}}_2 + \hat{\underline{P}}_3 = 0 \quad .$$

The CM coordinates for a system with atom, A, and diatom, BC, are:

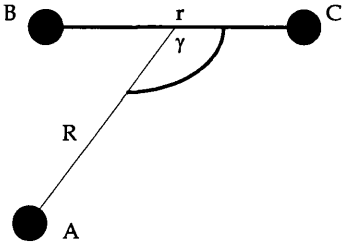

$$\underline{r} = \underline{r}_B - \underline{r}_C$$

and

$$\underline{R} = \underline{r}_A - \underline{r}_G = \underline{r}_A - \frac{m_B \underline{r}_B + m_C \underline{r}_C}{m_B + m_C}$$

with $\underline{r}_G$ representing the position vector of the centre of mass of diatom BC.

Thus, Eqn. (2.3) becomes:

$$\hat{T} = \frac{\hat{\underline{P}}_r^2}{2m_{BC}} + \frac{\hat{\underline{P}}_R^2}{2\mu},$$

where μ is the reduced mass of the whole system, given by:

$$\mu = \frac{m_A(m_B + m_C)}{m_A + m_B + m_C}$$

and m_{BC} is the reduced mass of the diatomic molecule:

$$m_{BC} = \frac{m_B\, m_C}{(m_B + m_C)}.$$

Given that the quantum mechanical definition of the momentum operator is:

$$\hat{P} = -i\hbar\nabla \quad ,$$

the Hamiltonian for the system, in its spherical polar form, can now be expressed as:

$$\hat{H} = -\frac{\hbar^2}{2\mu}\nabla_R^2 - \frac{\hbar^2}{2m_{BC}}\nabla_r^2 + \hat{V}_0(r) + \hat{V}(R, r, R', r') \qquad (2.4)$$

where R' represents (Θ, Φ), the polar angles associated with R, and r' represents (θ, ϕ), the polar angles associated with r. The potential energy function has here been separated into two parts: $\hat{V}_0(r)$ is the diatomic potential energy surface and $\hat{V}$ therefore now refers to the remainder of the potential, that due to the interaction between the diatom and the atom.

The Laplacians, ∇_R^2 and ∇_r^2, are given by:

$$\nabla_R^2 = \left[\left(\frac{\partial}{\partial R} + \frac{1}{R}\right)^2 + \frac{1}{(R\sin\Theta)^2}\left[\sin\Theta\frac{\partial}{\partial\Theta}\left(\sin\Theta\frac{\partial}{\partial\Theta}\right) + \frac{\partial^2}{\partial\Phi^2}\right]\right]$$

and

$$\nabla_r^2 = \left[\left(\frac{\partial}{\partial r} + \frac{1}{r}\right)^2 + \frac{1}{(r\sin\theta)^2}\left[\sin\theta\frac{\partial}{\partial\theta}\left(\sin\theta\frac{\partial}{\partial\theta}\right) + \frac{\partial^2}{\partial\phi^2}\right]\right]$$

or:

$$\nabla_R^2 = \left[\left(\frac{\partial}{\partial R} + \frac{1}{R}\right)^2 - \frac{\hat{l}^2(R')}{R^2}\right] \qquad (2.5)$$

and

$$\nabla_r^2 = \left[\left(\frac{\partial}{\partial r} + \frac{1}{r}\right)^2 - \frac{\hat{j}^2(r')}{r^2}\right] \qquad (2.6)$$

where $\hat{l}$ is the orbital angular momentum operator of the system and $\hat{j}$ is the angular momentum operator associated with the rotations of the diatomic molecule.

Hence, the total Hamiltonian has been split up into two parts, one representing the Hamiltonian of the diatomic molecule (the middle two terms of Eqn. (2.4)) and the other representing its interaction with the atom. Since the potential energy surface for the interaction of the diatom with the atom is only dependent on the angle, γ, between $\underline{R}$ and $\underline{r}$ and not on their absolute orientations in space, the final Hamiltonian can be written as:

$$\hat{H} = -\frac{\hbar^2}{2\mu}\left[\left(\frac{\partial}{\partial R} + \frac{1}{R}\right)^2 - \frac{\hat{l}^2(R')}{R^2}\right] + \hat{H}_{BC} + \hat{V}(R, r, \gamma) \quad . \qquad (2.7)$$

2.2 Close-Coupled Equations

As explained above, the aim of the calculation is to write the wavefunction for the system in terms of the internal states of the diatom, so as to ascertain the coefficients of each state. Therefore, the method used for the solution of the Schrödinger equation (2.1) with the Hamiltonian of Eqn. (2.7) involves expressing the wavefunction as a partial wave expansion over all the quantum numbers:

$$\Psi_{vjm_j} = \left(\frac{1}{R}\right) \sum_{v'j'm_j'l'm_l'} \psi_{l'm_l'}(R')\phi_{j'm_j'}(r')\chi_{v'j'}(r) g^{vjm_j}_{v'j'm_j'l'm_l'}(R) \tag{2.8}$$

Here, $\chi_{v'j'}$ is a rovibrational wavefunction for the diatomic molecule and $\phi_{j'm_{j'}}$ is a diatomic rotation wavefunction. $\psi_{l'm_{l'}}$ is an eigenfunction of the orbital angular momentum operators, $\hat{l}^2$ and $\hat{l}_z$.

Substituting the partial wave expansion into the Schrödinger equation, multiplying the resulting equation on the left by $\psi^*_{l''m_l''}(R')\phi^*_{j''m_j''}(r')\chi^*_{v''j''}(r)$ and integrating over r, r' and R' gives the set of coupled equations:

$$\left[\frac{d^2}{dR^2} + k^2_{v''j''} - \frac{l''(l''+1)}{R^2}\right] g_{v''j''m_j''l''m_l''}(R) = \frac{2\mu}{\hbar^2} \sum_{v'j'm_j'l'm_l'} \left\langle \psi_{l''m_l''}\, \phi_{j''m_j''}\, \chi_{v''j''} \middle| \hat{V} \middle| \psi_{l'm_l'}\, \phi_{j'm_j'}\, \chi_{v'j'} \right\rangle g_{v'j'm_j'l'm_l'}(R) \tag{2.9}$$

where $k^2_{v''j''} = \frac{2\mu}{\hbar^2}\left(E - \epsilon_{v''j''}\right)$ and $\epsilon_{v''j''}$ is an eigenvalue of $\hat{H}_{BC}$. Note that the summation on the right-hand side is over five quantum numbers.

These are the close-coupled equations which need to be solved to find *g(R)*.

The most sensible method of proceeding is to uncouple the equations by diagonalising the matrix of elements:

$$\left\langle v'' j'' m_j'' l'' m_l'' \middle| \hat{V} \middle| v' j' m_j' l' m_l' \right\rangle + \delta_{v''v'}\delta_{j''j'}\delta_{m_j''m_j'}\delta_{l''l'}\delta_{m_l''m_l'}\left(\frac{l''(l''+1)}{R^2} - k^2_{v''j''}\right) \tag{2.10}$$

which is constructed from the potential energy matrix elements of the right-hand side of Eqns. (2.9) added to a diagonal matrix containing the second and third terms of the

left-hand side. Such a diagonalisation would reduce the set of Eqns. (2.9) to a set of simple second-order differential equations.

However, if the basis set of Eqn. (2.8) is to be sufficiently large to give convergence in the results of the calculation of $g(R)$, this diagonalisation would be a mammoth task and would thus not be practicable. Hence, as noted in the Introduction, in order to reduce the amount of computational time and expense required, it is necessary to make some sort of an approximation.

2.3 The Centrifugal Sudden or Coupled States Approximation (CSA)

The coupled states approximation was formulated, simultaneously and independently, by Pack [22] and McGuire & Kouri [23]. The approximation originally consisted of replacing the orbital angular momentum operator in the Hamiltonian of Eqn. (2.7) by a constant parameter, $\bar{l}$, so that

$$\hat{l}^2 = \bar{l}(\bar{l}+1) \ ,$$

thus reducing the difficulty of diagonalising the matrix referred to above (Eqn. (2.10)).

However, it is simpler (and more effective) to apply the approximation if the formulation of the Schrödinger equation is transformed from space-fixed (SF) coordinates (i.e. the laboratory frame) to the body-fixed (BF) coordinate system [26, 27]. This system employs a rotating set of axes, defined such that the BF z-axis is constrained to lie along the vector $\underline{R}$ which relates the centre of mass of the diatom to the atom.

This means that the z component of the orbital angular momentum, m_l, is zero. Thus, the total angular momentum, $\hat{J}$, defined as

$$\hat{J} = \hat{j} + \hat{l}$$

will have z component

$$J_z = m_j + m_l = m_j = \Omega$$

where m_j is the projection of the rotational angular momentum on the (BF) z-axis.

In order to transform the Schrödinger equation for the system from the SF coordinate frame to the BF frame, the rotation function, $\Re$, is applied which rotates the z-axis so that it now lies along the vector $\underline{R}$ and the y-axis so that it now lies in the old (SF) xy-plane. The Schrödinger equation then becomes:

$$\Re\left(\hat{H}_{SF} - E\right)\Psi_{SF} = 0 \qquad . \qquad (2.11)$$

Since the potential surface, as a whole, is invariant under the rotation, the rotated bracket can be written simply as [22, 23] :

$$\Re\left(\hat{H}_{SF}-E\right)=-\frac{\hbar^2}{2\mu}\left[\left(\frac{\partial}{\partial R}+\frac{1}{R}\right)^2-\frac{\hat{l}_{BF}^2}{R^2}\right]+\hat{H}_{BC}\left(r,r'_{BF}\right)-E+\hat{V}(R,r,\gamma). \quad (2.12)$$

The rotated Hamiltonian is identical to Eqn. (2.7), except for the fact that the polar angles r' now describe the position of the vector $\underline{r}$ with respect to the BF-axes and that the operator $\hat{l}^2$ can no longer be exactly explicitly described. Instead, the operator $\hat{l}^2$ is written as $\left|\hat{J}-\hat{j}\right|^2$ and so the Hamiltonian becomes:

$$\hat{H}_{BF}=-\frac{\hbar^2}{2\mu}\left[\left(\frac{\partial}{\partial R}+\frac{1}{R}\right)^2-\frac{\left|\hat{J}-\hat{j}\right|^2}{R^2}\right]+\hat{H}_{BC}+\hat{V}(R,r,\gamma)$$

$$=-\frac{\hbar^2}{2\mu}\left[\left(\frac{\partial}{\partial R}+\frac{1}{R}\right)^2-\frac{\left(\hat{J}_x-\hat{j}_x\right)^2}{R^2}-\frac{\left(\hat{J}_y-\hat{j}_y\right)^2}{R^2}-\frac{\left(\hat{J}_z-\hat{j}_z\right)^2}{R^2}\right]+\hat{H}_{BC}+\hat{V}(R,r,\gamma)$$

$$=-\frac{\hbar^2}{2\mu}\left[\left(\frac{\partial}{\partial R}+\frac{1}{R}\right)^2-\frac{\left(\hat{J}^2+\hat{j}^2-2\hat{J}_z\hat{j}_z-\hat{J}_+\hat{j}_--\hat{J}_-\hat{j}_+\right)}{R^2}\right]+\hat{H}_{BC}+\hat{V}(R,r,\gamma) \quad (2.13)$$

where $\hat{J}_\pm=\hat{J}_x\pm i\hat{J}_y$

and $\hat{j}_\pm=\hat{j}_x\pm i\hat{j}_y$.

The SF wavefunction can be written in terms of a rotated BF wavefunction:

$$\Psi_{vjm_j}^{SF}=\left(\frac{1}{R}\right)\sum_{v'j'm'_jl'm'_l}\psi_{l'm'_l}(R')\phi_{j'm'_j}(r')\chi_{v'j'}(r)g_{v'j'm'_jl'm'_l}^{vjm_j}(R)=\Re^{-1}(R')\Psi_{vjm_j}^{BF} \quad . \quad (2.14)$$

In the SF frame, ψ_{lm_l} are the eigenfunctions of the orbital angular momentum operator, which are simply the spherical harmonics, such that

$$\hat{l}^2\,\mathrm{Y}_{lm_l}=l(l+1)\mathrm{Y}_{lm_l} \quad .$$

Thus, expressing the rotation function in terms of rotation matrices [28], Eqn. (2.14) becomes [29, 30]:

$$\Psi^{SF}_{v j m_j} = \left(\frac{1}{R}\right) \sum_{v' j' m'_j l' m'_l} \left(\sum_{m''_l} D^{l'}_{m''_l m'_l}(R',0) Y_{l' m''_l}(R'_{BF}) \right) \left(\sum_{\Omega'} D^{j'}_{\Omega' m'_j}(R',0)\, \phi_{j'\Omega'}(r'_{BF}) \right) \chi_{v' j'}(r)\, g^{v j m_j}_{v' j' m'_j l' m'_l}(R). \tag{2.15}$$

Since the rotation is about angles R'_{SF},

$$Y_{l' m''_l}(R'_{BF}) = Y_{l'0}(0,0) = \left[\frac{(2l'+1)}{4\pi}\right]^{1/2}$$

and hence:

$$\left(\hat{H}_{BF} - E\right) \left[\left(\frac{1}{R}\right) \sum_{v' j' m'_j l' m'_l} \left[\frac{(2l'+1)}{4\pi}\right]^{1/2} \left(\sum_{\Omega'} D^{j}_{\Omega' m'_j}(R',0) D^{l}_{0 m'_l}(R',0)\, \phi_{j'\Omega'}(r'_{BF}) \right) \chi_{v' j'}(r)\, g^{v j m_j}_{v' j' m'_j l' m'_l}(R) \right] = 0.$$

Making use of Wigner 3-j symbols, and the fact that $l + j = J$ and $m_j + m_l = M$, the wavefunction can be rewritten as:

$$\left[\left(\frac{1}{R}\right) \sum_{v' j' m'_j l' m'_l} \left[\frac{(2l'+1)}{4\pi}\right]^{1/2} \left(\sum_{\Omega' J M} D^{J\,*}_{\Omega' M}(R',0)(2J+1) \begin{pmatrix} j' & l' & J \\ \Omega' & 0 & -\Omega' \end{pmatrix} \begin{pmatrix} j' & l' & J \\ m'_j & m'_l & M \end{pmatrix} \phi_{j'\Omega'}(r'_{BF}) \right) \chi_{v' j'}\, g^{v j m_j}_{v' j' m'_j l' m'_l} \right] \tag{2.16}$$

and the Schrödinger equation therefore becomes:

$$\left(\hat{H}_{BF} - E\right) \left[\left(\frac{1}{R}\right) \sum_{\Omega' J M} \sum_{v' j'} D^{J\,*}_{\Omega' M}(R',0)\, \phi_{j'\Omega'}(r'_{BF})\, \chi_{v' j'}(r)\, f^{v j \Omega}_{v' j' \Omega' J M}(R) \right] = 0 \quad .$$

Thus, the time-independent Schrödinger equation for the system with the diatom initially in vibrational state v and rotational state j and with Ω the projection of j on the BF z-axis, can be expressed as:

$$\begin{aligned} \left(H_{BF} - E\right) \Psi^{J M v j \Omega} &= \left(H_{BF} - E\right) \left(\frac{1}{R}\right) \sum_{\Omega' v' j'} D^{J*}_{\Omega' M}(R',0)\, \phi_{j'\Omega'}(r') \chi_{v' j'}(r) f^{J v j \Omega}_{v' j' \Omega'}(R) \\ &= \left(H_{BF} - E\right) \sum_{\Omega'} D^{J*}_{\Omega' M}(R',0)\, \Psi^{J v j \Omega}_{\Omega'}(R,r,r') = 0 \end{aligned} \tag{2.17}$$

for total angular momentum quantum numbers J and M. (Note that r' are now the new polar angles, (θ, ϕ), associated with the vector $\underline{r}$ in the BF frame and that therefore angle θ is equivalent to angle γ).

Substitution of the Hamiltonian of Eqn. (2.13) into the Schrödinger equation (2.17), multiplying the result on the left by $D^{J}_{\Omega' M}$ and integrating over R', gives the coupled equations:

$$H_{\Omega'\Omega'-1}\Psi^{Jvj\Omega}_{\Omega'-1} + H_{\Omega'\Omega'+1}\Psi^{Jvj\Omega}_{\Omega'+1} + (H_{\Omega'\Omega'} - E)\Psi^{Jvj\Omega}_{\Omega'} = 0 \qquad (2.18)$$

where

$$H_{\Omega'\Omega'} = -\frac{\hbar^2}{2\mu}\left(\frac{\partial}{\partial R} + \frac{1}{R}\right)^2 + \frac{\hbar^2\left[J(J+1) - 2\Omega''^2 + \hat{j}^2\right]}{2\mu R^2} + \hat{H}_{BC} + \hat{V}(R,r,\gamma) \qquad (2.19)$$

and $$H_{\Omega'\Omega'\pm 1} = \frac{-\hbar^2\lambda_{\pm}(J,\Omega'')\hat{j}_{\mp}}{2\mu R^2} \quad . \qquad (2.20)$$

This result has made use of the relationships [22, 30]:

$$\hat{J}^2 D^{J*}_{M\Omega} = J(J+1) D^{J*}_{M\Omega}$$

$$\hat{J}_z D^{J*}_{M\Omega} = \Omega D^{J*}_{M\Omega}$$

$$\hat{J}_{\pm} D^{J*}_{\Omega M} = \lambda_{\mp}(J,\Omega) D^{J*}_{\Omega \mp 1 M}$$

$$\lambda_{\pm}(J,\Omega) = [J(J+1) - \Omega(\Omega \pm 1)]^{1/2} \quad .$$

Note that the raising and lowering operators, $\hat{J}_{\pm}$, in the BF frame have the opposite effect to those in the SF frame [29].

In this coordinate system, Schatz and Kuppermann [31] recommend a variation of the CSA which involves simply ignoring all terms non-diagonal in Ω", whilst leaving the diagonal terms unapproximated. This is equivalent to expressing the centrifugal term of the Hamiltonian as:

$$\left|\hat{J} - \hat{j}\right|^2 = \hat{J}^2 + \hat{j}^2 - 2\hat{J}_z\hat{j}_z \quad .$$

Hence, the Schrödinger equation becomes:

$$\left(-\frac{\hbar^2}{2\mu}\left(\frac{\partial}{\partial R}+\frac{1}{R}\right)^2+\frac{\hbar^2\left[J(J+1)-2\Omega''^2+\hat{j}^2\right]}{2\mu R^2}+\hat{H}_{BC}-E+\hat{V}(R,r,\gamma)\right)\Psi_{\Omega''}^{Jvj\Omega}=0 \qquad (2.21)$$

where

$$\Psi_{\Omega''}^{Jvj\Omega}=\frac{1}{R}\sum_{v'j'}\phi_{j'\Omega''}(r')\chi_{v'j'}(r)f_{v'j'\Omega''}^{Jvj\Omega}(R) \quad . \qquad (2.22)$$

Then, as for the SF coupled equations above (Eqn. (2.9)), multiplying the equation on the left by $\phi_{j''\Omega''}^{*}(r'_{BF})\chi_{v''j''}^{*}(r)$ and integrating over r and r' gives the set of BF coupled equations:

$$\left[\frac{d^2}{dR^2}+k_{v''j''}^2-\frac{\left[J(J+1)-2\Omega''^2+j''(j''+1)\right]}{R^2}\right]f_{v''j''\Omega''}^{Jvj\Omega}(R)=\frac{2\mu}{\hbar^2}\sum_{v'j'}\left\langle\phi_{j''\Omega''}\chi_{v''j''}\left|\hat{V}\right|\phi_{j'\Omega''}\chi_{v'j'}\right\rangle f_{v'j'\Omega''}^{Jvj\Omega}(R) \qquad (2.23)$$

with $k_{v''j''}^2=\frac{2\mu}{\hbar^2}\left(E-\epsilon_{v''j''}^{diatom}\right)$.

3 The Potential Energy Matrix

Prior to this research, as far as could be ascertained, all quantum mechanical studies of the vibrational relaxation of a diatom have assumed the diatom to have ground electronic state $^1\Sigma$. However, the molecular orbital description of the electronic configuration of O_2^+ is:

$$(1s\sigma_g)^2 (1s\sigma_u^*)^2 (2s\sigma_g)^2 (2s\sigma_u^*)^2 (2p\pi_u)^2 (2p\pi_u)^2 (2p\sigma_g)^2 (2p\pi_g^*)^1$$

meaning that the ground electronic state of O_2^+ is $^2\Pi$. Treating O_2^+ as $^1\Sigma$ would entail an approximation in the quantum mechanical model of the physical system. As mentioned in the Introduction, one of the major aims of this research is to assess the validity of such an approximation by carrying out calculations treating the diatom both as $^1\Sigma$ and as $^2\Pi$. In addition to which, another objective is to test the accuracy of the coupled states approximation for the O_2^+ / Kr system by comparing the results obtained using it to those obtained in classical and semi-classical studies, which used a semi-empirical potential energy surface.

Thus, as outlined in the Introduction, the coupled states approximation for the solution of the time-independent Schrödinger equation is here applied to three alternative descriptions of the inelastic scattering of O_2^+ with Kr:

a) Treating the diatom as $^1\Sigma$ and using the semi-empirical interaction potential energy surface of Tosi, Ronchetti and Lagana [11, 14] (TRL).

b) Treating the diatom as $^1\Sigma$ and using the single *ab initio* $1^2A''$ interaction potential energy surface of Ramiro-Diaz, Wahnon and Sidis (RDWS) [19]. The surface for the wavefunction of A" symmetry has been chosen over that for the wavefunction of A' symmetry since it is the lower of the two. (This is true despite the fact that, in the C_s symmetry group, A' is the representation of greater symmetry, since in the A' orientation the partly filled π-orbital of the diatom lies in the scattering plane and would thus have a greater affect on the ability of the incoming atom to interact with the diatom.)

c) Treating the diatom as $^2\Pi$ and using both the $1^2A''$ and the $1^2A'$ interaction potential energy surfaces of Ramiro-Diaz, Wahnon and Sidis (RDWS) [20].

Description c) follows the Hund's case (a) representation for the coupling of diatomic angular momentum such that the spin of the electrons and the electronic angular momentum are coupled together along the bond-axis. Hence, if Ω is the projection of the total angular momentum of the diatomic molecule along the molecular bond-axis, Λ the projection of the electronic orbital angular momentum along that axis and Σ the projection of the spin angular momentum, then:

$$\Omega = \Lambda + \Sigma .$$

For a $^2\Pi$ molecule, $\Lambda = \pm 1$ and $\Sigma = \pm \frac{1}{2}$ so that $|\Omega| = \frac{1}{2}$ or $^3/_2$.

However, in this analysis, in order to simplify the equations used, the spin of the electrons is assumed to have a negligible effect on the calculations and is therefore approximated to zero. Consequently, the system in this description has, in fact, been treated as one where the diatom is actually of electronic ground state $^1\Pi$, ignoring the doublet character of the O_2^+ diatom.

All the elements of the method discussed until now are equally applicable to all three descriptions of the O_2^+/Kr system. The differences between the three versions occur in the evaluation of the potential matrix terms of Eqn. (2.23).

3.1 The Diatomic Rotation Wavefunction

3.1.1 Diatomics in Σ States

The rotational part of the molecular wavefunction for a diatom with the ground electronic state of $^1\Sigma$ are the eigenfunctions that satisfy the equations:

$$\hat{j}^2 \phi_{j\Omega} = j(j+1)\phi_{j\Omega}$$

and

$$\hat{j}_z^{BF} \phi_{j\Omega} = \Omega \phi_{j\Omega}$$

which are, therefore, the normalised spherical harmonic functions, $Y_{j\Omega}(r')$.

3.1.2 Diatomics in Π States

The rotational part of the molecular wavefunction for a diatom with ground state of $^1\Pi$ are the eigenfunctions that satisfy the equations:

$$\hat{j}^2 \phi_{j\Omega\Lambda} = j(j+1)\phi_{j\Omega\Lambda}$$

$$\hat{j}_z^{BF} \phi_{j\Omega\Lambda} = \Omega \phi_{j\Omega\Lambda}$$

and

$$\hat{j}_z^{MF} \phi_{j\Omega\Lambda} = \Lambda \phi_{j\Omega\Lambda}$$

where MF is the molecule frame, which has the z-axis along the bond axis. Such functions are the normalised rotation matrices, $\left(\frac{2j+1}{8\pi^2}\right)^{1/2} D^j_{\Omega\Lambda}(r')$.

Because the value of the quantum number Λ can be either +1 or –1 and is dependent on the angular momentum of the electronic wavefunction, the partial wave expansion (Eqn. (2.22)) would now be either:

$$\Psi^{Jvj\Omega}_{\Omega'}|\Lambda\rangle = \sum_{v'j'} \left(\frac{2j'+1}{8\pi^2}\right)^{1/2} \chi_{v'j'}(r) f^{Jvj\Omega}_{v'j'\Omega'}(R) D^{j'}_{\Omega',1}(r')|\Lambda=1\rangle$$

or

$$\Psi_{\Omega''}^{Jvj\Omega}\left|\Lambda\right\rangle=\sum_{v'j'}\left(\frac{2j'+1}{8\pi^2}\right)^{1/2}\chi_{v'j'}(r)\,f_{v'j'\Omega'}^{Jvj\Omega}(R)\,D_{\Omega''-1}^{j'}(r')\left|\Lambda=-1\right\rangle \quad ,$$

dependent on the electronic angular momentum wavefunction, $\left|\Lambda\right\rangle$.

Due to symmetry requirements, a linear combination of the two wavefunctions is actually used, so that the definite symmetry partial wavefunction expansion for the Π diatom becomes:

$$\Psi_{\Omega'}^{Jvj\Omega}\left|\varepsilon\,\Lambda\right\rangle=\sum_{v'j'\varepsilon'}\left(\frac{2j'+1}{16\pi^2}\right)^{1/2}\chi_{v'j'}(r)\,f_{v'j'\Omega'}^{Jvj\Omega}(R)\left(D_{\Omega'1}^{j'}(r')\left|\Lambda=1\right\rangle+\varepsilon'\,D_{\Omega'-1}^{j'}(r')\left|\Lambda=-1\right\rangle\right) \quad (3.1)$$

where $\varepsilon'=\pm1$.

In this research, the Λ-doubling is neglected and the channel energies, $\epsilon_{vj\varepsilon}^{diat}$, are thus taken to be doubly degenerate with respect to ε.

3.2 Potential Energy Surfaces

3.2.1 Semi-Empirical Interaction Potential

The TRL potential energy surface is given by the formula first published in Ref. [17]:

$$\begin{aligned} V_{TRL}(R,r,\gamma) = {} & D_a \exp\left(-\bar{b}\left(R_a - R^*\right)\right)\left[\exp\left(-\bar{b}\left(R_a - R^*\right)\right) - 2\exp\left(-\Delta_a\left(\gamma_a - 139^\circ\right)^2\right)\right] \\ & + D_b \exp\left(-\bar{b}\left(R_b - R^*\right)\right)\left[\exp\left(-\bar{b}\left(R_b - R^*\right)\right) - 2\exp\left(-\Delta_b\left(\gamma_b - 139^\circ\right)^2\right)\right] \\ & - \frac{C}{2R^4}\left(1 - \tanh\left(R - \bar{R}_0\right)\right) + E\exp\left(-cR\right) \end{aligned} \quad (3.2)$$

where

$$R_a^2 = R^2 + \tfrac{1}{4}r^2 - R\,r\,\cos(\gamma)$$

$$R_b^2 = R^2 + \tfrac{1}{4}r^2 + R\,r\,\cos(\gamma)$$

$$\cos(\gamma_a) = \frac{\frac{1}{2}r - R\cos(\gamma)}{R_a}$$

$$\cos(\gamma_b) = \frac{\frac{1}{2}r - R\cos(\gamma)}{R_b} \quad .$$

The values of the constants of Eqn. (3.2) that were used are those given in Ref. [15]. They are:-

O_2^+ dissociation energy: $D_a = D_b = 0.2\,\text{eV}$

Equilibrium distance: $R^* = 2.56\,\text{Å}$

Angular dependence dampening function: $\Delta_a = \Delta_b = -\dfrac{\ln(0.1)}{\theta^2}$

with adjustable parameter: $\theta = 20^\circ$

$\bar{b} = 3.00\,\text{Å}^{-1}$

$C = 17.855\,\text{eV}$

$\bar{R}_0 = 15\,\text{Å}$

$E = 800\,\text{eV}$

$c = 3\,\text{Å}^{-1}$.

3.2.2 Ab Initio *Interaction Potential*

The *ab initio* potential energy surface of Ramiro-Diaz, Wahnon and Sidis [19, 20] was evaluated through the use of configuration interaction calculations in a basis of about one thousand projected-valence-bond state functions. Their calculations produced potential energy surface points, for both the 1A" and the 1A' electronic states, for 30 values of R, 10 values of r and 7 values of γ. In order to incorporate these points into the dynamics calculations, it is necessary to fit them to a function which can be used to describe the whole potential energy surface. The form of the PES function can be chosen to simplify the evaluation of the integrals in the potential energy matrix of Eqn. (2.23) by separating out the angular dependence.

Methods for incorporating a single potential energy surface into dynamics equations are much more common and better understood than those for multiple potential surfaces. However, a description of how to formulate both the A" and the A' potential surfaces in terms of a single function has been derived in a number of different ways [32 – 36]. This thesis will present the derivation proposed by Alexander [36] since it enables one to see easily how both the expression for the single potential surface, of the $^1\Sigma$ treatment, and that of the double potential surface, of the $^1\Pi$ treatment, are simply different examples of the same formulation.

The Hamiltonian of Eqn. (2.7) has been integrated over the coordinates of all the electrons of the system, based on the Born-Oppenheimer approximation which allows separation of the wavefunction into nuclear and electronic parts. The full Schrödinger equation in centre-of-mass coordinates, in atomic units, with the electronic part of the wavefunction written explicitly is:

$$\left[\hat{T}_R^{nucl} + \hat{T}_r^{nucl} + \hat{T}_{BC}^{el} + \hat{T}_A^{el} + \sum_{\substack{ij \\ i\neq j}} \frac{Z_i Z_j}{\left|\underline{r}_i^{BC} - \underline{r}_j^{BC}\right|} + \sum_{\substack{kl \\ k\neq l}} \frac{Z_k Z_l}{\left|\underline{r}_k^{A} - \underline{r}_l^{A}\right|} + \sum_{ik} \frac{Z_i Z_k}{\left|\underline{r}_i^{BC} - \underline{r}_k^{A}\right|} - E^{TOTAL}\right]$$

$$\Psi_R^{nucl}\Psi_r^{nucl}\Psi_{BC}^{el}\Psi_A^{el} = 0$$

with $\hat{T}$ being the kinetic energy operator and the vectors $\underline{r}$ are position vectors. The subscripts i and j label any two charged particles associated with the diatomic molecule BC, and k and l label any two charged particles associated with the atom A. Z_x is the charge of particle x and 'nucl' and 'el' label nuclear and electron terms, respectively.

Then, assuming possible electronic excitation in the molecule but not in the atom, multiplying on the left by $\Psi_{BC'}^{el\,*}\Psi_{A}^{el\,*}$ and integrating over the coordinates of the electrons gives the set of coupled equations:

$$\left[\hat{T}_R^{nucl}+\left(\hat{T}_r^{nucl}+\sum_{BC}\left\langle\Psi_{BC'}^{el}\left|\hat{T}_{BC}^{el}+\sum_{\substack{ij\\ i\neq j}}\frac{Z_iZ_j}{\left|\underline{r}_i^{BC}-\underline{r}_j^{BC}\right|}\right|\Psi_{BC}^{el}\right\rangle\right)+\left(\left\langle\Psi_A^{el}\left|\hat{T}_A^{el}+\sum_{\substack{kl\\ k\neq l}}\frac{Z_kZ_l}{\left|\underline{r}_k^{A}-\underline{r}_l^{A}\right|}\right|\Psi_A^{el}\right\rangle-E^{TOTAL}\right)\right.$$

$$\left.+\sum_{BC}\left\langle\Psi_{BC'}^{el}\Psi_A^{el}\left|\sum_{ik}\frac{Z_iZ_k}{\left|\underline{r}_i^{BC}-\underline{r}_k^{A}\right|}\right|\Psi_A^{el}\Psi_{BC}^{el}\right\rangle\right]\Psi_R^{nucl}\Psi_r^{nucl}=0$$

$$=\left[\hat{T}_R^{nucl}+\hat{H}_{BC}-E+\sum_{BC}\left\langle\Psi_{BC'}^{el}\Psi_A^{el}\left|\sum_{ik}\frac{Z_iZ_k}{\left|\underline{r}_i^{BC}-\underline{r}_k^{A}\right|}\right|\Psi_A^{el}\Psi_{BC}^{el}\right\rangle\right]\Psi_R^{nucl}\Psi_r^{nucl}=0 \qquad (3.3)$$

where E is the total energy of the system minus the energy of the atom. The Hamiltonian is now identical to that of Eqn. (2.7), but with the potential energy operator in that equation here expressed explicitly as a matrix.

Each of the inverse distances can be expanded as a linear combination of unnormalised spherical harmonics, C, [37] such that:

$$\sum_{ik}\frac{1}{\left|\underline{r}_i^{BC}-\underline{r}_k^{A}\right|}=\sum_{ik}\sum_{\substack{L_{BC}L_AL\\ M_{BC}M_AM}}\left(L_{BC}\,M_{BC}\,L_A\,M_A\middle|LM\right)F_{L_{BC}L_AL}\left(R,r_{BC_i},r_{A_k}\right)C_{L_{BC}M_{BC}}\left(r'_{BC_i}\right)C_{L_AM_A}\left(r'_{A_k}\right)C^{*}_{LM}\left(R'\right)$$

Here, $\left(r_{A_k},r'_{A_k}\right)$ are the coordinates of the particle k in the atom, relative to an origin fixed in the atom. $\left(r_{BC_i},r'_{BC_i}\right)$ are the coordinates of the particle i in the molecule, relative to an origin fixed at the centre of mass of the diatom but in an identical coordinate system to that for the atom. $\underline{R}$ is the vector which joins the two origins.

The first term of the summation is a Clebsch-Gordan coefficient, which arises as a result of the fact that the inverse-distance is invariant under simultaneous rotation of r_A, r_{BC} and R [37].

By setting the z-axis of the coordinate system to be along $\underline{R}$ i.e. as in the BF frame,

$$C_{LM}(R') = C_{LM}(\hat{z}) = \delta_{M0} \ .$$

If the atom, A, is spherically symmetric then the only terms which will contribute to integration of the atomic coordinates over all of space in Eqn. (3.3) will have $M_A = 0$. Then, the requirements of the Clebsch-Gordan coefficients means that $M_{BC} = 0$ as well. The inverse-distance expansion therefore reduces to:

$$\sum_{ik} \frac{1}{\left| \underline{r}_i^{BC} - \underline{r}_k^{A} \right|} = \sum_{ik} \sum_{L_{BC} L_A L} \left(L_{BC}\, 0\, L_A\, 0 \middle| L\, 0 \right) {}_{L_{BC} L_A L}F \left(R, r_{BC_i}, r_{A_k} \right) C_{L_{BC}0}\left(r'_{BC_i} \right) C_{L_A 0}\left(r'_{A_k} \right) \ , \qquad (3.4)$$

which is in the BF frame.

The molecular electronic wavefunction can be expanded as a linear combination of atomic orbitals. However, it is always defined in the molecule-fixed (MF) frame, where the z-axis is the bond-axis. So,

$$\Psi^{el}_{BC_i} = \sum_{anj} G^{i}_{anjm_j}(\rho_i) \mathrm{Y}_{jm_j}(\rho'_i) \ = \ \left| \Lambda = m_j \right\rangle$$

where $\underline{\rho}_i$ is the position vector of electron i from the origin in the molecule in the MF coordinate system. Obviously $|\rho_i| = \left| \underline{r}_{BC_i} \right|$. The labels n, j and m_j for atom a are the principal quantum number, the angular momentum quantum number and the projection of the angular momentum on the bond-axis, respectively.

In order to calculate the potential matrix elements of Eqn. (3.3), it is necessary to transform the molecular terms in the inverse distance expansion from the BF frame to the MF frame. This is expressed, using rotation matrices, as:

$$\sum_{ik} \frac{1}{\left| \underline{r}_i^{BC} - \underline{r}_k^{A} \right|} = \sum_{ik} \sum_{L_{BC} L_A L} \left(L_{BC}\, 0\, L_A\, 0 \middle| L\, 0 \right) C_{L_A 0}\left(r'_{A_k} \right) \sum_{\mu} D^{L_{BC}}_{0\mu}(0\gamma 0)\, C_{L_{BC}\mu}(\rho'_i)\, {}_{L_{BC} L_A L}F \left(R, \rho_i, r_{A_k} \right)$$

where γ is the angle between the diatomic bond-axis and the vector $\underline{R}$, as before. The x- and the y- axes in the MF frame are arbitrary and so, here, the angles of the rotation matrices have been chosen such that the xz-planes of the BF and MF frames coincide.

It is useful to note at this point that, if BC is a homonuclear molecule, then it must follow from the above equation that the C functions associated with the electrons of the molecule satisfy the relationship:

$$C_{L_{BC}\mu}(\rho_i') = C_{L_{BC}\mu}\left(\alpha_{BC_i}^{MF}, \beta_{BC_i}^{MF}\right) = (-1)^{\mu}\left[\frac{(L_{BC}+\mu)!}{(L_{BC}+\mu)!}\right]^{1/2} P_{L_{BC}}^{\mu}\left(\cos\left(\beta_{BC_i}^{MF}\right)\right) e^{i\mu\alpha_{BC_i}^{MF}}$$

$$= (-1)^{\mu}\left[\frac{(L_{BC}+\mu)!}{(L_{BC}+\mu)!}\right]^{1/2} P_{L_{BC}}^{\mu}\left(\cos\left(\pi - \beta_{BC_i}^{MF}\right)\right) e^{i\mu\alpha_{BC_i}^{MF}}$$

where P_l^m are the associated Legendre polynomials, which exhibit the parity:

$$P_l^m(-x) = (-1)^{l+m} P_l^m(x)$$

and so, for homonuclear diatomics, $(L_{BC} + \mu)$ would be limited to even values only.

The potential matrix elements now become:

$$\left\langle \Psi_{BC'}^{el}\Psi_A^{el}\left|\sum_{ik}\frac{Z_iZ_k}{\left|\underline{r}_i^{BC}-\underline{r}_k^{A}\right|}\right|\Psi_A^{el}\Psi_{BC}^{el}\right\rangle = \left\langle \Psi_A^{el}\left|\sum_{ik}Z_iZ_k\sum_{L_{BC}\mu}D_{0\mu}^{L_{BC}}(0\gamma 0)\sum_{j'j}\int \mathrm{Y}_{j'\Lambda_i'}^{*}(\rho_i')\,C_{L_{BC}\mu}(\rho_i')\mathrm{Y}_{j\Lambda_i}(\rho_i')d\rho_i'\right.\right.$$

$$\left.\left.\int\sum_{ana'n'}G_{a'n'j'\Lambda_i'}^{i^*}(\rho_i)\,G_{anj\Lambda_i}^{i}(\rho_i)\sum_{L_AL}(L_{BC}\,0\,L_A\,0|\,L\,0)C_{L_A0}(r_{A_k}')\,F_{L_{BC}L_AL}(R,\rho_i,r_{A_k})\rho_i^{2}d\rho_i\right|\Psi_A^{el}\right\rangle \quad (3.5)$$

which can be shortened to:

$$\hat{V}_{\Lambda'\Lambda}(R,r,\gamma) = \sum_{\mu}\sum_{L_{BC}}\sum_{i}D_{0\mu}^{L_{BC}}(0\gamma 0)\,V_{L_{BC}\mu}^{i}(R,r) \quad . \quad (3.6)$$

The first integral in Eqn. (3.5) can be calculated in terms of the Wigner 3-j symbols:

$$\int \mathrm{Y}_{j'\Lambda_i'}^{*}(\rho_i')\,C_{L_{BC}\mu}(\rho_i')\mathrm{Y}_{j\Lambda_i}(\rho_i')d\rho_i' = (-1)^{\Lambda_i'}\left[(2j'+1)(2j+1)\right]^{1/2}\begin{pmatrix} j & L_{BC} & j' \\ 0 & 0 & 0\end{pmatrix}\begin{pmatrix} j & L_{BC} & j' \\ \Lambda_i & \mu & -\Lambda_i'\end{pmatrix} \quad (3.7)$$

which, in order to be non-zero, must have $\mu = \Lambda_i' - \Lambda_i$.

Hence, Eqn. (3.6) can be written as:

$$\hat{V}_{\Lambda'\Lambda}(R,r,\gamma)=\sum_{L_{BC}}\sum_{i} D^{L_{BC}}_{0\,\Lambda'_i-\Lambda_i}(0\gamma 0)\,V^{i}_{L_{BC}\,\Lambda'_i-\Lambda_i}(R,r).$$

For all electrons other than those in unfilled orbitals with non-zero Λ, this becomes:

$$\hat{V}_{\Lambda'\Lambda}(R,r,\gamma)=\sum_{L_{BC}}\sum_{i} D^{L_{BC}}_{00}(0\gamma 0)\,V^{i}_{L_{BC}0}(R,r)=\sum_{L_{BC}} D^{L_{BC}}_{00}(0\gamma 0)\,V_{L_{BC}0}(R,r)$$

and so, if the diatom is taken to have ground electronic state Σ, where Λ= 0, the potential energy function can be expressed in the well known form:

$$\hat{V}(R,r,\gamma)=\sum_{l} V_{l0}(R,r)\,P_l(\cos\gamma) \qquad (3.8)$$

having used the identity:

$$D^{l}_{00}(\alpha\beta\gamma)=P_l(\cos\beta)\ .$$

The values of V_{l0} can then be found by fitting the single *ab initio* potential to an expansion in Legendre polynomials.

If the diatom has ground electronic state Π, with one electron in the unfilled π-orbital, then, as previously mentioned, (Eqn. (3.1)), the definite symmetry wavefunction is used:

$$\Psi^{rot}_{BC}\Psi^{el}_{BC}=\left(\frac{2j'+1}{16\pi^2}\right)^{1/2}\left(D^{j'}_{\Omega\,1}(r')\,|\lambda\rangle\,|\Lambda=1\rangle+\varepsilon\,D^{j'}_{\Omega\,-1}(r')\,|\lambda\rangle\,|\Lambda=-1\rangle\right)$$

where $\varepsilon=\pm1$. Here, $|\lambda\rangle$ represents the product of all the electronic molecular orbitals in the diatom other than that for the electron in the unfilled π-orbital, which is represented by the $|\Lambda\rangle$ term. The potential energy matrix will therefore consist of the terms:

$$\left\langle\lambda\left|\left\langle\Lambda=\pm1\left|\sum_{ik}\frac{1}{\left|\underline{r}_i^{BC}-\underline{r}_k^{A}\right|}\right|\Lambda=\pm1\right\rangle\right|\lambda\right\rangle=\sum_{L_{BC}} D^{L_{BC}}_{00}(0\gamma 0)\,V^{\lambda}_{L_{BC}0}(R,r)+\sum_{L_{BC}} D^{L_{BC}}_{00}(0\gamma 0)\,V^{\pi^1}_{L_{BC}0}(R,r)$$
$$=\sum_{L_{BC}} D^{L_{BC}}_{00}(0\gamma 0)\,V_{L_{BC}0}(R,r)$$

and:

$$\left\langle \lambda \left| \left\langle \Lambda = \pm 1 \left| \sum_{ik} \frac{1}{\left| \underline{r}_i^{BC} - \underline{r}_k^{A} \right|} \right| \Lambda = \mp 1 \right\rangle \right| \lambda \right\rangle = \sum_{L_{BC}} D_{02}^{L_{BC}}(0\gamma 0)\, V_{L_{BC}2}^{\pi^1}(R,r)$$

where superscript π^1 refers to the single electron in the unfilled π-orbital and λ to all the other electrons. This has made use of the fact that:

$$D_{02}^{l}(0\,\gamma\,0) = D_{0\,-2}^{l}(0\gamma 0) \quad \text{and} \quad V_{l\;\Lambda'-\Lambda}(R,r) = V_{l\;-\Lambda'+\Lambda}(R,r)\,.$$

The second of these two identities is due to the property of the 3-j symbols that:

$$\begin{pmatrix} j_1 & j_2 & j_3 \\ m_1 & m_2 & m_3 \end{pmatrix} = (-1)^{j_1+j_2+j_3} \begin{pmatrix} j_1 & j_2 & j_3 \\ -m_1 & -m_2 & -m_3 \end{pmatrix}$$

for then the first of the 3-j symbols in Eqn. (3.7) requires that $j' + L_{BC} + j$ be an even number.

In order to evaluate V_{l0} and V_{l2} it is necessary to express these expansions in terms of the A" and A' potential energy surfaces that have been calculated *ab initio*. The A' wavefunction is symmetric with respect to reflection in the triatomic plane and the A" wavefunction is anti-symmetric. Therefore, since the angles for the rotation of the BF frame on to the MF frame were fixed such that the xz-planes of the two coordinate frames coincide, these symmetry properties will also be true in the MF frame. The definite symmetry molecular electronic wavefunctions:

$$|\Lambda\varepsilon\rangle = \tfrac{1}{\sqrt{2}}\left(|\lambda\rangle\,|\Lambda=1\rangle + \varepsilon\,|\lambda\rangle\,|\Lambda=-1\rangle\right)$$

where $\varepsilon = \pm 1$, behave, under reflection in the MF xz-plane, as [38]:

$$\sigma_v(xz)|\,\Lambda\,\varepsilon\rangle = (-1)^{\Lambda}\,\varepsilon|\Lambda\,\varepsilon\rangle.$$

Consequently, it is possible to identify the A' wavefunction with the molecular electronic wavefunction $|\Lambda\ -1\rangle$ in the Π-state and the A" wavefunction with $|\Lambda\ 1\rangle$.

Thus, the A" and A' potential energy surfaces can be described by the potential matrix elements:

$$V_{A''}(R,r,\gamma)=\left\langle \Lambda\ 1\left|\sum_{ik}\frac{1}{\left|\underline{r}_i^{BC}-\underline{r}_k^{A}\right|}\right|\Lambda\ 1\right\rangle=\sum_{L_{BC}}D_{00}^{L_{BC}}(0\gamma 0)V_{L_{BC}0}(R,r)+\sum_{L_{BC}}D_{02}^{L_{BC}}(0\gamma 0)V_{L_{BC}2}^{\pi^1}(R,r)$$

$$V_{A'}(R,r,\gamma)=\left\langle \Lambda\ -1\left|\sum_{ik}\frac{1}{\left|\underline{r}_i^{BC}-\underline{r}_k^{A}\right|}\right|\Lambda\ -1\right\rangle=\sum_{L_{BC}}D_{00}^{L_{BC}}(0\gamma 0)V_{L_{BC}0}(R,r)-\sum_{L_{BC}}D_{02}^{L_{BC}}(0\gamma 0)V_{L_{BC}2}^{\pi^1}(R,r).$$

It is therefore apparent that:

$$\sum_{L_{BC}}D_{00}^{L_{BC}}(0\gamma 0)V_{L_{BC}0}(R,r)=\frac{1}{2}[V_{A''}+V_{A'}]$$

and:

$$\sum_{L_{BC}}D_{02}^{L_{BC}}(0\gamma 0)V_{L_{BC}2}^{\pi^1}(R,r)=\frac{1}{2}[V_{A''}-V_{A'}]\quad .$$

Transforming the rotation matrices into Legendre polynomials and associated Legendre polynomials, yields:

$$\sum_{l=0}^{\infty}P_l(\cos\gamma)V_{l0}(R,r)=\frac{1}{2}[V_{A''}+V_{A'}] \qquad (3.9)$$

and

$$\sum_{l=2}^{\infty}\left[\frac{(l-2)!}{(l+2)!}\right]P_l^2(\cos\gamma)V_{l2}(R,r)=\frac{1}{2}[V_{A''}-V_{A'}] \qquad (3.10)$$

and thus reveals that the V_{l0} terms can be evaluated by fitting the average of the A" and A' potential energy surfaces to an expansion in Legendre polynomials, whilst the V_{l2} terms can be evaluated by fitting one-half the difference of the two surfaces to an expansion in associated Legendre polynomials. Note that the sum over l in Eqn. (3.10) starts at $l=2$ due to the requirements of the 3-j symbols in Eqn. (3.7).

This derivation has made clear that the ability to express the potential energy functions as linear combinations of Legendre and associated Legendre polynomial functions of the separation angle γ, for both the Σ treatment and the Π treatment of the diatom, arises from the same source – the relative orientation of the molecular electronic wavefunction with respect to the inverse-distance potential energy terms.

To construct the full 3D potential energy function then, for the Σ treatment the potential is expanded as [39]:

$$\hat{V}_0(R,r,\gamma) = V_{A''} = \sum_{n=1}^{N} \sum_{\substack{l=0 \\ even\ l}}^{L} P_l(\cos\gamma) A_{ln}(R)(r-r_e)^{n-1} \tag{3.11}$$

whilst, for the Π treatment, two expressions are employed:

$$\hat{V}_0(R,r,\gamma) = \frac{V_{A'} + V_{A''}}{2}(R,r,\gamma) = \sum_{n=1}^{N} \sum_{\substack{l=0 \\ even\ l}}^{L} P_l(\cos\gamma) A_{ln}(R)(r-r_e)^{n-1} \tag{3.12}$$

and

$$\hat{V}_2(R,r,\gamma) = \frac{V_{A'} - V_{A''}}{2}(R,r,\gamma) = \sum_{n=1}^{N} \sum_{\substack{l=2 \\ even\ l}}^{L} \left[\frac{(l-2)!}{(l+2)!}\right]^{\frac{1}{2}} P_l^2(\cos\gamma) B_{ln}(R)(r-r_e)^{n-1} \quad . \tag{3.13}$$

Here, $P_l(\cos\gamma)$ is a Legendre polynomial; $P_l^2(\cos\gamma)$ is an associated Legendre polynomial; r_e is the equilibrium molecular bond distance ($r_e = 2.11\,a_0$ for O_2^+); A_{ln} and B_{nl} are expansion coefficients. Since the diatom in the O_2^+ / Kr system is homonuclear, the sum over l is for even values only, as explained above.

The expansion coefficients are found using the procedure described by Werner *et al* [39]. One can rewrite Eqns. (3.11), (3.12) and (3.13) in matrix form as:

$$\hat{V}_0(R,r,\gamma) = \underline{p}_0^T . \underline{\underline{A}}(R) . \underline{s} \qquad ; \qquad \hat{V}_2(R,r,\gamma) = \underline{p}_2^T . \underline{\underline{B}}(R) . \underline{s}$$

where vectors $\underline{p}$ and $\underline{s}$ have the elements:

$$p_{0l} = P_l(\cos\gamma) \qquad p_{2l} = \left[\frac{(l-2)!}{(l+2)!}\right]^{\frac{1}{2}} P_l^2(\cos\gamma) \qquad s_n = (r-r_e)^{n-1} .$$

The matrices $\underline{\underline{A}}(R)$ and $\underline{\underline{B}}(R)$ can be expressed as:

$$\underline{\underline{A}}(R) = \underline{\underline{P}}_0^{T\,-1} . \underline{\underline{W}}(R) . \underline{\underline{S}}^{-1} \qquad ; \qquad \underline{\underline{B}}(R) = \underline{\underline{P}}_2^{T\,-1} . \underline{\underline{Z}}(R) . \underline{\underline{S}}^{-1} \tag{3.14}$$

where

$$P_{0\,lk} = P_l(\cos\gamma_k) \qquad P_{2\,lk} = \left[\frac{(l-2)!}{(l+2)!}\right]^{\frac{1}{2}} P_l^2(\cos\gamma_k) \qquad S_{nm} = (r_m - r_e)^{n-1}$$

and γ_k and r_m are angles and bond distances for which the potential has been calculated *ab initio*. At each γ_k and r_m the R-dependent potentials are fit independently, to the form

$$W_{ln}(R) = a_1^{ln}\exp(-a_2^{ln}R)(1 + a_3^{ln}R + a_4^{ln}R^2 + a_5^{ln}R^3) - \tanh(R)\left(\frac{a_6^{ln}}{R^4} + \frac{a_7^{ln}}{R^6} + \frac{a_8^{ln}}{R^8}\right) \qquad (3.15)$$

and

$$Z_{ln}(R) = a_1^{ln}\exp(-a_2^{ln}R)(1 + a_3^{ln}R + a_4^{ln}R^2 + a_5^{ln}R^3) \quad . \qquad (3.16)$$

The $\frac{(V_{A'} - V_{A''})}{2}$ is a purely repulsive potential and so $Z_{ln}(R)$ does not contain the last three terms of Eqn. (3.15).

3.3 The Potential Matrix Elements

3.3.1 Single-Surface Interaction Potential – Σ Treatment

The TRL potential is already expressed in a functional form (Eqn. (3.2)). However, in order to simplify the calculation of the potential energy matrix elements (more specifically, the integration over angles r') it is advantageous to fit it, too, as an expansion in Legendre polynomials, as in Eqn. (3.8). The coefficients of such an expansion, V_{l0}^{TRL}, are found by multiplying $V_{TRL}(R,r,\gamma)$ of Eqn. (3.2) by each of the Legendre polynomials of the expansion in turn and then integrating with respect to $\cos\gamma$, numerically, over all γ.

Thus, the potential matrix elements for the O_2^+ / Kr system treating the diatom as $^1\Sigma$, for both the semi-empirical potential surface of TRL and the *ab initio* $1^2A''$ potential surface of RDWS, can be expressed as:

$$\left\langle \chi_{v'j'}(r)\phi_{j'\Omega'}(r')\middle|\hat{V}(R,r,\gamma)\middle|\phi_{j''\Omega''}(r')\chi_{v''j''}(r)\right\rangle = \sum_l \int dr\, \chi^*_{v'j'}(r)\, V_{l0}(R,r)\chi_{v''j''}(r) \int dr'\, Y^*_{j'\Omega'}(r')P_l(\cos\gamma)Y_{j''\Omega''}(r')$$

$$= \left[\frac{(2j'+1)}{(2j''+1)}\right]^{1/2} \sum_l^{\infty} \int dr\, \chi^*_{v'j'}(r)\, V_{l0}(R,r)\chi_{v''j''}(r) \left\langle j'\ \Omega''\ l\ 0 \middle| j''\ \Omega''\right\rangle \left\langle j'\ 0\ l\ 0 \middle| j''\ 0\right\rangle$$

in terms of Clebsch-Gordan coefficients, which, using 3-j symbols, is equivalent to:

$$(2j'+1)^{1/2}(2j''+1)^{1/2}(-1)^{\Omega''} \sum_l^{\infty} \int dr\, \chi^*_{v'j'}(r)\, V_{l0}(R,r)\chi_{v''j''}(r) \begin{pmatrix} j' & l & j'' \\ \Omega'' & 0 & -\Omega'' \end{pmatrix} \begin{pmatrix} j' & l & j'' \\ 0 & 0 & 0 \end{pmatrix}.$$

This expression reveals a selection rule for the transition in the scattering of a homonuclear diatom, such as O_2^+. The second of these 3-j symbols, due to the requirement that:

$$\begin{pmatrix} j_1 & j_2 & j_3 \\ m_1 & m_2 & m_3 \end{pmatrix} = (-1)^{j_1+j_2+j_3} \begin{pmatrix} j_1 & j_2 & j_3 \\ -m_1 & -m_2 & -m_3 \end{pmatrix},$$

means that $j'+l+j''$ must be an even number. Thus, since for a homonuclear diatomic l will be even, j'' and j' must be either both even or both odd. There will be no coupling between even and odd states and so, if the initial state of the diatom has j even, only

states of even j' need be included in the basis and, for odd initial j, only states of odd j' need be included.

3.3.2 *Two-Surface* Ab Initio *Interaction Potential – Π Treatment*

The potential matrix elements for the treatment of the diatom as $^1\Pi$, using the combination of the ab initio $1^2A''$ and $1^2A'$ potentials of RDWS, can be expressed as:

$$\left\langle v'' j'' \Omega'' \varepsilon'' \middle| \hat{V} \middle| v' j' \Omega'' \varepsilon' \right\rangle = \left(\frac{(2j''+1)^{1/2}(2j'+1)^{1/2}}{16\pi^2} \right) \times$$
$$\left\langle \chi_{v''j''}(r) \left(D^{j''}_{\Omega'' 1}(r') \middle| \Lambda \right\rangle + \varepsilon'' D^{j''}_{\Omega'' -1}(r') \middle| -\Lambda \right\rangle \Big| \hat{V} \Big| \chi_{v'j'}(r) \left(D^{j'}_{\Omega'' 1}(r') \middle| \Lambda \right\rangle + \varepsilon' D^{j'}_{\Omega'' -1}(r') \middle| -\Lambda \right\rangle \Big) \Big\rangle$$

which upon substitution of Eqn. (3.6) becomes:

$$\frac{(2j''+1)^{1/2}(2j'+1)^{1/2}}{16\pi^2} \Bigg\{ \sum_{l}^{\infty} \int \chi^*_{v''j''} V_{l0} \chi_{v'j'} dr \left[\int dr' (-1)^{\Omega''-1} D^{j''}_{-\Omega''-1} D^{l}_{00} D^{j'}_{\Omega'' 1} + \varepsilon'' \varepsilon' (-1)^{\Omega''+1} D^{j''}_{-\Omega'' 1} D^{l}_{00} D^{j'}_{\Omega'' -1} \right]$$
$$+ \sum_{l=2}^{\infty} \int \chi^*_{v''j''} V_{l2} \chi_{v'j'} dr \left[\int dr' \varepsilon' (-1)^{\Omega''-1} D^{j''}_{-\Omega''-1} D^{l}_{0\,2} D^{j'}_{\Omega''-1} + \varepsilon'' (-1)^{\Omega''+1} D^{j''}_{-\Omega'' 1} D^{l}_{0\,-2} D^{j'}_{\Omega'' 1} \right] \Bigg\} . \quad (3.17)$$

This has made use of the relationship:

$$D^{j''*}_{\Omega'' \Lambda'} = (-1)^{\Omega'-\Lambda'} D^{j''}_{-\Omega''-\Lambda'} \quad .$$

Converting the integrals into Wigner 3-j symbols, Eqn. (3.17) becomes:

$$= \frac{(2j''+1)^{1/2}(2j'+1)^{1/2}}{2} (-1)^{\Omega''+1} \quad \times$$
$$\Bigg\{ \sum_{l}^{\infty} \int \chi^*_{v''j''}(r) V_{l0}(R,r) \chi_{v'j'}(r) dr \begin{pmatrix} j' & l & j'' \\ \Omega'' & 0 & -\Omega'' \end{pmatrix} \left[\begin{pmatrix} j' & l & j'' \\ 1 & 0 & -1 \end{pmatrix} + \varepsilon'' \varepsilon' (-1)^{j'+j''+l} \begin{pmatrix} j' & l & j'' \\ 1 & 0 & -1 \end{pmatrix} \right]$$
$$+ \sum_{l=2}^{\infty} \int \chi^*_{v''j''}(r) V_{l2}(R,r) \chi_{v'j'}(r) dr \begin{pmatrix} j' & l & j'' \\ \Omega'' & 0 & -\Omega'' \end{pmatrix} \left[\varepsilon' \begin{pmatrix} j' & l & j'' \\ -1 & 2 & -1 \end{pmatrix} + \varepsilon'' (-1)^{j'+j''+l} \begin{pmatrix} j' & l & j'' \\ -1 & 2 & -1 \end{pmatrix} \right] \Bigg\}$$

$$= (2j''+1)^{1/2}(2j'+1)^{1/2}\sum_{l}(-1)^{\Omega''+1}\left(\frac{1+\varepsilon''\varepsilon'(-1)^{j'+j''+l}}{2}\right)\begin{pmatrix} j' & l & j'' \\ \Omega'' & 0 & -\Omega'' \end{pmatrix}$$
$$\left[\begin{pmatrix} j' & l & j'' \\ 1 & 0 & -1 \end{pmatrix}\int\chi^{*}_{v''j''}(r)V_{l0}(R,r)\chi_{v'j'}(r)dr + \varepsilon'\begin{pmatrix} j' & l & j'' \\ -1 & 2 & -1 \end{pmatrix}\int\chi^{*}_{v''j''}(r)V_{l2}(R,r)\chi_{v'j'}(r)dr\right] \quad (3.18)$$

which has used the property of the 3-j symbols:

$$\begin{pmatrix} j_1 & j_2 & j_3 \\ m_1 & m_2 & m_3 \end{pmatrix} = (-1)^{j_1+j_2+j_3}\begin{pmatrix} j_1 & j_2 & j_3 \\ -m_1 & -m_2 & -m_3 \end{pmatrix} \quad .$$

This is exactly equivalent to the result given by Klar using Clebsch-Gordan coefficients [32].

Here too, the expression for the potential matrix elements reveals a selection rule for the Π treatment of a homonuclear diatomic such as O_2^+, since Eqn. (3.18) will only be non-zero for

$$\varepsilon''\varepsilon'(-1)^{j'+j''+l} = +1$$

and, if the diatom is homonuclear, l will be an even number. Thus, since the parity of the molecular wavefunctions is determined by [38]

$$p = \varepsilon(-1)^{j},$$

only basis functions with the same parity are coupled.

3.4 Discrete Variable Representation

The $\chi_{vj}(r)$ basis functions of the partial wave expansion, which must be evaluated in order to calculate the potential energy matrix of Eqn. (2.23), are the rovibrational wavefunctions of the diatomic molecule, satisfying the diatomic Schrödinger equation:

$$\hat{H}_{diatom}\chi_{vj}(r)=\left[-\frac{1}{2\mu}\frac{d^2}{dr^2}-\frac{j(j+1)}{2\mu r^2}+\hat{V}_{diatom}(r)\right]\chi_{vj}(r)=\epsilon_{vj}^{diatom}\chi_{vj}(r) \qquad (3.19)$$

where μ is the reduced mass of the diatom.

The diatomic potential energy surface of Eqn. (3.19) has been described using the functional form of Huxley and Murrell [40]:

$$\hat{V}_{diatom}(r)=D_e\left[1-\left(1+c_1(r-r_e)+c_2(r-r_e)^2+c_3(r-r_e)^3\right)\times\exp(-c_1(r-r_e))\right] \qquad (3.20)$$

where D_e and c_i are calculated in terms of the spectroscopic constants and r_e is the equilibrium bond-length of the diatom.

The parameters used in Eqn. (3.20) are:-

$$r_e=2.11\ a_0 \quad ; \quad c_1=2.5716\ a_0^{-1}$$
$$c_2=1.1022\ a_0^{-2} \quad ; \quad c_3=0.4846\ a_0^{-3}$$
$$D_e=0.249145\ hartree$$

and were found using the formulation described by Huxley and Murrell [40].

The diatomic Schrödinger equation is solved through the method of potential-optimised discrete variable representation (PO-DVR) [41 – 43]. This process involves choosing a primitive orthonormal one-dimensional basis set

$$\{h_n(r)\ ,\ n=1,\ 2,\ .....,\ N_b\ \} \qquad (3.21)$$

from which one obtains the corresponding DVR basis functions

$$|r_k\rangle=\sum_{n=1}^{N_b}M_{nk}h_n(r) \qquad . \qquad (3.22)$$

$\underline{\underline{M}}$ is the matrix which diagonalises the coordinate matrix $\underline{\underline{\hat{r}}}$ that represents the coordinate operator $\hat{r}$ in the representation defined by (3.21). Hence $|r_k\rangle$ is the eigenfunction corresponding to the eigenvalue, r_k, of the $\hat{r}$ operator and is localised around that eigenvalue.

In order to obtain functions that have some information about the potential energy surface, the one-dimensional basis set of (3.21) is chosen by means of the numerical solution of a one-dimensional reference Schrödinger equation:

$$\hat{H}_{ref}\, h_l(r) = \left[-\frac{1}{2\mu}\frac{d^2}{dr^2} + \hat{V}_{diat} \right] h_l(r) = \varepsilon_l\, h_l(r) \qquad (3.23)$$

i.e. where the rotational quantum number has been taken to be zero. The eigenvalues, ε_l, can be taken as a first approximation to be $(v+\frac{1}{2})\hbar\omega$, as for an harmonic oscillator, and are then refined, through a numerical algorithm, to give the actual eigenvectors and eigenvalues.

The h_l functions are then used to obtain potential-optimised DVR localised functions:

$$\left|r_\lambda^{PO}\right\rangle = \sum_{l=1}^{N_b} M_{l\lambda}\, h_l(r) \qquad . \qquad (3.24)$$

The coefficients, $M_{l\lambda}$, are determined by the following method:

$$\left\langle h_{l'}(r)\middle|\hat{r}\middle|r_\lambda^{PO}(r)\right\rangle = \left\langle h_{l'}(r)\middle|r_\lambda\middle|r_\lambda^{PO}\right\rangle$$

$$\sum_l M_{l\lambda}\left\langle h_{l'}(r)\middle|\hat{r}\middle|h_l(r)\right\rangle = r_\lambda \sum_l M_{l\lambda}\delta_{l'l}$$

This is an eigenfunction equation, expressed in matrix form as:

$$\underline{\underline{\hat{r}}}\,\underline{\underline{M}} = \underline{\underline{M}}\,\underline{\underline{r}} \qquad (3.25)$$

and this can be solved to give values of the coefficients, $M_{l\lambda}$, and the eigenvalues of the $|r_\lambda\rangle$ functions, r_λ.

Since the $|r_\lambda\rangle$ functions are localised around their eigenvalues, r_λ, and are orthogonal, any arbitrary coordinate operator matrix involving them can be considered to be practically diagonal:

$$\langle r_n|F(r)|r_m\rangle \approx F(r_m)\langle r_n|r_m\rangle = F(r_m)\delta_{nm} \quad .$$

Hence, the intergration over r on the right-hand side of Eqn. (2.23) is made very easy if the rovibrational part of the wavefunction, $\chi_{vj}(r)$, is expressed as a linear combination of the PO-DVR basis set:

$$|\chi_{vj}(r)\rangle = \sum_\lambda T_{vj\lambda}|r_\lambda^{PO}(r)\rangle$$

for then

$$\langle\chi_{v'j'}(r)|\hat{V}(R,r,\gamma)|\chi_{v''j''}(r)\rangle = \sum_\lambda V(R,r_\lambda,\gamma)T_{v'j'\lambda}T_{v''j''\lambda} \quad . \tag{3.26}$$

The coefficients, $T_{vj\lambda}$, are determined by a similar method to that used for $M_{l\lambda}$:

$$\langle r_{\lambda'}^{PO}|\hat{H}_{diatom}|\chi_{vj}(r)\rangle = \langle r_{\lambda'}^{PO}|\in_{vj}^{diatom}|\chi_{vj}(r)\rangle$$

$$\sum_\lambda T_{vj\lambda}\langle r_{\lambda'}^{PO}|\hat{H}_{diatom}|r_\lambda^{PO}\rangle = \left(\sum_\lambda T_{vj\lambda}\langle r_{\lambda'}^{PO}|\hat{H}_{vib}|r_\lambda^{PO}\rangle\right) + T_{vj\lambda'}\frac{j(j+1)}{2mr_\lambda^2}\delta_{\lambda'\lambda}$$

$$= \left(\sum_\lambda T_{vj\lambda}\sum_{l'l} M_{l'\lambda'}M_{l\lambda}\langle h_{l'}|\hat{H}_{vib}|h_l\rangle\right) + T_{vj\lambda'}\frac{j(j+1)}{2mr_\lambda^2}\delta_{\lambda'\lambda} = \in_{vj}^{diatom}\sum_\lambda T_{vj\lambda}\delta_{\lambda'\lambda} \,. \tag{3.27}$$

Since $\hat{H}_{vib}$ is the reference Hamiltonian of Eqn. (3.23) from which the $|h_l\rangle$ functions were derived,

$$\langle h_{l'}|\hat{H}_{vib}|h_l\rangle = \varepsilon_l\delta_{l'l} \quad .$$

Equation (3.27) is an eigenfunction equation, expressed in matrix form as:

$$(\underline{\underline{\tilde{M}}}\,\underline{\underline{M}}\,\underline{\underline{H}}_{vib} + \underline{\underline{H}}_{rot})\underline{\underline{T}} = \underline{\underline{T}}\,\underline{\underline{\in}}_{diatom}$$

and can be solved to give values of the coefficients, $T_{vj\lambda}$, and the energy levels of the diatomic molecule, $\in_{vj}^{diatom}$.

The application of the PO-DVR method therefore results in an expression for the rovibrational terms in the potential energy matrix, χ_{vj}, and the energy levels of the diatomic molecule, ϵ_{vj}^{diatom}, both of which are required for the solution of the close-coupled equations (2.23).

4 Propagation of the Wavefunction

4.1 Introduction

As mentioned at the start of Chapter 2, the method by which the rate constants of the inelastic scattering are calculated is through the evaluation of the probability of the O_2^+ diatom being found in the scattered internal quantum state, after having undergone quenching through collision with a Kr atom from a given initial internal state. This is achieved through the solution of the set of coupled Schrödinger equations:

$$\left[\frac{d^2}{dR^2}+k_{v''j''}^2-\frac{\left[J(J+1)-2\Omega''^2+j''(j''+1)\right]}{R^2}\right]f_{v''j''\Omega''}^{Jvj\Omega}(R)=\frac{2\mu}{\hbar^2}\sum_{v'j'}\left\langle\phi_{v''j''\Omega''}\chi_{v''j''}\left|\hat{V}\right|\phi_{v'j'\Omega''}\chi_{v'j'}\right\rangle f_{v'j'\Omega''}^{Jvj\Omega}(R) \tag{4.1}$$

with the potential energy matrix elements on the right-hand side taking the form discussed in the previous chapter.

There is a separate set of these coupled equations for each initial internal state of the diatom, so the coupled equations can be expressed in matrix form as:

$$\left[\frac{d^2}{dR^2}+k_{v''j''}^2-\frac{\left[J(J+1)-2\Omega''^2+j''(j''+1)\right]}{R^2}\right]\underline{\underline{F}}=\underline{\underline{\hat{V}}}\,\underline{\underline{F}}$$

with $\underline{\underline{\hat{V}}}$ having matrix elements $\hat{V}_{ij}=\frac{2\mu}{\hbar^2}\langle\phi_i\chi_i|\hat{V}|\phi_j\chi_j\rangle$ and with each column of $\underline{\underline{F}}$ containing the R-dependent components of the wavefunction expansion for a given initial state of the diatom.

At the asymptotic limit (i.e. at the surface of the sphere of the region of interaction), where the observables of the system are measured, the interaction potential energy can be considered to be universally zero and consequently the form of the matrix $\underline{\underline{F}}$ at that point can be written in terms of spherical waves such that

$$\underline{\underline{F}}(R)\xrightarrow[R\to\infty]{}\underline{\underline{c}}\left(\underline{\underline{I}}-\underline{\underline{O}}\,\underline{\underline{S}}\right) \tag{4.2}$$

where $\underline{\underline{I}}$ is a diagonal matrix of incoming waves of momentum $-k_{v_j}\hbar$, with elements:

$$I_{nn} = \exp\left(-i\left(k_n R - \frac{(J+j)\pi}{2}\right)\right) \qquad (4.3)$$

and $\underline{\underline{O}}$ is a diagonal matrix of outgoing waves of momentum $k_{v_j}\hbar$, with elements:

$$O_{nn} = \exp\left(i\left(k_n R - \frac{(J+j)\pi}{2}\right)\right) \qquad (4.4)$$

where n labels internal diatomic state (v, j) and $k_n^2 = \frac{2\mu}{\hbar^2}\left(E - \epsilon_n^{diatom}\right)$. $\underline{\underline{c}}$ is a constant matrix.

The S-matrix of Eqn. (4.2) is the 'scattering matrix' and it is this which contains the information about the probabilities of the transitions which occur due to the scattering reaction. Each column of the S-matrix consists of the coefficients of the partial wave expansion over internal states for a given initial internal state of the diatom. The square of each element in a column, therefore, gives the probability of the state of the diatom measured, after excitation (or relaxation) from the initial state of that column, being the particular internal state for which that element is the coefficient.

The formal definition of the scattering matrix is as follows [44]:

If $\psi_j(\underline{s})$ are the eigenfunctions of the internal Hamiltonians of a system in collision, then the internal state of the system before or after the collision can be written as:

$$\psi(\underline{s}) = \sum_j a_j \psi_j(\underline{s})$$

where:

$|a_j|^2$ = probability of finding system in state $\psi_j(\underline{s})$.

If the a_j coefficients are written as a column vector, $\underline{A}$, then the scattering matrix is defined as:

$$\underline{A}_f = \underline{\underline{S}}\,\underline{A}_i$$

where $\underline{A}_i, \underline{A}_f$ are for the initial and final states of the colliding molecules in the asymptotic region. The probability of a transition from state i to state j is then given by

$$P_{ij}=|S_{ij}|^2 \quad .$$

Since,

$$\sum_j |a_j|^2 = 1,$$

it follows that:

$$\underline{A}_f^{*T}\,\underline{A}_f = \underline{A}_i^{*T}\,\underline{\underline{S}}^{*T}\,\underline{\underline{S}}\,\underline{A}_i = \mathrm{I}$$
$$\underline{\underline{S}}^{*T}\,\underline{\underline{S}} = \mathrm{I}$$

where I is the identity matrix, and so the S-matrix must be unitary.

The matrix $\underline{\underline{c}}$ of Eqn. (4.2) is set so that the outward flux density for the scattering reaction is $|S_{nn}|^2 - 1$ in the entrance channel, and $|S_{nm}|^2$ in the other channels, ensuring that the total flux remains constant. The flux density function is defined by:

$$\underline{j} = \frac{-i\hbar}{2\mu}\left(\Psi^* \underline{\nabla}\Psi - \Psi \underline{\nabla}\Psi^*\right)$$

and this results in the asymptotic form of the translational wavefunction being written as:

$$\underline{\underline{F}}(R) \xrightarrow[R\to\infty]{} \left(\underline{\underline{k}}^{-½}\,\underline{\underline{I}} - \underline{\underline{k}}^{-½}\,\underline{\underline{O}}\,\underline{\underline{S}}\right)$$

with $\underline{\underline{k}}$ being the diagonal matrix of elements k_n, where:

$$k_n^2 = \frac{2\mu}{\hbar^2}\left(E - \epsilon_n^{diatom}\right)$$

and n labels internal diatomic state (v, j).

In order to obtain the S-matrix at the asymptotic limit, it is necessary to solve the coupled equations to calculate the functions $f(R)$ and apply boundary conditions, which, at the asymptotic limit, are the boundary conditions defined by Eqn. (4.2). However, since the potential matrix in Eqns. (4.1) is, firstly, not diagonal and secondly, a function of R, the solution of these equations is not a simple task. Even if the matrix could be diagonalised, which itself would not be easy since each element is a function rather than a constant, the resulting matrix would still be a function of R, making any solution very hard to compute.

One way around this problem is to divide the interaction space with respect to R into a set of discrete sectors. If the sectors are small enough, the potential in each sector could then be considered to be constant with respect to R, which would greatly facilitate the diagonalisation of the potential matrix in each sector. The coupled equations would then become uncoupled and, in addition, the potential matrix would no longer be a function of R within each sector, making the subsequent solution of the equations within each sector a trivial matter. The wavefunctions $f(R)$ are thus calculated initially in a sector where the form of the wavefunction is known and then propagated out to 'infinite' distance, where the boundary conditions of Eqn. (4.2) can be applied to yield the asymptotic S-matrix.

The method of propagation used in this research is the R-matrix propagation theory. This method has long been of use in the theory of nuclear reactions and for about twenty years in the theory of non-reactive, inelastic scattering, the latter having been developed by Stechel, Walker & Light [45].

One of the major advantages of the R-matrix method is that it ensures that the final S-matrix produced at the end of the propagation meets the necessary requirement that it be a unitary matrix. For, rather than finding the S-matrix directly, it is easier to guarantee this condition by finding a real symmetric matrix which is related to the S-matrix as:

$$\underline{\underline{S}} = \left(\mathrm{I} - i\underline{\underline{R}}\right)^{-1}\left(\mathrm{I} + i\underline{\underline{R}}\right) \quad ,$$

for then the S-matrix will be unitary by definition.

The R-matrix is defined as the inverse log-derivative of the wavefunction, namely

$$\underline{\underline{R}}^{-1} = \left[\frac{d\underline{\underline{\Psi}}}{dR}\right]\left[\underline{\underline{\Psi}}\right]^{-1} \qquad (4.5)$$

At the asymptotic limit, therefore, where

$$\underline{\underline{\Psi}} = \underline{\underline{c}}\left(\underline{\underline{I}} - \underline{\underline{O}}\,\underline{\underline{S}}\right),$$

with $\underline{\underline{I}}$ and $\underline{\underline{O}}$ defined by Eqns. (4.3) and (4.4) respectively, we find that

$$\underline{\underline{R}} = \underline{\underline{c}}\left(\underline{\underline{I}} - \underline{\underline{O}}\,\underline{\underline{S}}\right)\left[-i\underline{\underline{k}}\left(\underline{\underline{I}} + \underline{\underline{O}}\,\underline{\underline{S}}\right)\right]^{-1}\underline{\underline{c}}^{-1}$$

where $\underline{\underline{k}}$ is a diagonal matrix of the k_{vj} terms. This rearranges to

$$\underline{\underline{S}} = \underline{\underline{c}}^{-1}\,\underline{\underline{I}}\left(\mathrm{I} - i\underline{\underline{R}}\,\underline{\underline{k}}\right)^{-1}\left(\mathrm{I} + i\underline{\underline{R}}\,\underline{\underline{k}}\right)\underline{\underline{I}}\,\underline{\underline{c}} \qquad (4.6)$$

as desired. Thus, as long as it can be assured that the final R-matrix is real symmetric, the final S-matrix will be unitary.

The final R-matrix can be considered as describing the effect of the interaction region on the external region and Eqn. (4.5) can be written as

$$F_R(i) = \underline{\underline{R}}\,F'_R(i) \qquad (4.7)$$

where $F_R(i)$ is the value of the function at the outer surface of the interaction region. Since we are only interested in the asymptotic value of the S-matrix, it is only necessary to propagate the R-matrix, not the whole wavefunction, and then calculate from it the S-matrix at the asymptotic limit, where the boundary conditions are applied.

The next section describes the method of propagation of the R-matrix through the interaction space, based largely on the treatment of Stechel, Walker & Light [45]. The subsequent section shows the application of the method to the system under consideration – the inelastic scattering of a diatom with an atom – and the solution of the coupled equations (4.1).

4.2 Propagation of the R-Matrix

Consider a set of coupled, second order differential equations of the form

$$\frac{d^2}{d\rho^2} g_n(\rho) = \sum_{n'} \langle \phi_n(x) | W(\rho) | \phi_{n'}(x) \rangle g_{n'}(\rho) = \sum_{n'} W_{nn'}(\rho) g_{n'}(\rho) \qquad (4.8)$$

obtained from the expansion:

$$\Psi(\rho, x) = \sum_{n'} \phi_{n'}(x)\, g_{n'}(\rho) \quad .$$

If the coordinate space is split up into discrete sectors such that, within each sector, i, $\underline{\underline{W}}$ is assumed to be independent of ρ, then a transformation could be made such that:

$$\psi_n^{(i)}(x) = \sum_{n'} \phi_{n'}(x) T_{n'n}^{(i)}$$

which would diagonalise the matrix $\underline{\underline{W}}$, where $\underline{\underline{T}}^{(i)}$ will also be independent of ρ. Thus, if $\underline{\underline{T}}^{(i)}$ is the transformation matrix for sector i, which is made up of the orthonormal eigenvectors of $\underline{\underline{W}}(\rho_i)$, and $\overline{\underline{\underline{T}}}^{(i)}$ is its transpose and inverse, then:

$$\overline{\underline{\underline{T}}}^{(i)}\, \underline{\underline{W}}(\rho_i)\, \underline{\underline{T}}^{(i)} = -\underline{\underline{\lambda^2}}^{(i)} \quad , \qquad (4.9)$$

where $\underline{\underline{\lambda^2}}$ is the diagonal matrix of eigenvalues, λ^2. This transformation is achieved by saying:

$$\Psi(\rho, x) = \underline{\phi}_n(x)\, \underline{\underline{T}}^{(i)}\, \overline{\underline{\underline{T}}}^{(i)}\, \underline{g}_n(\rho)$$

$$= \underline{\psi}^{(i)}(x)\, \underline{F}^{(i)}(\rho) \quad .$$

Thus, Eqns. (4.8) becomes:

$$\frac{d^2}{d\rho^2} F_n^{(i)}(\rho) = -\lambda_n^{2(i)} F_n^{(i)}(\rho) \quad . \qquad (4.10)$$

This is a second order, ordinary differential equation with two linearly independent solutions for each sector, denoted by F_1 and F_2. Thus it is possible, without loss of generality to write

$$F_n = \alpha F_1^n + \beta F_2^n$$

which implies that

$$F_n' = \alpha F_1'^n + \beta F_2'^n \quad .$$

We now define the sector R-matrix for boundaries $\rho = a$ and $\rho = b$ (for $a < b$) using the definition of the R-matrix (Eqn. (4.7)) :-

$$\begin{pmatrix} F_n(a) \\ F_n(b) \end{pmatrix} = \begin{pmatrix} (\underline{\underline{r}}_1)_{nn} & (\underline{\underline{r}}_2)_{nn} \\ (\underline{\underline{r}}_3)_{nn} & (\underline{\underline{r}}_4)_{nn} \end{pmatrix} \begin{pmatrix} -F_n'(a) \\ F_n'(b) \end{pmatrix}.$$

Substituting in the definitions of F_n and F_n', we find

$$\begin{pmatrix} \alpha F_1^n(a) + \beta F_2^n(a) \\ \alpha F_1^n(b) + \beta F_2^n(b) \end{pmatrix} = \begin{pmatrix} -(\underline{\underline{r}}_1)_{nn}(\alpha F_1'^n(a) + \beta F_2'^n(a)) & + & (\underline{\underline{r}}_2)_{nn}(\alpha F_1'^n(b) + \beta F_2'^n(b)) \\ -(\underline{\underline{r}}_3)_{nn}(\alpha F_1'^n(a) + \beta F_2'^n(a)) & + & (\underline{\underline{r}}_4)_{nn}(\alpha F_1'^n(b) + \beta F_2'^n(b)) \end{pmatrix}$$

from which we can conclude that:

$$\begin{aligned} F_1^n(a) &= -(\underline{\underline{r}}_1)_{nn} F_1'^n(a) + (\underline{\underline{r}}_2)_{nn} F_1'^n(b) \\ F_2^n(a) &= -(\underline{\underline{r}}_1)_{nn} F_2'^n(a) + (\underline{\underline{r}}_2)_{nn} F_2'^n(b) \\ F_1^n(b) &= -(\underline{\underline{r}}_3)_{nn} F_1'^n(a) + (\underline{\underline{r}}_4)_{nn} F_1'^n(b) \\ F_2^n(b) &= -(\underline{\underline{r}}_3)_{nn} F_2'^n(a) + (\underline{\underline{r}}_4)_{nn} F_2'^n(b) \quad . \end{aligned} \qquad (4.11)$$

Now, the solutions to the original differential equation (4.10) are of the forms

$$F_1^n = \exp(i\lambda_n \rho); \qquad F_2^n = \exp(-i\lambda_n \rho) \quad .$$

Substituting into Eqn. (4.11) gives:

$$\begin{aligned} e^{i\lambda_n a} &= -(\underline{\underline{r}}_1)_{nn} i\lambda_n e^{i\lambda_n a} + (\underline{\underline{r}}_2)_{nn} i\lambda_n e^{i\lambda_n b} \\ e^{-i\lambda_n a} &= (\underline{\underline{r}}_1)_{nn} i\lambda_n e^{-i\lambda_n a} - (\underline{\underline{r}}_2)_{nn} i\lambda_n e^{-i\lambda_n b} \\ e^{i\lambda_n b} &= -(\underline{\underline{r}}_3)_{nn} i\lambda_n e^{i\lambda_n a} + (\underline{\underline{r}}_4)_{nn} i\lambda_n e^{i\lambda_n b} \\ e^{-i\lambda_n b} &= (\underline{\underline{r}}_3)_{nn} i\lambda_n e^{-i\lambda_n a} - (\underline{\underline{r}}_4)_{nn} i\lambda_n e^{-i\lambda_n b} \quad . \end{aligned}$$

If we now introduce h, the sector width $(b - a)$, then, by multiplying each of the above equations by one of the functions

$$\exp(i\lambda_n a); \qquad \exp(-i\lambda_n a); \qquad \exp(i\lambda_n b); \qquad \exp(-i\lambda_n b)$$

and solving simultaneously, we find that the diagonal matrices may be written:

$$(\underline{\underline{r}}_1^{(i)})_{lm} = (\underline{\underline{r}}_4^{(i)})_{lm} = \delta_{lm} \begin{cases} \left|\lambda_m^{(i)}\right|^{-1} \coth\left|h\lambda_m^{(i)}\right| & \lambda_m^{(i)2} \le 0 \\ -\left|\lambda_m^{(i)}\right|^{-1} \cot\left|h\lambda_m^{(i)}\right| & \lambda_m^{(i)2} > 0 \end{cases}$$

$$(\underline{\underline{r}}_2^{(i)})_{lm} = (\underline{\underline{r}}_3^{(i)})_{lm} = \delta_{lm} \begin{cases} \left|\lambda_m^{(i)}\right|^{-1} \operatorname{csch}\left|h\lambda_m^{(i)}\right| & \lambda_m^{(i)2} \le 0 \\ -\left|\lambda_m^{(i)}\right|^{-1} \csc\left|h\lambda_m^{(i)}\right| & \lambda_m^{(i)2} > 0 \end{cases} .$$

The next step is to calculate the new global R-matrix, $\underline{\underline{R}}^{(i)}$, from the sector R-matrix, $\underline{\underline{r}}^{(i)}$, and the old global R-matrix, $\underline{\underline{R}}^{(i-1)}$. The sector R-matrix carries information about both surfaces of the sector, whilst the global R-matrix retains information about only a single surface (the outer one). Thus, whereas the sector R-matrix will be of dimension $(2N \times 2N)$, the global R-matrix will have dimension $(N \times N)$.

From Eqn. (4.7) we see that

$$\underline{F}_R^{(i)} = \underline{\underline{R}}^{(i)} \underline{F'}_R^{(i)} \tag{4.12}$$

and

$$\underline{F}_R^{(i-1)} = \underline{\underline{R}}^{(i-1)} \underline{F'}_R^{(i-1)} \tag{4.13}$$

where $\underline{F}_R$ and $\underline{F}_L$ are defined at the surfaces of each sector, R labelling the outer (right-hand side) surface and L labelling the inner (left-hand side) surface.

However, at the boundaries between sector i and sector $(i - 1)$, the values of g_n and g_n' must be continuous. Hence,

$$\underline{\underline{T}}^{(i-1)} \underline{F}_R^{(i-1)} = \underline{\underline{T}}^{(i)} \underline{F}_L^{(i)}$$

$$\underline{F}_R^{(i-1)} = \underline{\underline{Q}}(i-1, i) \underline{F}_L^{(i)}$$

and $$\underline{F'}_R^{(i-1)} = \underline{\underline{Q}}(i-1,i)\underline{F'}_L^{(i)}$$

where the matrix $\underline{\underline{Q}}$ represents the overlap between the eigenvector bases in adjacent sectors and is given by

$$\underline{\underline{Q}}(i-1,i) = \underline{\underline{\overline{T}}}^{(i-1)}\underline{\underline{T}}^{(i)}.$$

Hence,

$$\begin{aligned}\underline{F}_L^{(i)} &= \underline{\underline{\overline{Q}}}(i-1,i)\underline{F}_R^{(i-1)} = \underline{\underline{\overline{Q}}}(i-1,i)\underline{\underline{R}}^{(i-1)}\underline{F'}_R^{(i-1)} \\ &= \underline{\underline{\overline{Q}}}(i-1,i)\underline{\underline{R}}^{(i-1)}\underline{\underline{Q}}(i-1,i)\underline{F'}_L^{(i)} \quad .\end{aligned} \tag{4.14}$$

From Eqn. (4.11) we know that

$$\underline{F}_L^{(i)} = -\underline{\underline{r}}_1^{(i)}\underline{F'}_L^{(i)} + \underline{\underline{r}}_2^{(i)}\underline{F'}_R^{(i)} \quad . \tag{4.15}$$

Comparing Eqn. (4.14) and Eqn. (4.15) we find that

$$\begin{aligned}\underline{F'}_L^{(i)} &= \left[\underline{\underline{r}}_1^{(i)} + \underline{\underline{\overline{Q}}}(i-1,i)\underline{\underline{R}}^{(i-1)}\underline{\underline{Q}}(i-1,i)\right]^{-1}\underline{\underline{r}}_2^{(i)}\underline{F'}_R^{(i)} \\ &= \underline{\underline{Z}}^{(i)}\underline{\underline{r}}_2^{(i)}\underline{F'}_R^{(i)}\end{aligned}$$

where

$$\underline{\underline{Z}}^{(i)} = \left[\underline{\underline{r}}_1^{(i)} + \underline{\underline{\overline{Q}}}(i-1,i)\underline{\underline{R}}^{(i-1)}\underline{\underline{Q}}(i-1,i)\right]^{-1} \quad . \tag{4.16}$$

Now, Eqn. (4.11) also gives us that

$$\begin{aligned}\underline{F}_R^{(i)} &= -\underline{\underline{r}}_3^{(i)}\underline{F'}_L^{(i)} + \underline{\underline{r}}_4^{(i)}\underline{F'}_R^{(i)} \\ &= \left[\underline{\underline{r}}_4^{(i)} - \underline{\underline{r}}_3^{(i)}\underline{\underline{Z}}^{(i)}\underline{\underline{r}}_2^{(i)}\right]\underline{F'}_R^{(i)}\end{aligned}$$

which, upon comparison with Eqn. (4.12), yields the relationship:

$$\underline{\underline{R}}^{(i)} = \underline{\underline{r}}_{4}^{(i)} - \underline{\underline{r}}_{3}^{(i)} \underline{\underline{Z}}^{(i)} \underline{\underline{r}}_{2}^{(i)} \quad . \qquad (4.17)$$

This equation furnishes us with a method of calculating the global R-matrix at the outer surface of a sector, given the sector R-matrix and the global R-matrix produced from the preceding sector, thus enabling propagation of the R-matrix.

This formulation preserves the symmetry of the R-matrix, which is necessary in order that the final S-matrix be unitary: if $\underline{\underline{R}}^{(i-1)}$ and $\underline{\underline{r}}^{(i)}$ are both symmetric, then $\underline{\underline{R}}^{(i)}$ is also symmetric. Since $\underline{\underline{r}}^{(i)}$ is diagonal and thus trivially symmetric, it follows that if the R-matrix for one sector is symmetric, the R-matrix in the next will be as well.

4.3 Application to Atom-Diatom Scattering

In the system under consideration, the coupled equations (Eqn. (4.1)), can be written as:

$$\frac{d^2 g_{v'j'}(R)}{dR^2} = \frac{2\mu}{\hbar^2}\left[\sum_{v''j''\varepsilon''}\langle v'j'\Omega''\varepsilon'|\hat{V}|v''j''\Omega''\varepsilon''\rangle g_{v''j''} + \left[\frac{\hbar^2}{2\mu}\left(\frac{J(J+1)-2\Omega''^2+j'(j'+1)}{R^2}\right)+\left(\in_{v'j'}-E\right)\right]g_{v'j'}\right] \tag{4.18}$$

which is of similar form to Eqn. (4.8). For each R-sector, this equation can be decoupled by diagonalisation of the matrix, $\underline{\underline{W}}$, consisting of the potential matrix elements (calculated using the value of R at the centre of the i^{th} sector) added to a diagonal matrix containing the values of

$$\frac{\hbar^2}{2\mu}\left(\frac{J(J+1)-2\Omega''^2+j'(j'+1)}{R^{(i)2}}\right)+\in_{v'j'} \quad ,$$

so that

$$\underline{\underline{T}}^{(i)}\underline{\underline{W}}(R^{(i)})\underline{\underline{T}}^{(i)} = \underline{\underline{e}}^{(i)}$$

where $e_l^{(i)}$, the elements of the diagonal matrix $\underline{\underline{e}}^{(i)}$, are the eigenvalues of the eigenvectors $T_l^{(i)}$.

Thus, Eqns. (4.18) become

$$\frac{d^2}{dR^2}F_l(R) = -\frac{2\mu}{\hbar^2}(E-e_l^{(i)})F_l(R) \quad .$$

Identifying $\frac{2\mu}{\hbar^2}(E-e_l^{(i)})$ as the $\lambda^{2(i)}$ term of Eqn. (4.10) allows the application of the R-matrix method as detailed in the previous section.

It remains only to define the R-matrix for sector 1, so that the propagation of Eqns. (4.16) and (4.17) can be carried out:

For a system with a large repulsive potential near the origin, the wavefunction in that area will follow the relationship:

$$g(R) \to 0 \text{ as } R \to 0$$

and so, since $(E - e_l^{(1)})$ will be negative, the wavefunction there can be written as:

$$\underline{F}(r) = \underline{\underline{A}}\,\underline{e}^{\lambda R}$$

and thus the initial R-matrix, $\underline{\underline{R}}^{(1)}$, would have elements:

$$R_{lk}^{(1)} = \delta_{lk} \left| \lambda^{(1)}{}_l \right|^{-1}.$$

The propagation is then carried out until the boundary of the global R-matrix lies in the asymptotic region of the scattering potential, at which point the asymptotic boundary conditions, as defined by Eqn. (4.6), are applied. At the asymptotic region, $e^{(\infty)} = \in_{v'j'}$, so that $\lambda^{(\infty)} = k$.

Thus, the S-matrix is given by

$$\underline{\underline{S}} = \underline{\underline{k}}^{1/2} \underline{\underline{W}}^{-1} \underline{\underline{W}}^{*} \underline{\underline{k}}^{-1/2} \qquad (4.19)$$

where

$$\underline{\underline{W}} = \underline{\underline{R}}^{fin} \underline{\underline{O}}' - \underline{\underline{O}}$$

with $\underline{\underline{R}}^{fin}$ being the global R-matrix determined in the last sector and:

$$O_{nq} = \delta_{nq} \exp(ik_n R^{\infty})$$
$$O'_{nq} = \delta_{nq}\, ik_n \exp(ik_n R^{\infty}) \ .$$

The matrices

$$k_{nq}^{-1/2} = \delta_{nq} \left| k_n \right|^{-1/2}$$
$$k_{nq}^{1/2} = \delta_{nq} \left| k_n \right|^{1/2}$$

are included in Eqn. (4.19) in order to conserve the flux of each channel, as discussed above.

5 Total Cross Sections and Rate Constants

For a given initial internal state of the diatom, the asymptotic radial wavefunction for the system will be:

$$\Psi_j(R_\infty) = A\left(\delta_{ij}\, k_j^{-\frac{1}{2}} e^{-ik_i R} - \sum_i k_i^{-\frac{1}{2}} S_{ij}\, e^{ik_i R} \right) \quad .$$

The total cross sections for a transition from a given initial vibrational and rotational state (and, for the Π treatment, for a given initial value of ε) to another vibrational state will therefore be [30]:

$$\sigma(v' \leftarrow v\, j(\varepsilon)) = \frac{\pi}{k_{vj}^2 (2j+1)} \sum_{j'} \sum_{J} \sum_{\Omega} (2J+1) \left| S^{J\Omega}_{v'j' \leftarrow vj(\varepsilon)} \right|^2 \quad . \qquad (5.1)$$

Here, the $(2j+1)$ term is included to account for the rotational degeneracy of the entrance channel and the $(2J+1)$ is from Eqn. (2.16).

It should be noted that, the higher the initial rotational state, the greater the number of Ω terms there will be in the partial wave expansion and that the S-matrix propagation must be repeated for each value of Ω, as well as J.

The total cross sections are calculated over a range of collision energies and the rate constants for transitions from a given initial rotational and vibrational state are then calculated, as a function of temperature, by averaging the cross sections over the Maxwell-Boltzmann distribution, using the equation:

$$k^{j(\varepsilon)}(v' \leftarrow v\, j(\varepsilon)) = \left(\frac{8}{\pi\mu} \right)^{\frac{1}{2}} (k_B T)^{-\frac{1}{2}} \int_0^\infty \sigma(v' \leftarrow v\, j(\varepsilon)) e^{\left(-E_C / k_B T\right)} E_C\, dE_C \qquad (5.2)$$

where E_c is the collision energy (i.e. $E - \epsilon_{vj}^{diatom}$) and k_B is the Boltzmann constant.

The integration of Eqn. (5.2) has been carried out in these calculations through recognising that, by making the substitution:

$$x = \frac{E_c}{k_B T} \quad , \tag{5.3}$$

Eqn. (5.2) reduces to:

$$k^{j(\varepsilon)}(v' \leftarrow v\, j(\varepsilon)) = \left(\frac{8}{\pi\mu}\right)^{1/2} (k_B T)^{1/2} \int_0^\infty \sigma(E_c)\, e^{(-x)} x\, dx$$

and is then of the correct form to be evaluated using, for example, the method of Gauss-Laguerre integration which states that:

$$\int_0^\infty e^{-x} f(x) dx = \sum_{i=1}^{n} w_i\, f(x_i) \quad .$$

Since this method requires calculating the function, $f(x)$, at specific values of x and applying specific weighting coefficients, w, dependent on the value of n, it follows from Eqn. (5.3) that, at higher temperatures, evaluation of the rate constants would require knowledge of cross sections at larger collision energies.

Boltzmann averaging the results of Eqn. (5.2) over all initial j states gives the vibrational relaxation rate constant:

$$k(v' \leftarrow v) = \frac{\sum_j (2j+1) k(v' \leftarrow v\, j(\varepsilon)) \exp\left(-\epsilon_{vj} / k_B T\right)}{\sum_j (2j+1) \exp\left(-\epsilon_{vj} / k_B T\right)} \quad . \tag{5.4}$$

6 Results of Calculations on O_2^+ + Kr

6.1 Potential Fit

Since the calculations on the TRL potential and on the single, $1^2A''$, RDWS *ab initio* potential were carried out by S.K. Pogrebnya prior to my research, a more detailed report will be given to the results of the potential fit for the Π-state treatment of the system than to these.

6.1.1 Semi-Empirical Interaction Potential

The TRL potential surface was fitted to an expansion in Legendre polynomials as explained in Section 3.3.1. Due to the highly anisotropic nature of the potential surface, a large number of terms had to be included in the series expansion. It was found that Legendre terms up to the 24^{th} order were necessary to achieve convergence in the results of the dynamics calculations. This means that, despite its analytical form, calculations using this potential were rather costly, typically requiring about 1 hour on a Silicon Graphics Origin 2000 for each J evaluated.

6.1.2 Single Ab Initio *Interaction Potential*

The points supplied by Ramiro Diaz *et al* [19] for the *ab initio* A'' potential surface were fitted as an expansion in Legendre polynomials using the method described at the end of Section 3.2.2 and taking the values of r_m of Eqn. (3.14) to be:

$$r_m = 1.8\, a_0\,,\ 2.05\, a_0\,,\ 2.11\, a_0\,,\ 2.2\, a_0\,,\ 2.5\, a_0$$

and the values of γ_k as:

$$\gamma_k = 0°, 30°, 60°, 90° \quad ,$$

with $L = 4$ and $N = 5$.

The potential fit was tested by comparing the predictions of the potential expansion function created to the remaining *ab initio* points that were not used in the fitting of the expansion.

6.1.3 *Combined* Ab initio *A" and A' Potential*

For the Π treatment of the O_2^+ diatom, using the points calculated *ab initio* by Ramiro Diaz *et al*, for both the A" and the A' potential surfaces of Ref. [19, 20], the average of the two potential surfaces (V_A) was fit to an expansion in Legendre polynomials whilst the one-half difference of the two potentials (V_{HD}) was fit to an expansion in associated Legendre polynomials, as described in Section 3.2.2. For both fits, the values of r_m of Eqn. (3.14) were taken to be:

$$r_m = 1.8\ a_0\ ,\ 2.05\ a_0\ , 2.11\ a_0\ , 2.2\ a_0\ , 2.5\ a_0$$

and the values of γ_k used were:

$$\gamma_k = 0°, 30°, 60°, 90°.$$

Both surfaces had $L = 4$ and $N = 5$.

Some cross-sections of the fitted potential surfaces are shown in Figure 1 and Figure 2, at values of r and γ which were used in the matrices of Eqn. (3.14) to create the potential energy functions.

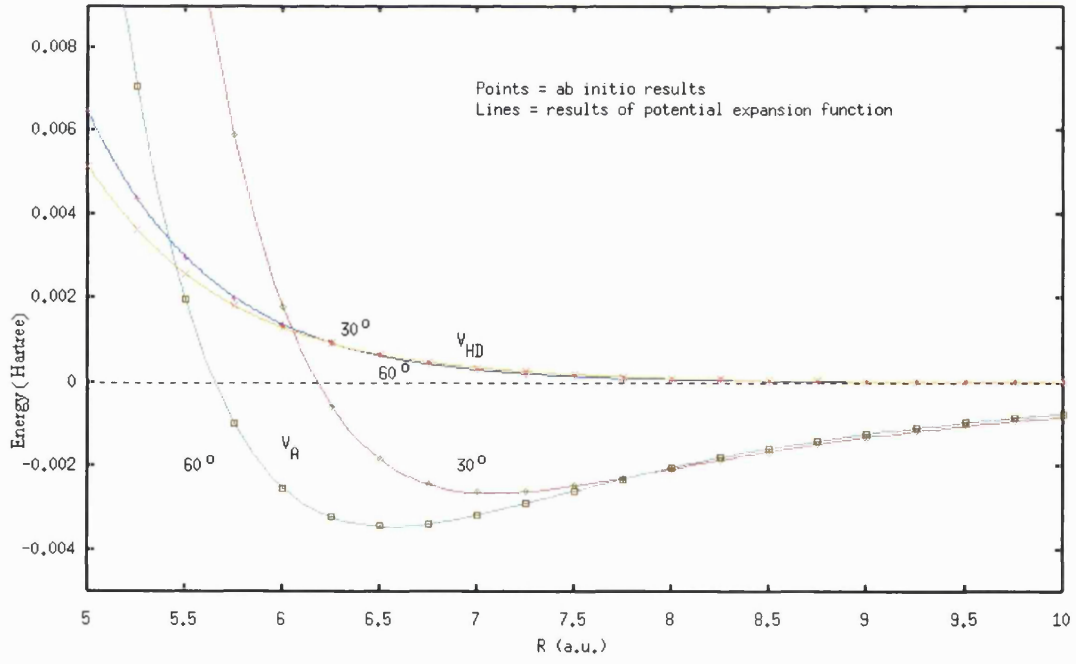

Figure 1 Cuts of potential energy surfaces V_A and V_{HD} at r =1.8 a_0 ; γ = 30°, 60°.

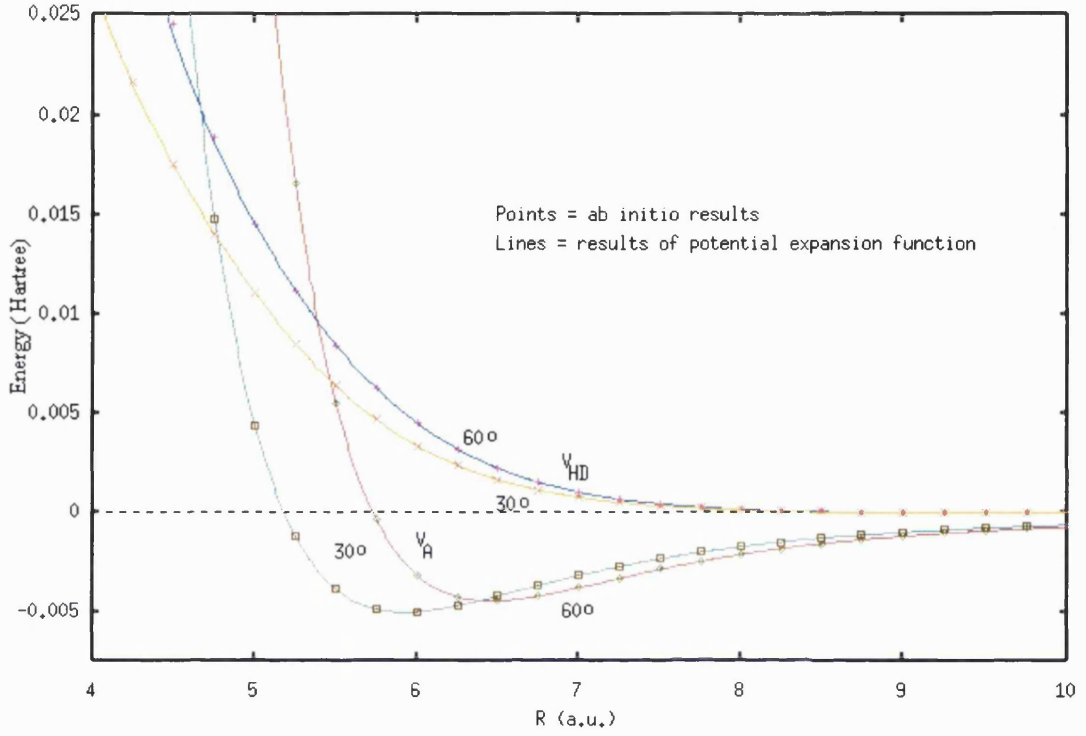

Figure 2 Cuts of potential energy surfaces V_A and V_{HD} at r =2.5 a_0 ; $\gamma = 30°, 60°$.

The potential fits were tested by comparing the values of V_A and V_{HD} generated by the expansion functions to those provided by RDWS for values of r and γ other than those included in the fitting procedure.

Figure 3 shows results of a test of the fitted potential expansion functions at a value of γ which was used in the fitting procedure, but at a value of r which was not. Figure 4 shows results of a test of the fitted potential expansion functions at a value of r which was used in the fitting procedure, but at a value of γ which was not. Finally, Figure 5 shows results of a test of the fitted potential expansion functions at a value of r and a value of γ which were both not used in the fitting procedure.

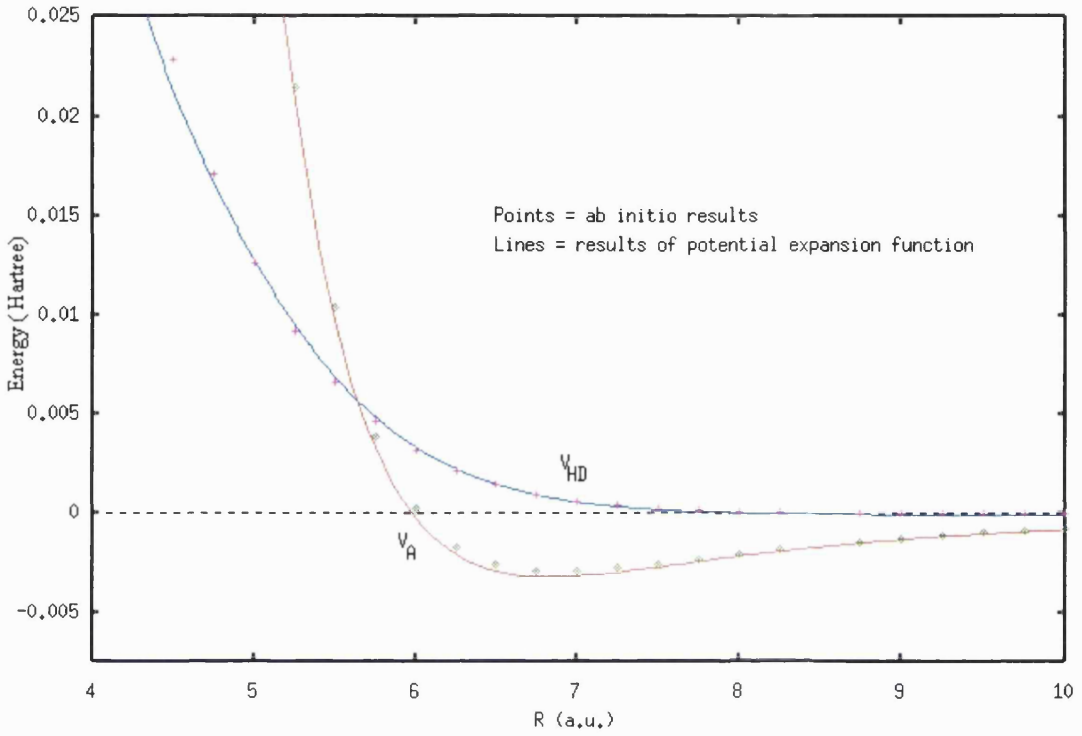

Figure 3 Cuts of potential energy surfaces V_A and V_{HD} at r =2.28 a_0 ; γ =30°.

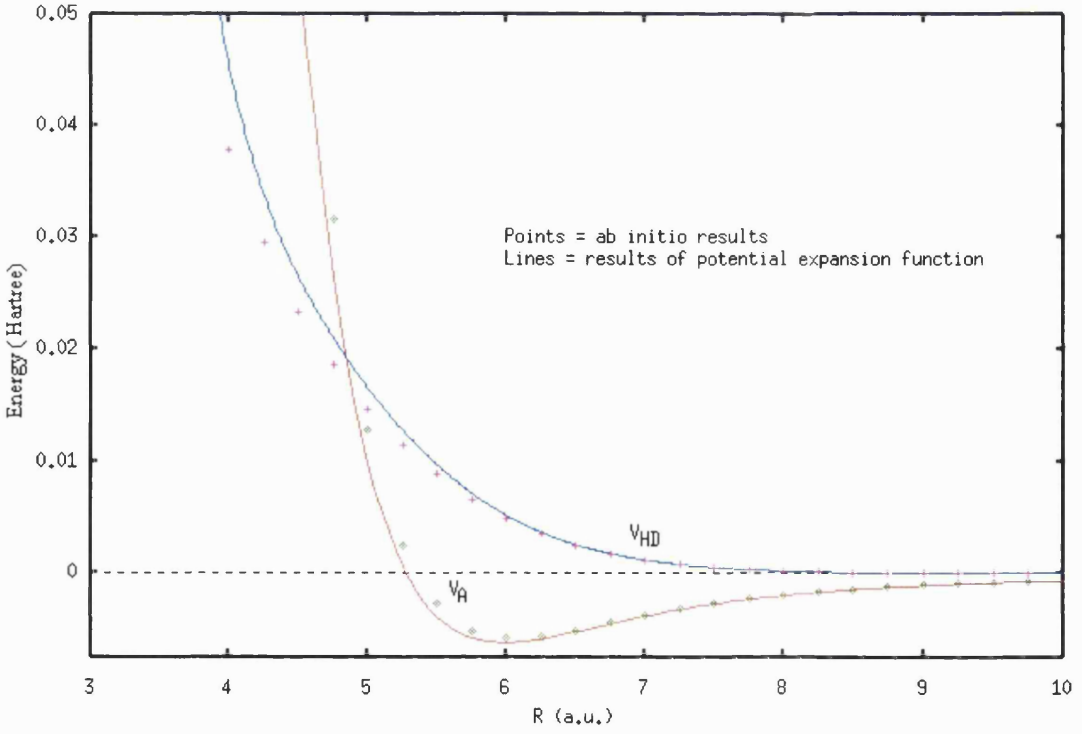

Figure 4 Cuts of potential energy surfaces V_A and V_{HD} at r =2.5 a_0 ; γ = 45°.

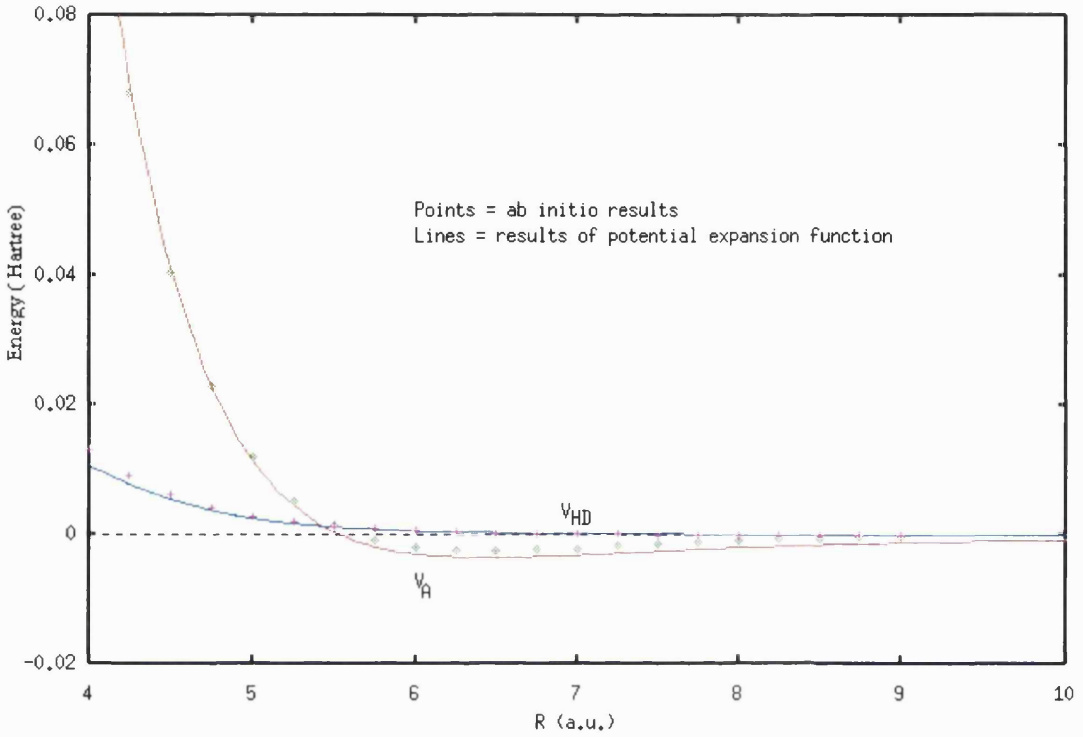

Figure 5 Cuts of potential energy surfaces V_A and V_{HD} at r =1.9 a_0 ; γ = 75°.

6.2 Total Cross Sections and Rate Constants

The results of all coupled-states calculations are essentially meaningless unless a sufficiently large basis set, and thus number of channels, is used to achieve convergence in the values of the probabilities and cross sections obtained. Naturally, the number of channels which must be made available would be expected to increase with an increase in the collision energy of the interaction and so, testing for this convergence must be done for each collision energy at which the calculations are carried out. Similarly, such convergence must be found with variation in other parameters, such as the maximum value of the total angular momentum, J_{max} , the value of $R = R^{\infty}$ at which the boundary conditions are applied and the number of sectors, *M*, into which the propagation space is divided. Throughout this research, we have considered these requirements to have been reached when the results are converged to within 2%.

6.2.1 Calculations Using TRL Potential

The accuracy of the CSA method has been tested by comparing the results obtained with it using the TRL potential energy surface with previously published, alternative methods which have used the same potential surface.

Thus, cross sections were calculated for $\sigma_{\Sigma}^{TRL}(v'=0 \leftarrow v=1, j=0)$ at a range of collision energies and are presented in Figure 6 along with the results of the classical trajectory calculations carried out by Tosi, Ronchetti and Lagana [14] and the semi-classical calculations performed by Zenevich *et al* [15]. The necessary parameters required to achieve convergence in the cross sections for these calculations are shown in Table 1. The basis set description (m_1, m_2, m_3) means that m_i rotational functions are associated with the *i*th vibrational level. It can be seen that there is very good agreement between the quantum dynamical and the classical trajectory results, with the semi-classical being about a factor of 2 lower.

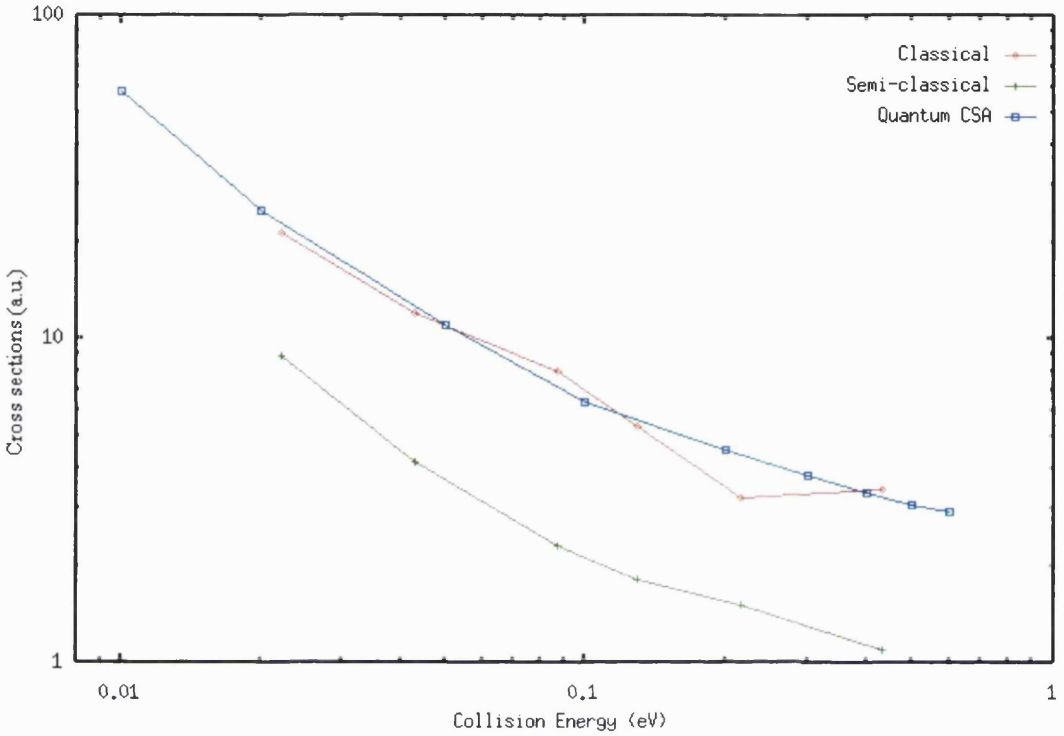

Figure 6 Cross sections $\sigma_{\Sigma}^{TRL}(v'=0 \leftarrow v=1, j=0)$ calculated with the TRL potential.

Collision Energy (eV)	Cross Section (a_0^2)	J_{max}	R^{∞} (a_0)	M	Basis
0.005	0.12240E+03	90	20	200	28, 26, 6
0.01	0.58848E+02	100	20	200	28, 26, 6
0.02	0.25195E+02	120	20	200	28, 26, 6
0.05	0.11128E+02	148	20	250	28, 26, 6
0.1	0.64299E+01	180	20	250	28, 30, 10
0.2	0.45632E+01	230	20	250	32, 30, 10
0.3	0.37904E+01	260	20	250	32, 30, 10
0.4	0.33460E+01	300	20	300	34, 34, 12
0.5	0.30848E+01	320	20	300	34, 34, 12
0.6	0.29435E+01	350	20	300	34, 34, 12

Table 1 Parameters required for convergence in the cross sections of quantum dynamical CSA calculations of $\sigma_{\Sigma}^{TRL}(v'=0 \leftarrow v=1, j=0)$ using TRL potential surface.

A further test of the use of the coupled states approximation has been made by comparing the total cross sections obtained with those calculated using the fully close coupling (CC) treatment of Gianturco *et al* [17]. They found the cross sections $\sigma_{\Sigma}^{TRL}(v'=0 \leftarrow v=1, j=1)$ at the collision energy of 0.022 eV for total angular momentum J = 0 and J = 60. The CSA and the CC methods are, of course, identical for J = 0, but a calculation of $\sigma_{\Sigma}^{TRL}(v'=0 \leftarrow v=1, j=1)$ for J = 60, using the CSA, produced a cross section of 0.178 a_0^2 as compared with the result of 0.115 a_0^2 obtained by the CC method [17].

These results are very encouraging and are an assurance as to the applicability of the CSA to our system.

The rate constants, $k_{\Sigma}^{TRL}(v'=0 \leftarrow v=1, j=0)$, as a function of temperature were found, using the coupled states approximation on the TRL surface, by averaging the cross sections over the Maxwell-Boltzmann distribution as described in Chapter 5. These results can then be compared with those obtained by the two experimental studies which have been carried out on the O_2^+ / Kr system [5, 7]. However, as has previously been pointed out [14], the energy distribution of reactants under the experimental conditions is not well known and may well fall somewhere in between a Maxwell-Boltzmann distribution and a delta function one. In this study, since the Maxwell-Boltzmann distribution has been adopted, the mean collision energy, E_m , on which the experimental results are dependent, is given by:

$$E_m = (3/2)k_B T \quad ,$$

where k_B is the Boltzmann constant and T is the temperature.

The results are shown in Figure 7. Since the TRL potential requires a large number of Legendre polynomials in its expansion, as mentioned earlier, it is unfortunately too expensive to calculate the rate constants at high temperatures where a larger basis would be required. Nevertheless, Figure 7 does show that at low temperatures the calculations using the TRL potential surface are in fair agreement with the experimental data. The relationship is better for the data of

Ref. [7] than for that of Ref. [5], the difference between the two sets of data being due to the fact that Ref. [7] actually corresponds to the vibrational relaxation rate constants of O_2^+ with Kr where the diatom is initially in a mixture of excited states, of proportion $O_2^+(v=1)/O_2^+(v=2) \approx 3$, as opposed to the pure $O_2^+(v=1)$ of Ref. [5].

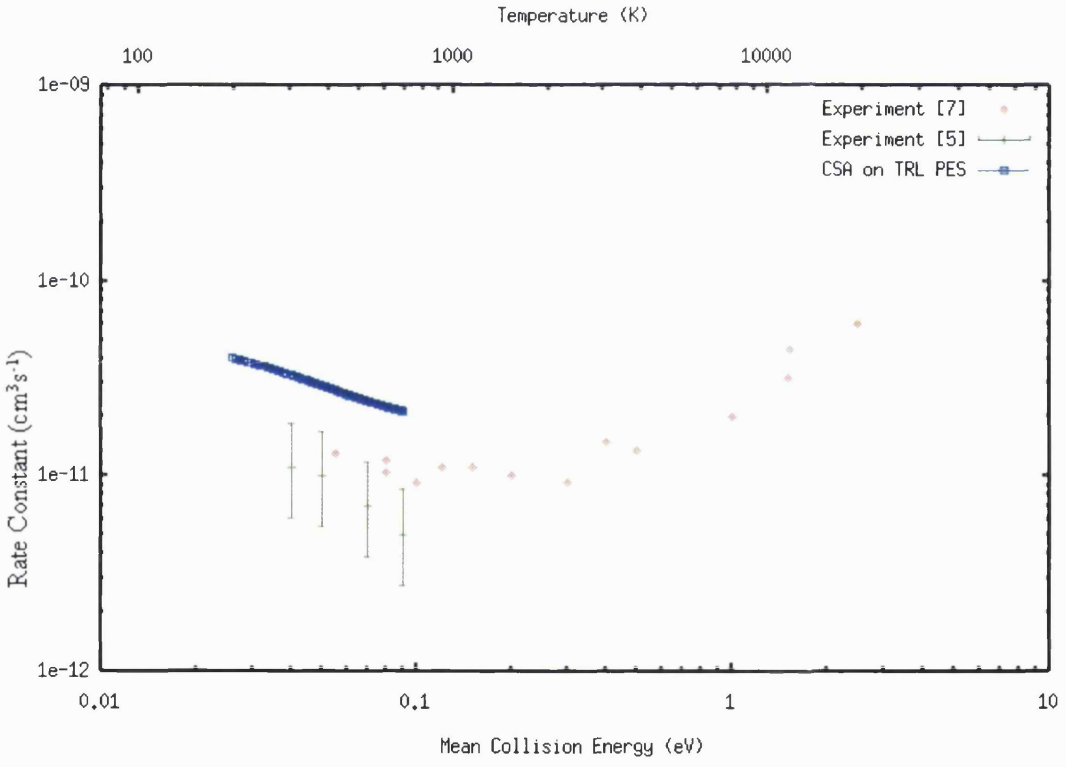

Figure 7 Comparison of the calculated rate constant, $k_{\Sigma}^{TRL}(v'=0 \leftarrow v=1, j=0)$, as a function of temperature and E_m, with the experimentally observed rate constants for O_2^+ / Kr inelastic scattering.

6.2.2 *Calculations Using* Ab Initio *A" Interaction Potential*

As explained in Section 3.3.1, since O_2^+ is homonuclear, the basis set used for the Σ treatment of the system need include only even states of j if the initial-j state is even and only odd states if it is odd. However, in addition, the nuclear spin of ^{16}O equals zero. This means that the nuclei are bosons and so the wavefunction of the diatom must satisfy the Pauli principle that

$$\hat{P}\Psi = +\Psi$$

where $\hat{P}$ is the label permutation operator for the two nuclei. Since:

$$\hat{P}\Psi = \left(\sigma_{el}(yz)\, i_{el}\, \psi^{el}\right)\psi^{vib}\left(C_2(x)\,\psi^{rot}\right)\left(p_{nuc}\,\psi^{nuc}\right) \qquad (6.1)$$

where i is an inversion operator, C_2 is a rotation of 180°, σ is a reflection operator and p permutes the states of the nuclei [46], this results in a further requirement for the Σ treatment of the system, namely that j always be even.

The cross sections, $\sigma_\Sigma(v'=0 \leftarrow v=1, j=0)$, were calculated at a range of collision energies and are shown, along with the values of the various parameters required to achieve convergence, in Table 2.

Collision Energy (eV)	Cross Section (a_0^2)	J_{max}	R^∞ (a_0)	M	Basis
0.001	0.1504E+00	90	30	300	26, 24, 22
0.005	0.2606E-01	90	30	300	26, 24, 22
0.010	0.1156E-01	100	30	300	26, 24, 22
0.100	0.5054E-02	130	30	300	28, 26, 22
0.250	0.1873E-01	160	20	200	28, 26, 22
0.500	0.5084E-01	230	20	200	36, 34, 28

Table 2 Total cross sections, with parameters required for convergence, for CSA calculations of $\sigma_\Sigma(v'=0 \leftarrow v=1, j=0)$ using lowest, 1A", *ab initio* potential energy surface.

From these results, the rate constant, $k_{\Sigma}(v'=0 \leftarrow v=1, j=0)$, was calculated as a function of temperature and mean collision energy, using the Maxwell-Boltzmann distribution as described in Chapter 5. The results are shown in Figure 8 along with the equivalent results using the TRL potential surface and the experimental results (as in Figure 7).

It appears that use of the single *ab initio* potential leads to rate constants which are more than one thousand times smaller than those found in experiment and through use of the semi-empirical TRL potential surface.

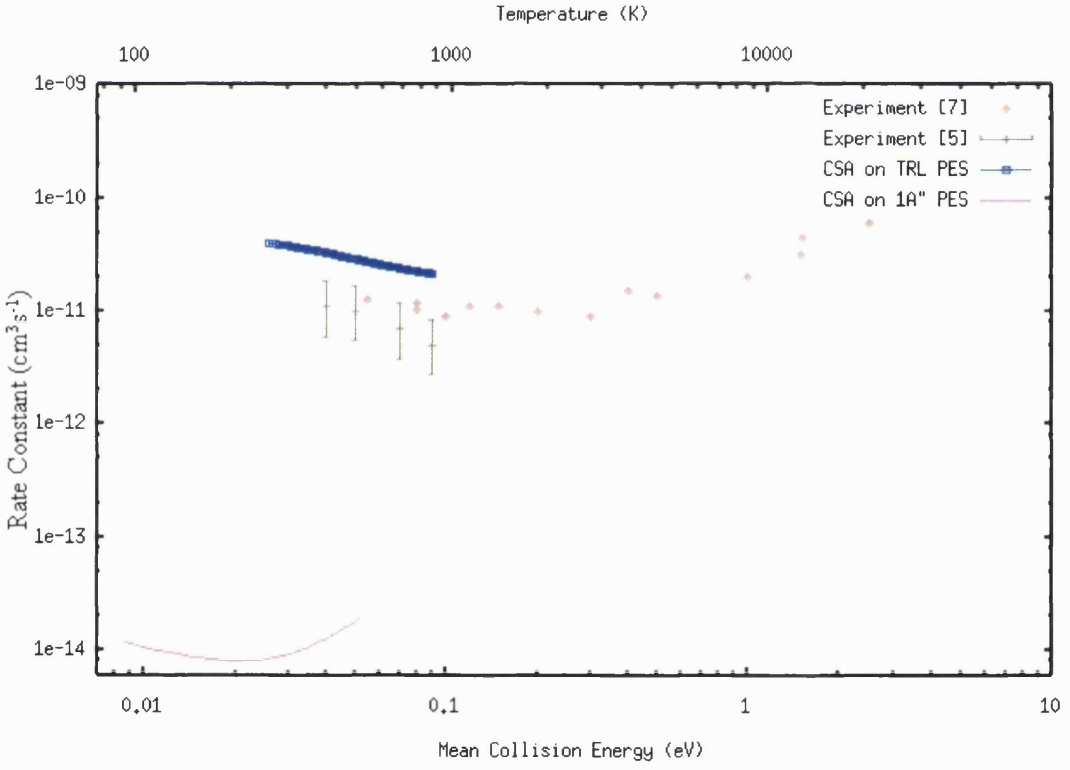

Figure 8 Rate constant, $k_{\Sigma}(v'=0 \leftarrow v=1, j=0)$, as a function of temperature and E_m, on a single *ab inito* potential surface, compared with that found using the TRL surface and the experimentally observed rate constants for O_2^+ / Kr inelastic scattering.

It must be remembered that the curves of the two theoretical calculations depicted in Figure 8, are the rate coefficients for the relaxation of the diatom from the lowest rotational state of the excited vibration only, (v = 1, j = 0), whilst the experiments measured the vibrational relaxation ($v = 0 \leftarrow v = 1$) from all initial rotational states. However, previous CSA calculations of vibrational

relaxation in ion-neutral systems [24, 25] have found that $k_{\Sigma}^{j=0}(T)$ is generally only about 1.5 times smaller than $k_{\Sigma}(T)$ and so could be expected to act as a good approximation to it. Nevertheless, rate constants have been calculated for values of initial-j up to $j = 8$ and the results have then been extrapolated to give an estimate of the total vibrational rate constant, $k_{\Sigma}(T)$, as shown in Figure 9. As expected, the ratio of $k_{\Sigma}^{j=0}(T) : k_{\Sigma}(T)$ is not greater than 1: 2.

It appears, then, that the use of the single $1^2A''$ *ab initio* potential energy surface leads to rate constants more than 1000 times smaller than those found in experiment.

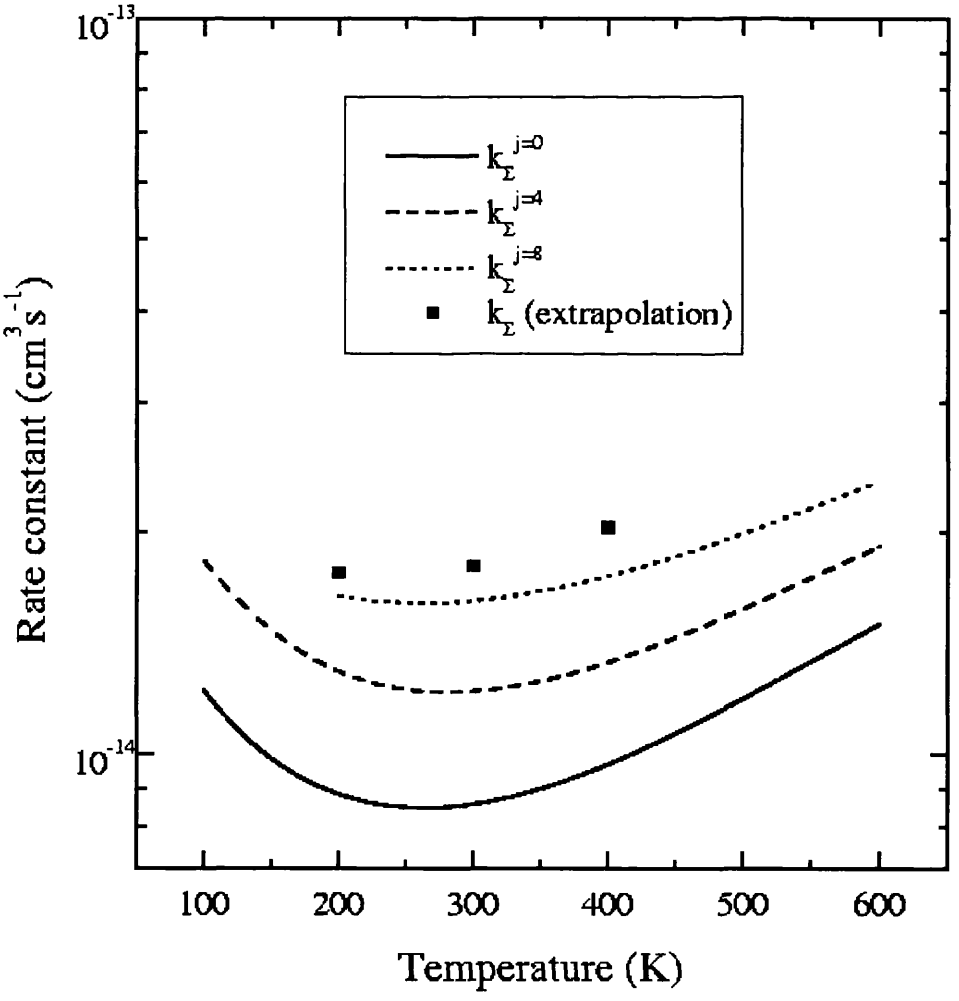

Figure 9 The initial rotational state selected rate constants calculated on a single lowest, $1^2A''$, RDWS surface.

6.2.3 Calculations Using Combined A" and A' Potentials

As explained in Section 3.3.2, the selection rule for the Π treatment of the system, due to the diatom being homonuclear, allows only terms of same parity, p, to be coupled together, where:

$$p = \varepsilon(-1)^j,$$

and so the basis set need only include those states of j and ε which have equivalent parity to that of the initial-j and -ε state of the diatom. However, here too the Pauli principle and Eqn. (6.1) furnish us with an additional requirement since, in the Π treatment of the system, $\sigma_{el}(yz)\psi^{el} = \varepsilon\psi^{el}$ [38]. Thus, only terms with even j with $\varepsilon = 1$ or odd j with $\varepsilon = -1$ can be included in the basis.

The cross sections, $\sigma_{\Pi}(v' = 0 \leftarrow v = 1, j = 1, \varepsilon = -1)$ (there is no $j = 0$ state for a Π-state diatom), were calculated at a range of collision energies and are shown, along with the values of the various parameters required to achieve convergence, in Table 3.

Collision Energy (eV)	Cross Section (a_0^2)	J_{max}	R^{∞} (a_0)	M	Basis
0.001	4.422E-01	70	38	320	48, 47, 38
0.005	1.669E-01	100	50	517	48, 47, 38
0.010	4.687E-02	100	50	517	48, 47, 38
0.027	1.412E-02	125	50	517	48, 47, 38
0.032	1.237E-02	125	50	517	48, 47, 38
0.050	7.530E-03	150	50	517	48, 47, 38
0.072	3.280E-03	150	50	517	48, 47, 38
0.100	1.906E-03	200	50	517	48, 47, 38
0.122	1.716E-03	200	50	517	48, 47, 38
0.200	2.977E-03	250	50	517	55, 53, 47
0.300	6.460E-03	250	50	517	70, 63, 52, 5
0.500	1.658E-02	300	50	517	71, 65, 59, 7
0.700	2.723E-02	400	50	517	75, 68, 62, 17

Table 3 Total cross sections, with parameters required for convergence, for CSA calculations of $\sigma_{\Pi}(v' = 0 \leftarrow v = 1, j = 1, \varepsilon = -1)$ using combined, 1A" and 1A', ab inito potential energy surfaces.

The rate constants, $k_{\Pi}(v'=0 \leftarrow v=1, j=1, \varepsilon=-1)$, were then calculated as a function of temperature and mean collision energy from these cross sections, using the Maxwell-Boltzmann distribution as described in Chapter 5. The results are shown in Figure 10 and compared to the equivalent rate constants calculated in the Σ treatment, $k_{\Sigma}(v'=0 \leftarrow v=1, j=0)$ (as in Figure 8). The inclusion of the second potential surface has resulted in the rate constant at low temperatures being several times higher than that found using just the single, 1^2A", potential energy surface.

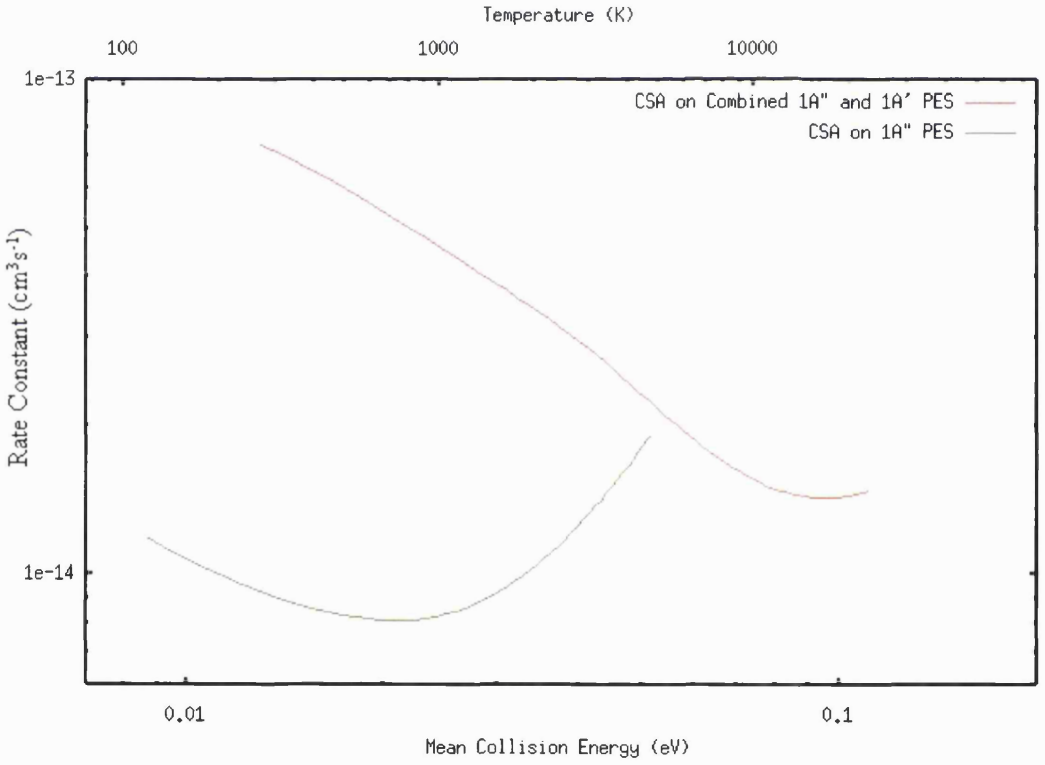

Figure 10 Rate constant, $k_{\Pi}(v'=0 \leftarrow v=1, j=1, \varepsilon=-1)$, as a function of temperature and E_m, for O_2^+ + Kr, using the *ab initio* potential surfaces of both symmetries of the system, compared with $k_{\Sigma}(v'=0 \leftarrow v=1, j=0)$ which uses just the 1A" surface.

In order to evaluate $k_{\Pi}(v'=0 \leftarrow v=1)$, the rate constants were calculated for initial-j up to $j=9$ (which corresponds to the maximum of the Boltzmann distribution at room temperature) and the results then extrapolated to give an estimate of the total vibrational rate constant, $k_{\Pi}(T)$. It turns out that the dependence of $k_{\Pi}^{j\varepsilon}$ on initial-j is much stronger than that of k_{Σ}^{j}. The rate constant $k_{\Pi}^{j=9,\varepsilon=-1}$ is more than an order of magnitude higher than $k_{\Pi}^{j=1,\varepsilon=-1}$ as can be seen in Figure 11. This results in $k_{\Pi}(T)$ being over 100 times greater than $k_{\Sigma}(T)$ in the range $T=200-400K$ (Figure 11).

Thus, the inclusion of the second potential energy surface has greatly increased the calculated efficiency of the vibrational relaxation. However, despite this significant effect, the vibrational relaxation rate constants obtained within the CSA approach, utilising the two adiabatic *ab initio* potential surfaces of Ref. [19, 20], are still about a factor of 10 below the reported experimental data [5, 7].

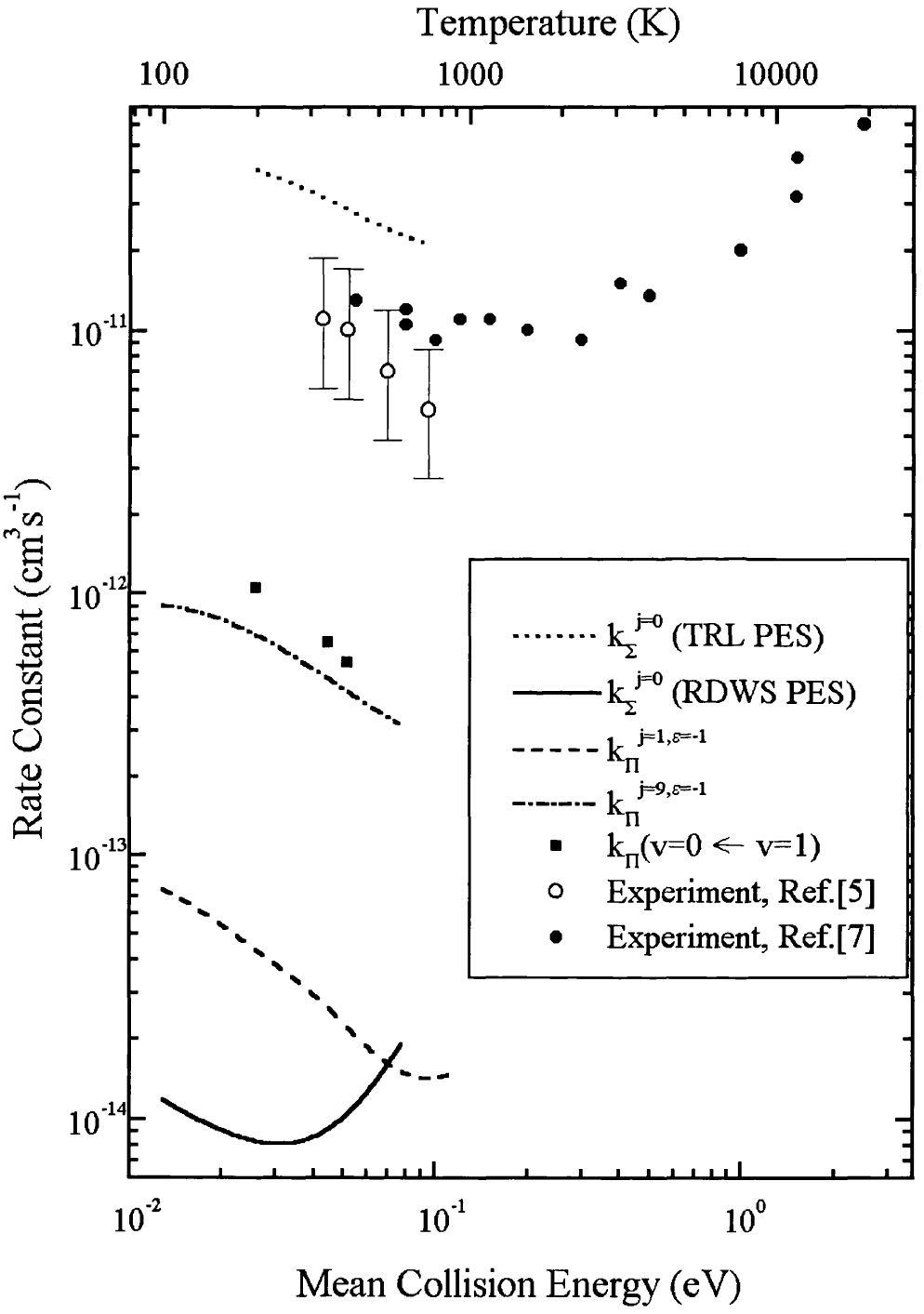

Figure 11 Comparison of all the quantum dynamically calculated, temperature dependent rate constants for O_2^+ / Kr vibrational relaxation using the CSA and the experimentally observed results.

7 Discussion of Results of Calculations on O_2^+ + Kr

One of the aims of this study is to analyse the effects that the major differences between the potential surface calculated *ab initio* [19, 20] and that presented by Tosi *et al* [14] would have on the cross sections and rate constants. Figure 8 shows that, when quantum calculations for the vibrational quenching of the O_2^+ ($v=1$) diatom with Kr, using the coupled states approximation, were applied to both the TRL potential and the RDWS A" potential, in both cases treating the diatom as having the ground electronic state Σ, the latter potential surface yielded much lower cross sections and rate constants than the former.

This effect was expected, since the RDWS potential surface has a shallower well depth and a less steep repulsive wall than the TRL potential surface. This results in weaker coupling between vibrational states and, therefore, less efficient vibrational relaxation. For example, the matrix elements

$$V_{v'v}(R,\gamma)=\langle \chi_{v'0}(r)|V(R,r,\gamma)|\chi_{v0}(r)\rangle \ ,$$

calculated with the TRL potential, were generally observed to be much greater than those calculated with the RDWS potential.

It should be noted that good agreement between calculations using the TRL potential energy surface and the experimental results of Ref. [7] is also to be expected (once the accuracy of the CSA method has been assured), given that this potential contains adjustable parameters which were designed to obtain the best agreement between the results of classical trajectory calculations [14] and the experimental vibrational relaxation rate constants [7]. In particular, varying the parameter which controls the angular width of the potential well, changes the rate constants by orders of magnitude at small and moderate collision energies.

The other principal aim of this study is to contrast the results of quantum dynamical calculations which treat the diatom of the O_2^+ / Kr system as a Π-state molecule and thus use both A" and A' *ab initio* potential surfaces, with those which treat the diatom as a Σ-state molecule and use only the lower, A", *ab initio* surface.

Figures 10 and 11 reveal two major differences between the Π treatment and the Σ treatment. Firstly, the rate constants of vibrational relaxation from the lowest initial rotational state of the $v = 1$ vibration are significantly higher, at low temperatures, for $k_{\Pi}^{j=1,\varepsilon=-1}$ than for $k_{\Sigma}^{j=0}$. Secondly, increasing the initial rotational state of the diatom results in the typical increase in rate constant for k_{Σ}, with $k_{\Sigma} \approx 2 \times k_{\Sigma}^{j=0}$ (Figure 9), whereas k_{Π} shows an increase in efficiency of more than one order of magnitude with increase in initial-*j*.

In order to explain the first of these effects, it is instructive to look at the vibronic energy curves of the different symmetries of the O_2^+ / Kr system. These are defined by:

$$U_A^v(R,\gamma) = \langle v | \hat{V}_A(R,r,\gamma) | v \rangle + \epsilon_v$$

and can be understood as being the effective potential for the diatom in the particular vibrational state, *v*.

Figure 12 reveals that, at certain values of γ, the two vibronic curves

$$U_{A''}^{v=1}(R,\gamma) = \langle v=1 | \hat{V}_{A''}(R,r,\gamma) | v=1 \rangle + \epsilon_{v=1} \ ,$$

and

$$U_{A'}^{v=0}(R,\gamma) = \langle v=0 | \hat{V}_{A'}(R,r,\gamma) | v=0 \rangle + \epsilon_{v=0} \ ,$$

– i.e. the curve for the lower potential of the two symmetries, at the higher vibrational state and for the higher potential, at the lower vibrational state, respectively – cross, at low energies. Since, in reality, the A" and A' surfaces are mixed to produce the true potential surfaces of the interaction, the crossing shown in Figure 12 does not actually occur. However, observation of this pseudo-crossing does suffice to offer a qualitative understanding of the extra

efficiency caused by the inclusion of the additional potential surface at low temperatures. It indicates that, at low collision energies, in the region of the pseudo-crossing, the probability for vibrational relaxation from the $v = 1$ state of the diatom to the $v = 0$ state will be high. This is a direct result of the existence of the two alternative symmetries of the system.

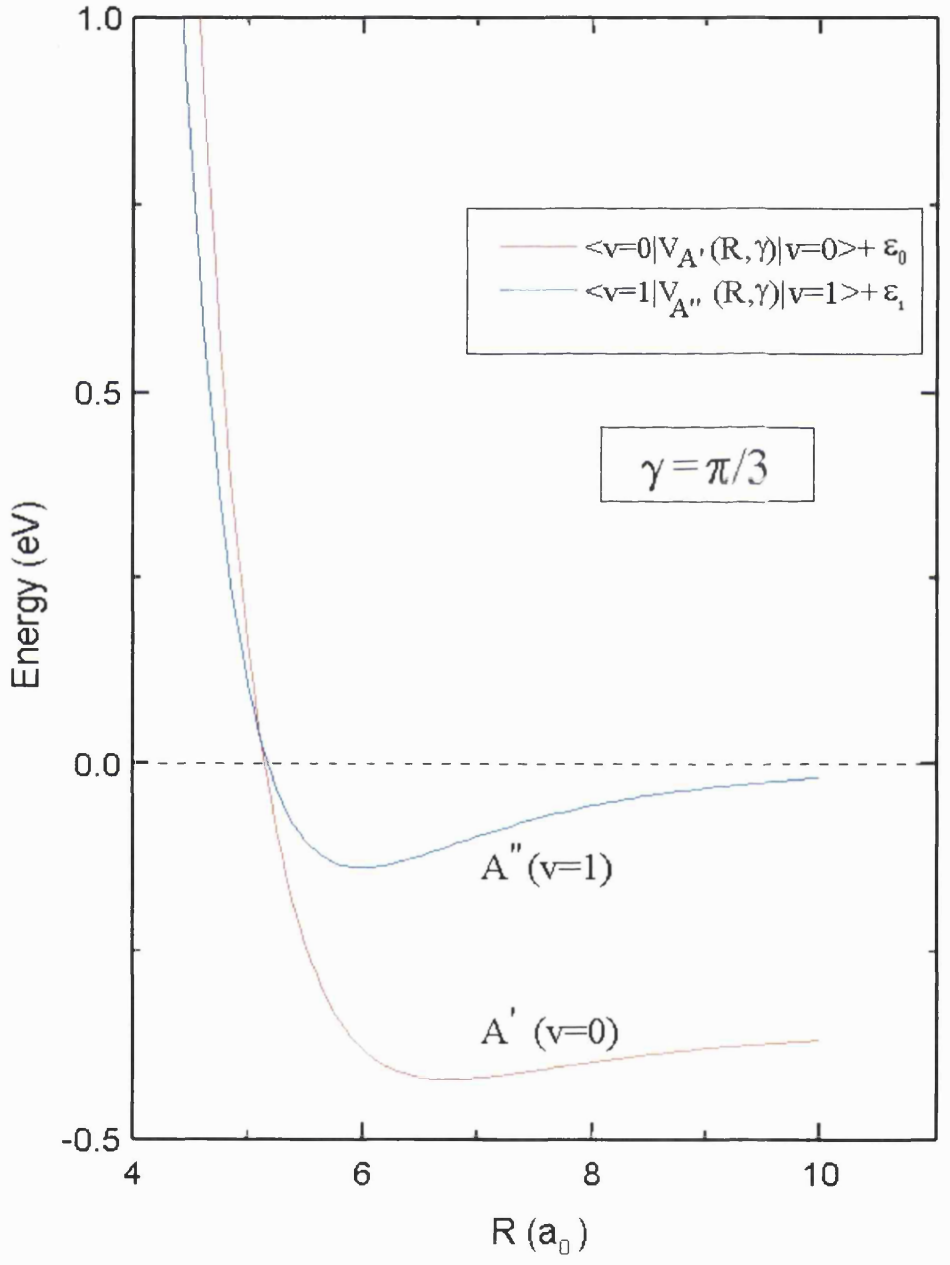

Figure 12 Vibronic curves $U_{A''}^{v=1}$ and $U_{A'}^{v=0}$ at γ = 60°, with respect to $U_{A''}^{v=1}(R \to \infty)$.

Thus, these calculations appear to support the suggestion, put forward in Ref. [6], that the increased efficiency of the O_2^+ / Kr system over that of a system with approximately equivalent electrostatic attraction, such as NO^+ / Kr, is due to the open-shell of the O_2^+ diatom, since it is that which leads to the presence of the potentials of different symmetry.

The greater dependence on initial-j of the rate constants $k_\Pi^{j\varepsilon}$, than that shown by the rate constants k_Σ^j, can be explained by an extension of the vibronic energy curve pseudo-crossing observation.

The contributions given by different values of $|\Omega|$ to the cross sections $\sigma_\Sigma(v'=0 \leftarrow v=1, j=9)$ and $\sigma_\Pi(v'=0 \leftarrow v=1, j=9, \varepsilon=-1)$ have been calculated and are shown in Figure 13 for $J = 70$ and collision energy 0.05 eV. In the Σ case, σ_Σ^Ω is an oscillating function with a small amplitude and each $|\Omega|$ gives practically the same contribution to the total cross section. In the Π case, however, σ_Π^Ω has a strong tendency to peak at some value $|\Omega| >> 1$. It is this which leads to the increase in $k_\Pi^{j\varepsilon}$ with increase in initial-j, since Ω is limited to being never greater than the smaller of the two values of j – initial-j and final-j.

The explanation for this uneven contribution of the σ_Π^Ω to $\sigma_\Pi^{j\varepsilon}$ at large initial-j becomes clear when we note that, at $\Omega = 0$ (or $\Omega = 1$, in the Π case) the interaction angle, γ, will be zero whereas, for large values of j, as $|\Omega| \rightarrow j$, $\gamma \rightarrow 90°$. Hence, Figure 13 reveals that, when the interaction angle takes the values $90° > \gamma >> 0°$, there is a greater probability for vibrational relaxation. Now, the pseudo-crossing of $U_{A''}^{v=1}$ and $U_{A'}^{v=0}$, an example of which was seen in Figure 12, is observed at the geometries $30° < \gamma < 70°$. So, we would expect to see a maximum for σ_Π^Ω at values of Ω which correspond to these configurations and, thus, the effects of the pseudo-crossing of the vibronic energy curves will be magnified at higher values of initial-j.

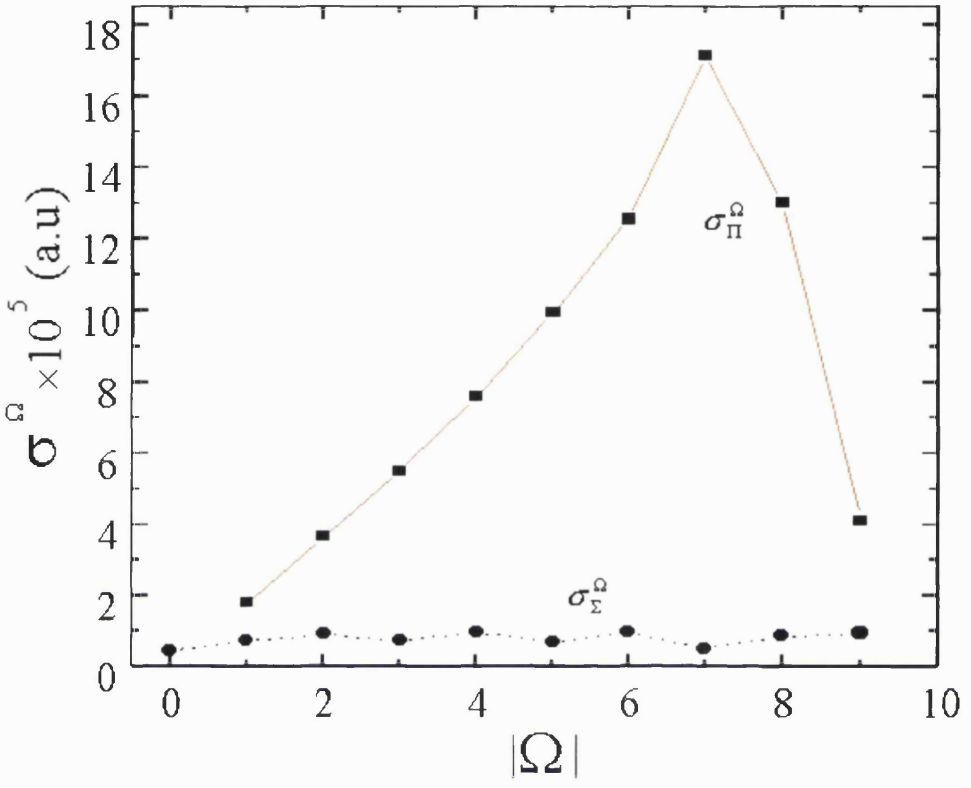

Figure 13 Ω-contributions to the cross sections $\sigma_{\Sigma}(v'=0 \leftarrow v=1, j=9)$ (circles) and $\sigma_{\Pi}(v'=0 \leftarrow v=1, j=9, \varepsilon=-1)$ (squares) at $J=70$, $E_c = 0.05\,\text{eV}$.

As the results in Figure 11 show, there is one feature which the quantum calculations on all the descriptions of the O_2^+ / Kr system have in common: they all show negative dependence on temperature for low temperatures. For temperatures up to T ≈ 700K, the rate constants obtained using the TRL potential and all the $k_{\Pi}^{j\varepsilon}$ rate constants are monotonically decreasing functions of temperature, whilst the rate constants obtained using the single A" RDWS potential surface show a minimum at about room temperature.

As discussed in the Introduction, it is suggested that this property of the O_2^+ / Kr system, which is observed in the experimental studies of Refs. [5, 7], is due to the formation of a complex at low temperatures.

A support for this suggestion can be advanced by examining the dependence of the cross sections on the total angular momentum, J. Figure 14 shows the partial cross section $\sigma_{\Sigma}^{J}(v'=0 \leftarrow v=1, j=0)$ as a function of J and Figure 15 presents a similar plot for $\sigma_{\Pi}^{J}(v'=0 \leftarrow v=1, j=1, \varepsilon=-1)$. Both diagrams show a pronounced resonance structure to be present at low collision energies, which disappears at higher collision energies. This behaviour strongly suggests the formation of a rotating complex occurring (or at least being dominant) at low energies and temperatures, as proposed by Ferguson [1].

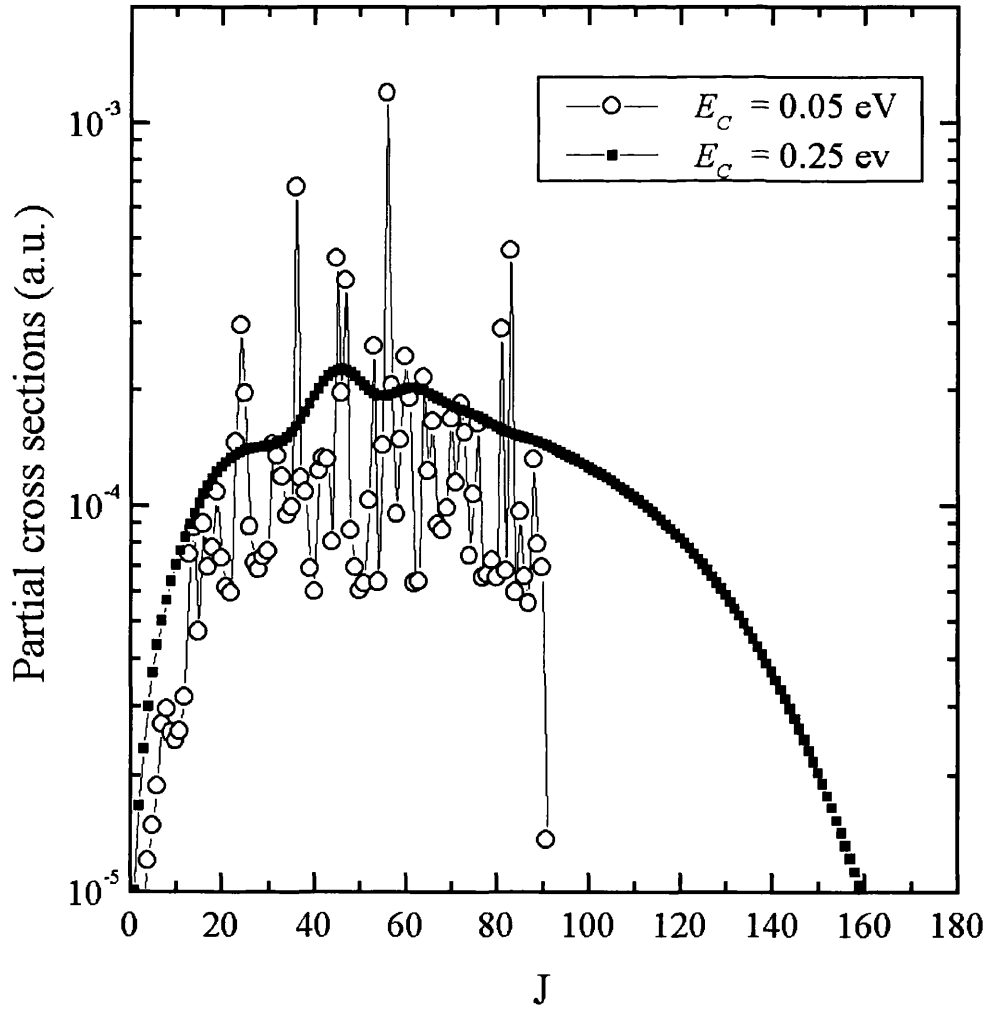

Figure 14 Partial cross sections $\sigma_{\Sigma}^{J}(v'=0 \leftarrow v=1, j=0)$ at two collision energies.

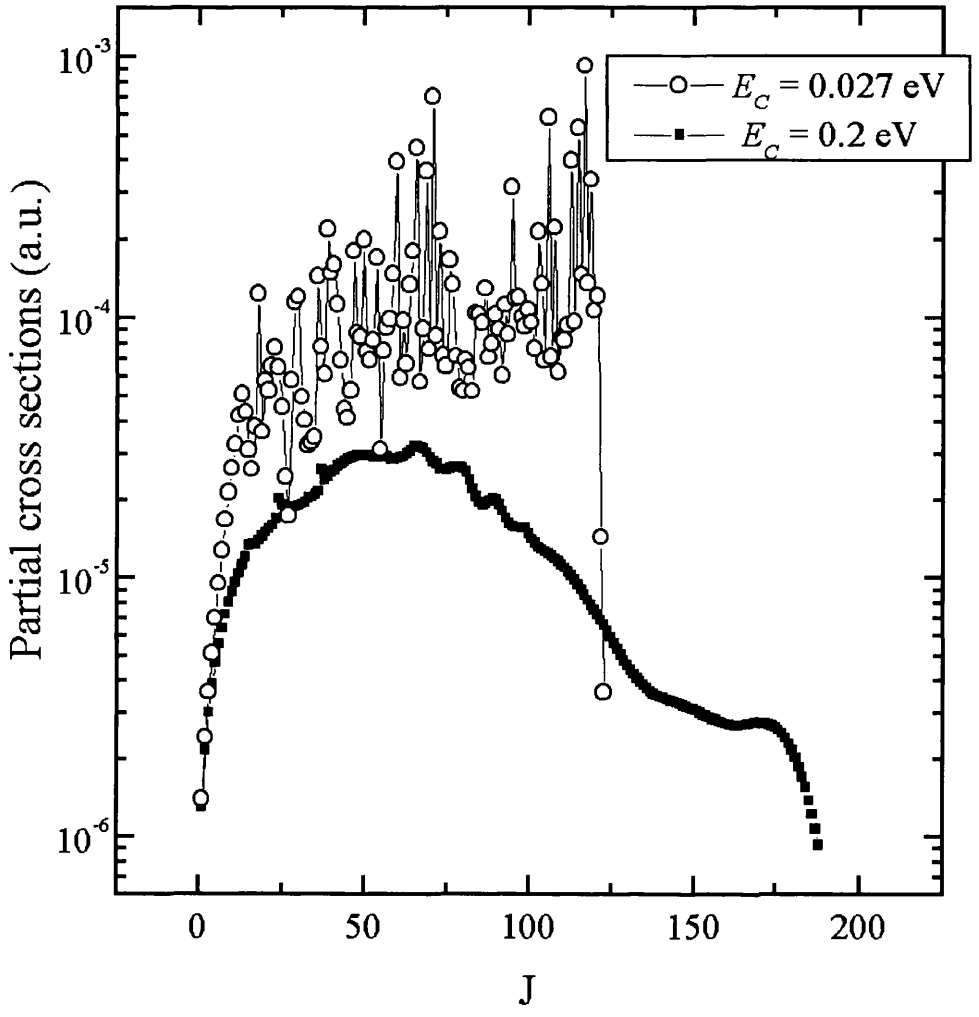

Figure 15 Partial cross sections $\sigma_{\Pi}^{J}(v'=0 \leftarrow v=1, j=1, \varepsilon=-1)$ at two collision energies.

8 Conclusions of Analysis of O_2^+ + Kr

The quantum dynamical coupled states approximation has been tested for applicability to the vibrational relaxation of O_2^+ (v = 1) through collision with Kr. It has then been performed using an *ab initio* potential energy surface for the system and compared to experimental data. The calculations were originally carried out on a single potential surface, but then subsequently, to take into account the Π-state nature of the diatom, were extended to enable the inclusion of both the *ab initio* adiabatic surfaces calculated by Ramiro Diaz *et al* [19, 20], for the two symmetries present in the system. This is the first time quantum scattering calculations have been done for the vibrational relaxation of a molecule in a Π electronic state which includes two potential energy surfaces.

The results of the calculations on the semi-empirical TRL potential energy surface show that the coupled states approximation is valid for describing vibrational relaxation, even for the extreme case of a heavy atomic partner and a very anisotropic and deep interaction potential such as the TRL one.

Calculations on the single, $1^2A''$, *ab initio* potential surface result in rate constants far below experimental data. This highlights the difference between the semi-empirical potential energy surface of Tosi *et al* [14], which was designed to fit results of classical trajectory calculations to the rate constants found experimentally, and the RDWS potential surface, calculated *ab initio*.

The inclusion of the second *ab initio* potential energy surface results in an increase in rate constants of about 100 times, at low temperatures. In addition, the dependence of the rate constants on the initial rotational state of the diatom is much greater for this Π-state treatment of the diatom. These differences can be explained as being due to the pseudo-crossing of vibronic energy curves of different symmetry and the localisation of the wavefunction for higher initial-j at configurations where this pseudo-crossing is observed.

The conclusion of this study, therefore, is that calculations on vibrational relaxation of O_2^+ / Kr and similar systems should include the potential energy

surfaces of all the various symmetries present. Approximating the diatom as having the ground electronic state Σ, when in reality it does not, is not a good approximation.

The theoretical analysis of the O_2^+ / Kr system also leads to a support for the complex formation mechanism at low temperatures and collision energies put forward by Ferguson [1], which leads to the negative dependence of the rate constants on temperature observed in both experimental and theoretical studies of the system, at low temperatures.

Further Work

The rate constants calculated by means of the quantum scattering method, utilising the two adiabatic *ab initio* surfaces, are still about an order of magnitude lower than experimental data. Collision dynamics results are very sensitive to even small variations in the interaction potential and so further improvements to the potential energy surfaces would be very useful. In addition, new experiments, especially at low temperatures, would be of great interest.

PART 2

9 Introduction

9.1 Dissociation of the Ozone Dication

9.1.1 Background

Molecules with a doubly positive charge (molecular dications) are generally unstable and extremely chemically reactive and are therefore of great interest, both theoretically and experimentally. Most molecular dications dissociate to give two charged ion fragments and it has been proven experimentally, by Newson and Price [47], that the ozone dication, O_3^{2+}, is one such example. They have carried out an ion-ion coincidence technique, using time-of-flight mass spectroscopy, to investigate the fragmentation of the O_3^{2+} cation created by the double ionisation of ozone through electron impact. This study is of particular interest considering the recent focus on the properties of ozone and its role in the atmosphere.

The process:

$$O_3 \xrightarrow{e^-} O_3^{2+} \longrightarrow O_2^+ + O^+ + \text{K.E.} \quad , \qquad (2)$$

detected by Newson and Price, results in the release of an amount of kinetic energy in the ionic products, as seen from the schematic potential energy curves shown in Figure 16, and a measurement of this kinetic energy release (KER), together with knowledge of the energies of the fragments produced, enables the evaluation of the double ionisation energy of O_3.

Newson and Price [47] found the KER of process (2) by measuring the relative velocity of the O_2^+ and O^+ fragments formed and found it to be 7.5 ± 0.3 eV, giving a value of 34.3 ± 0.3 eV for the excitation energy of the lowest energy state of O_3^{2+} to dissociate to O_2^+ and O^+, relative to the ground state of O_3. This result for

the excitation energy, however, is dependent on the assumption that the O_2^+ fragment formed has no significant internal energy.

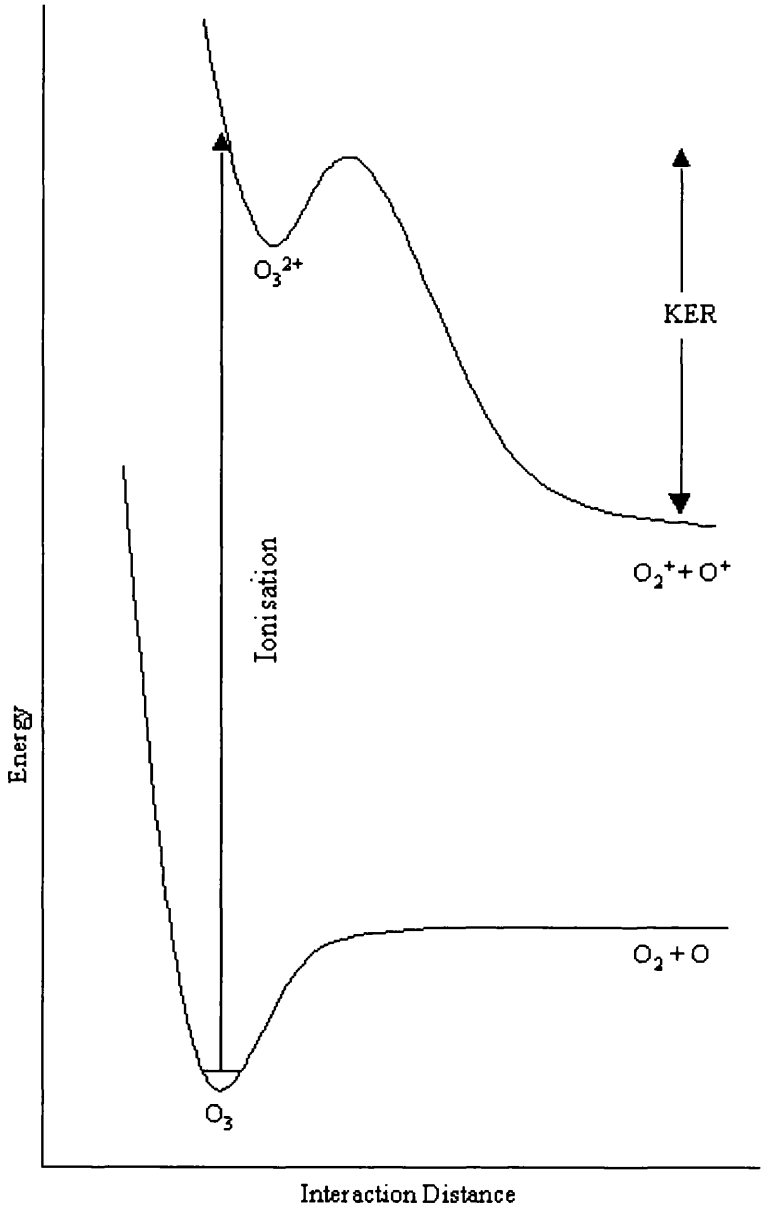

Figure 16 Schematic potential energy curves for ionisation of ozone and subsequent dissociation of the ozone dication.

In order to verify the validity of this assumption, Newson and Price carried out an alternative method for determining the energy of the lowest energy O_3^{2+} state to

decay to the fragments O_2^+ and O^+ which involved monitoring the yield of the fragments produced, as a function of the energy of the impact electrons. This more direct, but less accurate, method gave a state energy of 34 ± 2 eV, which appears to confirm their supposition.

9.1.2 This Research

The distribution of internal energy states in the diatomic ion, O_2^+, formed from the dissociation of O_3^{2+} excited from neutral ozone, can be determined theoretically using quantum dynamical methods. This product distribution can be calculated through the evaluation of the overlap of the wavefunction for the bound ground energy state of O_3 with the scattering wavefunction for the process:

$$O_2^+ + O^+ \leftrightarrow O_3^{2+} \quad , \qquad (3)$$

and involves much of the same theory described in Part 1 of this thesis.

Although the O_3^{2+} dication formed by the double ionisation of O_3 may initially be created as a quasi-bound molecule before fragmenting, the excited system can still be described by a scattering wavefunction since the Hamiltonian for the dissociation of the quasi-bound state is identical to that for the scattering process (3). Similarly, the wavefunction for the bound O_3 molecule, Ψ_{O_3}, is described in this analysis using the same form of the coordinates as that employed for the scattering wavefunction, $\Psi_{O_2^+ + O^+}$. As will be seen in the method, this greatly simplifies the calculations.

An *ab initio* potential energy surface for process (3) has recently been developed by Champkin *et al* [48]. The current research is therefore able to span a number of different fields of chemistry by incorporating this new surface into quantum dynamical calculations, in order to facilitate the interpretation of the experiments carried out by Newson and Price [47]. The potential energy surface for the bound

ozone molecule uses the harmonic oscillator model described by Barbe, Secroun and Jouve [49], based on the results of infrared spectra.

Just as with the scattering process of Part 1, the evaluation of the scattering wavefunction for process (3) requires the application of suitable boundary conditions which describe the system at an infinite distance from the collision. However, unlike the system discussed there, process (3) entails the scattering of two charged species, O_2^+ and O^+, and will therefore have a Coulombic term in the potential surface which dominates at large distances. As a result, the scattering particles are prevented from assuming the form of simple plane waves even at infinite distances. Consequently, an accurate portrayal of the wavefunction in the asymptotic region will involve the use of different boundary conditions to those used in Chapter 4.

Most calculations of this nature until now have used only the 'regular' boundary conditions, appropriate to a system without a long-range Coulombic potential, and so it would be of interest to investigate the necessity of using the correct asymptotic boundary conditions when dealing with a system which has a Coulombic potential. This requires the adaptation of the theory for the propagation of the overlapping wavefunctions, since the method used has previously only been illustrated for non-Coulombic systems.

The aim of the research in this part of the thesis, therefore, is to calculate the product distribution of O_2^+ in the process (2) and to test the effects of the use of the more accurate, but less commonly used, asymptotic boundary conditions in the calculations. However, in order to gain some understanding of the differences resulting from the use of the alternative boundary conditions, a preliminary investigation has been undertaken on a simple, one-dimensional elastic scattering interaction which also contains a Coulomb potential energy term and this study is presented here first.

9.2 Elastic Scattering with a Coulombic Potential

The system chosen to test the effects of the use of asymptotic boundary conditions appropriate to a Coulombic potential, instead of the more commonly used 'regular' boundary conditions, is the elastic scattering of H^+ and Cl^+.

This system has been chosen due to its simplicity and the fact that a recently published paper by Bennett and McNab [50] presents the results of accurate *ab initio* calculations of the potential energy for the doubly charged molecule HCl^{2+}. In addition to providing the one-dimensional potential surfaces for the four lowest electronic states of the dication, these authors evaluate the energies and lifetimes of the quasi-bound vibrational levels which are supported by those states, using the Numerov-Cooley algorithm [51] and a uniform semi-classical approximation. The potential surface of Ref. [50] is treated as that of a bound molecular dication which dissociates to give two charged fragments, H^+ and Cl^+, and thus the metastable vibrational levels are described as quasi-bound states. However, the same potential could be equally seen as describing the elastic scattering of $H^+ + Cl^+$, forming orbiting resonances (HCl^{2+}) at certain collision energies.

The aim of this study of the process

$$H^+ + Cl^+ \leftrightarrow HCl^{2+}$$

is to calculate, through R-matrix propagation, the total cross sections of the elastic scattering on the *ab initio* potential surface of Ref. [50] and to locate resonances in the phase shifts and cross sections as a function of collision energy, using both regular and Coulombic boundary conditions. The energies, widths and lifetimes of the orbiting resonances can be compared to the values found by Bennett and McNab [50].

Hence, this study allows an assessment of the requirement of theoretical studies of systems with Coulombic potentials to use the boundary conditions appropriate to such potentials when calculating a variety of observable quantities. This is,

therefore, a useful prelude to the main investigation of this part of the thesis – the double ionisation of ozone followed by its fragmentation – which includes a comparison of the product distribution of the internal states of O_2^+ using both regular and Coulombic boundary conditions.

The structure of this part of the thesis is as follows: Firstly, a brief description of the theory of elastic scattering used in the analysis of $H^+ + Cl^+$ will be presented, showing the cause of the requirement for different boundary conditions for systems with Coulombic potentials than those for the regular, non-Coulombic systems and deriving the various observables from the solution of the Schrödinger equation. Since the theory of inelastic scattering is anyway an extension of the theory for elastic scattering, this is a useful precursor to the treatment of the O_3 / $O_2^+ + O^+$ system. The results of calculations on the elastic scattering of H^+ and Cl^+ are then presented, followed by a discussion of the conclusions made from this analysis.

Chapter 11 then turns to the O_3 / $O_2^+ + O^+$ system and describes the procedure of calculating the product distribution of O_2^+ through the evaluation of the overlap matrix between the bound and the scattering wavefunctions. The method of determining each of the wavefunctions through solution of the relevant coupled equations is outlined, with reference to the theory discussed in Part 1, followed by a detailed account of the method used for calculating their overlap, using both regular and Coulombic boundary conditions. Chapter 12 presents the results of these calculations and, finally, Chapter 13 discusses the conclusions which can be drawn from them.

10 Elastic Scattering of H^+ and Cl^+

10.1 Method

The time-independent Schrödinger equation for an atom colliding with another atom, with an interaction potential $V(R)$, can be written as:

$$[\nabla^2 + k^2 - U(R)]\Psi(R,\theta,\phi) = 0 \qquad (10.1)$$

where $$k^2 = \frac{2\mu}{\hbar^2}E \quad ; \quad U(R) = \frac{2\mu}{\hbar^2}V(R)$$

and μ is the reduced mass of the two atoms.

For an isotropic potential, the wavefunction can be expanded as a linear combination of Legendre polynomials such that:

$$\Psi(R,\theta) = \sum_{l=0}^{\infty} A_l \psi_l(R) P_l(\cos\theta) \qquad (10.2)$$

where l is the orbital angular momentum quantum number.

If the radial wavefunction is taken as

$$\psi_l(R) = \frac{g_l(R)}{R} \quad , \qquad (10.3)$$

then substituting the partial wave expansion of the wavefunction into the Schrödinger equation (10.1), multiplying both sides by $P_{l'}(\cos\theta)\sin\theta$ and integrating over θ gives the radial Schrödinger equation:

$$\frac{d^2 g_l(R)}{dR^2} + \left[k^2 - U(R) - \frac{l(l+1)}{R^2}\right] g_l(R) = 0 \quad . \qquad (10.4)$$

In a case where $U(R) = 0$ for all values of R, Eqn. (10.4) can be solved even for small R, since it becomes simply a variant of the well-known 'Bessel's equation'. Eqn. (10.4) would then have linearly independent solutions:

$$g_l(R) = kR \times j_l(kR) \qquad \text{and} \qquad g_l(R) = kR \times n_l(kR),$$

where $j_l(kR)$ and $n_l(kR)$ are spherical Bessel functions, which are known to have the properties [52]:

$$j_l(kR) \underset{R\to\infty}{\to} \frac{1}{kR}\sin\left(kR-\frac{\pi l}{2}\right)$$

$$n_l(kR) \underset{R\to\infty}{\to} \frac{1}{kR}\cos\left(kR-\frac{\pi l}{2}\right)$$

and

$$j_l(kR) \underset{R\to 0}{\to} \begin{array}{l} 1 \text{ for } l=0 \\ 0 \text{ for } l>0 \end{array}$$

$$n_l(kR) \underset{R\to 0}{\to} \infty \quad .$$

However, since $g_l(R)$ must be well-behaved at the origin, the solution to Eqn. (10.4) with zero potential would be just:

$$g_l(R) = kR\, j_l(kR) \quad . \qquad (10.5)$$

In the case where the potential in the interaction region is non-zero, the form of $g_l(R)$ in the asymptotic region, where the potential tends to zero, would be expected to be similar to the asymptotic form of Eqn. (10.5) but with the argument of the sine function 'shifted' to account for the effects of the potential. Hence,

$$g_l(R) \underset{R\to\infty}{\to} C\sin\left(kR-\frac{\pi l}{2}+\delta_l\right) \qquad (10.6)$$

where δ_l is called the 'phase shift' and carries all the information about the scattering due to the interaction potential. C is an arbitrary constant.

In order to check whether C is indeed a constant, Eqn. (10.6) can be written as:

$$g_l(R) \underset{R\to\infty}{\to} C(R)\left(e^{i\left(kR-\pi l/2+\delta_l\right)} - e^{-i\left(kR-\pi l/2+\delta_l\right)}\right)$$

and substituted into the radial Schrödinger equation (10.4). Taking just the positive exponential term for the sake of brevity, this gives:

$$\frac{d^2\left(C(R)e^{i(kR+\varepsilon)}\right)}{dR^2}+\left[k^2-U(R)-\frac{l(l+1)}{R^2}\right]C(R)e^{i(kR+\varepsilon)}=0$$

and since,

$$\frac{d}{dR}\left(C(R)\,e^{i(kR+\varepsilon)}\right)=\left[C'+ikC\right]e^{i(kR+\varepsilon)} \quad ,$$

$$\frac{d^2}{dR^2}\left(C(R)\,e^{i(kR+\varepsilon)}\right)=\left[(C''+ikC')+ik(C'+ikC)\right]e^{i(kR+\varepsilon)}=\left[C''+2ikC'-k^2C\right]e^{i(kR+\varepsilon)}$$

this becomes:

$$C''+2ikC'-\left[U(R)+\frac{l(l+1)}{R^2}\right]C=0 \quad .$$

For large R, C can be assumed to be sufficiently close to a constant such that [52]:

$$C'' \ll kC'$$

and so, neglecting the second derivative, separating the variables and integrating both sides gives:

$$2ik\ln C=\int^{R}\left[U(R)+\frac{l(l+1)}{R^2}\right]dR \quad .$$

Thus, for C to be a constant, the right-hand side of this equation must tend to a constant as R tends to infinity. That will be the case as long as $U(R)$ tends to zero faster than $1/R$. Hence, for systems with a potential of the order of $1/R^2$ or less, C will be a constant and the asymptotic form of the radial wavefunction can be written as Eqn. (10.6).

In the case of the scattering of a charged species by another charged species, the potential energy term in the Schrödinger equation includes a term:

$$V_{Coul}(R)=\frac{Z_A Z_B \varepsilon^2}{R}$$

where $Z_i\varepsilon$ is the charge on particle i. This does not fulfil the aforementioned condition and consequently, for such a system, the asymptotic form of the radial wavefunction cannot be written simply as a sum of e^{ikr} terms. The Coulombic potential is considered to have an 'infinite' range such that the scattering species is affected by it at all distances.

However, consider the function $f(R)$, such that (again taking as an example only the positive exponential term):

$$g_l(R)=C(R)\,e^{ikR}e^{f(R)}$$

and thus:

$$\frac{dg_l(R)}{dR}=\left[C'+Cik+Cf'\right]e^{ikR}e^{f(R)}$$

and

$$\frac{d^2g_l(R)}{dR^2}=\left[\left(C''+C'ik+C'f'+Cf''\right)+\left[ik+f'\right]\left(C'+Cik+Cf'\right)\right]e^{ikR}e^{f(R)}.$$

Substituting into the radial Schrödinger equation (10.4) this gives:

$$C''+C'(2ik+2f')+C\left(f''+2ikf'+(f')^2-U(R)-\frac{l(l+1)}{R^2}\right)=0.$$

Again, neglecting the second derivative of C, separating the variables and integrating both sides, one obtains:

$$\ln C=-\int^{R}\frac{1}{(2ik+2f')}\left(f''+2ikf'+(f')^2-U(R)-\frac{l(l+1)}{R^2}\right)dR \qquad . \quad (10.7)$$

Now, if $f(R)$ is defined as the function:

$$f(R)=a\ln(bR),$$

then Eqn. (10.7) reduces to:

$$\ln C = -\int^{R} \frac{dR}{\left(2ik + 2a/R\right)} \left[\frac{\left(a^2 - a - l(l+1)\right)}{R^2} + \left(\frac{2ika}{R} - U(R) \right) \right],$$

which, for a Coulombic potential, where $U(R) = \beta / R$, becomes:

$$\ln C = -\int^{R} \frac{dR}{\left(2ik + 2a/R\right)} \left[\frac{\left(a^2 - a - l(l+1)\right)}{R^2} + \left(\frac{2ika - \beta}{R} \right) \right].$$

In order for C to be a constant as R tends to infinity, the right-hand side must tend to a constant. This can be achieved if a is defined such that:

$$a = -i\frac{\beta}{2k}$$

for then the last bracketed term becomes zero.

Hence, for scattering over a Coulomb potential, the solution to Eqn. (10.4) is taken asymptotically to be [52]:

$$g_l(R) \underset{R\to\infty}{\to} C\left(e^{i\left(kR - \pi/2 + \delta_l - \gamma \ln 2kR\right)} - e^{-i\left(kR - \pi/2 + \delta_l - \gamma \ln 2kR\right)} \right)$$

or

$$g_l(R) \underset{R\to\infty}{\to} C \sin\left(kR - \frac{\pi l}{2} + \delta_l - \gamma \ln 2kR \right) \qquad (10.8)$$

where

$$\gamma = \frac{2\mu}{\hbar^2}\left(\frac{Z_A Z_B \varepsilon^2}{2k} \right)$$

which, for scattering involving two singly charged cations, as is the case in the Coulombic systems studied in this thesis, becomes simply

$$\gamma = \frac{\mu}{k}$$

when written in atomic units.

Both Eqn. (10.6) and Eqn. (10.8) can be written in terms of incoming and outgoing components:

$$g_l(R) \underset{R\to\infty}{\to} C(k)\left(e^{-ikR} - (-1)^l S_l(k) e^{ikR}\right)$$

and

$$g_l(R) \underset{R\to\infty}{\to} C(k)\left(e^{-i(kR-\gamma \ln 2kR)} - (-1)^l S_l(k) e^{i(kR-\gamma \ln 2kR)}\right)$$

where

$$S_l(k) = e^{2i\delta_l}$$

is the elastic scattering equivalent of the S-matrix of Chapter 4 and represents the effect of the scattering potential on the relative amplitudes of the incoming and outgoing parts of the radial wavefunction.

Just as for the inelastic scattering in Chapter 4, S_l can be calculated through propagation of the R-matrix by rewriting Eqn. (10.4) as

$$\frac{d^2 g_l(R)}{dR^2} = -\left[k^2 - U(R) - \frac{l(l+1)}{R^2}\right] g_l(R) \qquad (10.9)$$

and dividing the interaction space into sectors within each of which $U(R)$ can be taken to be constant, so that Eqn. (10.9) can then be written as

$$\frac{d^2 g_l^{(i)}(R)}{dR^2} = -\lambda_l^{2(i)} g_l^{(i)}(R) \qquad . \qquad (10.10)$$

The general solution to Eqn. (10.10) is

$$g_l^{(i)}(R) = \alpha e^{i\lambda_l^{(i)} R} + \beta e^{-i\lambda_l^{(i)} R} \qquad (10.11)$$

so that the sector R-matrix, defined as:

$$\begin{pmatrix} g_l^{(i)}(a) \\ g_l^{(i)}(b) \end{pmatrix} = \begin{pmatrix} r_{l1}^{(i)} & r_{l2}^{(i)} \\ r_{l3}^{(i)} & r_{l4}^{(i)} \end{pmatrix} \begin{pmatrix} -g_l'^{(i)}(a) \\ g_l'^{(i)}(b) \end{pmatrix},$$

with a and b the sector boundaries ($a < b$), will once again have the elements:

$$r_{l1}^{(i)} = r_{l4}^{(i)} = \begin{cases} \left|\lambda_l^{(i)}\right|^{-1} \coth\left|h\lambda_l^{(i)}\right| & \lambda_l^{(i)2} \le 0 \\ -\left|\lambda_l^{(i)}\right|^{-1} \cot\left|h\lambda_l^{(i)}\right| & \lambda_l^{(i)2} > 0 \end{cases}$$

$$r_{l2}^{(i)} = r_{l3}^{(i)} = \begin{cases} \left|\lambda_l^{(i)}\right|^{-1} \operatorname{csch}\left|h\lambda_l^{(i)}\right| & \lambda_l^{(i)2} \le 0 \\ -\left|\lambda_l^{(i)}\right|^{-1} \csc\left|h\lambda_l^{(i)}\right| & \lambda_l^{(i)2} > 0 \end{cases}$$

as with the inelastic scattering.

Note that Eqn. (10.11) is true even for elastic scattering with a Coulombic potential since, within each sector, the potential is seen as constant with respect to R. The effects of the Coulombic potential need only be considered later, when applying the asymptotic boundary conditions.

The propagation of the global R-matrix for elastic scattering is considerably quicker, computationally, than that for the inelastic scattering of Chapter 4, since all the matrices involved are reduced to a single element (1×1 matrix) and no diagonalisation is required. Thus,

$$\mathfrak{R}^{(i)} = r_4^{(i)} - r_3^{(i)} Z^{(i)} r_2^{(i)}$$

where

$$Z^{(i)} = \left[r_1^{(i)} + \mathfrak{R}^{(i-1)}\right]^{-1}$$

and so, taking

$$\mathfrak{R}^{(1)} = \frac{1}{\left|\lambda^{(1)}\right|} \quad ,$$

leads to the evaluation of $\mathfrak{R}^{(\infty)}$.

The S-matrix and thus the phase shift is then calculated by applying the asymptotic boundary conditions in accordance with Eqn. (10.6), or Eqn. (10.8) if the potential has a Coulombic term. Thus:

$$S_l^{reg} = e^{2i\delta_l^{reg}} = \left(e^{-ik_l R} + ik_l \mathfrak{R}_l^{(\infty)} e^{-ik_l r}\right)\left(e^{ik_l R} - ik_l \mathfrak{R}_l^{(\infty)} e^{ik_l r}\right)^{-1} \tag{10.12}$$

and:

$$S_l^{Coul} = e^{2i\delta_l^{Coul}} = \left(e^{-i(k_l R - \gamma \ln 2k_l R)} + i\left(k_l - \frac{\gamma}{R}\right)\mathfrak{R}_l^{(\infty)} e^{-i(k_l r - \gamma \ln 2k_l R)}\right)\left(e^{i(k_l R - \gamma \ln 2k_l R)} - i\left(k_l - \frac{\gamma}{R}\right)\mathfrak{R}_l^{(\infty)} e^{i(k_l r - \gamma \ln 2k_l R)}\right)^{-1}. \tag{10.13}$$

Cross sections

The phase shift itself is not a directly observable quantity in a scattering reaction. Instead, the differential cross section and the total cross section are measured as a function of collision energy. These quantities can be related to the phase shift by assuming that the wavefunction in the asymptotic region, where the measurements are made, can be written as the sum of two components, each of which satisfy the Schrödinger equation (10.1): an incident wave moving along the z-axis with momentum $\hbar k$ and a scattered spherical wave. Hence,

$$\Psi(R,\theta) \underset{R\to\infty}{\rightarrow} \Psi_{Incident} + \Psi_{Scattered} = e^{ikz} + \frac{f(\theta)}{R} e^{ikR} \quad . \qquad (10.14)$$

The differential cross section, defined as the number of scattered particles, per unit time per unit solid angle, divided by the number of incident particles, per unit time per unit area, is therefore:

$$\frac{d\sigma}{d\Omega} = \frac{\left|\Psi_{Scattered}\right|^2}{\left|\Psi_{Incident}\right|^2 / R^2} = \left|f(\theta)\right|^2 .$$

Since the incident plane wave is also a solution of the Schrödinger equation, it too can be written as a partial wave expansion such as Eqn. (10.2):

$$e^{ikz} = e^{ikR\cos\theta} = \sum_{l=0}^{\infty} B_l \psi_l(R) P_l(\cos\theta) \quad . \qquad (10.15)$$

Multiplying both sides of Eqn. (10.15) by $P_{l'}(\cos\theta)\sin\theta$ and integrating over angle θ from 0 to π gives:

$$\frac{2}{(2l'+1)} B_{l'} \psi_{l'}(R) = \int_{-1}^{1} e^{ikRt} P_{l'}(t) dt \qquad (10.16)$$

where the substitution $t = \cos\theta$ has been made. The right-hand side can be integrated by parts, to give:

$$\frac{2}{(2l'+1)}B_{l'}\psi_{l'}(R) = \frac{1}{ikR}\left[e^{ikRt}P_{l'}(t)\right]_{-1}^{1} - \frac{1}{ikR}\int_{-1}^{1}e^{ikRt}\frac{d}{dt}P_{l'}(t)\,dt$$

and further integration by parts of the second term on the right-hand side reveals it to be of order $\frac{1}{R^2}$. Thus, in the asymptotic region, Eqn. (10.16) can be taken as:

$$\frac{2}{(2l'+1)}B_{l'}\psi_{l'}(R) \approx \frac{1}{ikR}\left[e^{ikRt}P_{l'}(t)\right]_{-1}^{1}$$

which, since $P_l(1) = 1$ and $P_l(-1) = (-1)^l$, gives:

$$B_l\psi_l(R) = \frac{(2l+1)i^l}{kR}\sin\left(kR - \frac{\pi l}{2}\right).$$

Hence, Eqn. (10.15) becomes:

$$e^{ikz} = e^{ikR\cos\theta} = \sum_{l=0}^{\infty}\frac{(2l+1)i^l}{kR}\sin\left(kR - \frac{\pi l}{2}\right)P_l(\cos\theta)$$

$$= \sum_{l=0}^{\infty}\frac{(2l+1)i^l}{kR}\frac{1}{2i}\left(e^{i\left(kR-\frac{\pi l}{2}\right)} - e^{-i\left(kR-\frac{\pi l}{2}\right)}\right)P_l(\cos\theta)$$

and the total asymptotic wavefunction can therefore be written as:

$$\Psi(R,\theta) \underset{R\to\infty}{\to} \sum_{l=0}^{\infty}\frac{(2l+1)i^l}{kR}\frac{1}{2i}\left(e^{i\left(kR-\frac{\pi l}{2}\right)} - e^{-i\left(kR-\frac{\pi l}{2}\right)}\right)P_l(\cos\theta) + \frac{f(\theta)}{R}e^{ikR} \quad . \qquad (10.17)$$

The partial wave expansion of the total asymptotic wavefunction, Eqn. (10.2), using the form of the radial wavefunction appropriate to a non-Coulombic potential, Eqn. (10.6), is:

$$\Psi(R,\theta) \underset{R\to\infty}{\to} \sum_{l=0}^{\infty}A_l\left(e^{i(kR-\pi/2+\delta_l)} - e^{-i(kR-\pi/2+\delta_l)}\right)P_l(\cos\theta) \quad . \qquad (10.18)$$

Comparing the coefficients of e^{-ikR} in Eqns. (10.17) and (10.18) leads to the expression for the coefficients of the partial wave expansion of Eqn. (10.18):

$$A_l = \frac{(2l+1)i^l}{kR}\frac{1}{2i}e^{i\delta_l}$$

and then, comparing the coefficients of e^{ikR}, leads to:

$$f(\theta) = \sum_{l=0}^{\infty}\frac{(2l+1)}{2ik}\left(e^{2i\delta_l}-1\right)P_l(\cos\theta) = \sum_{l=0}^{\infty}\frac{(2l+1)}{k}e^{i\delta_l}\sin\delta_l\ P_l(\cos\theta).$$

The differential cross section is then:

$$\frac{d\sigma}{d\Omega} = |f(\theta)|^2$$

and the total cross section is:

$$\sigma = 2\pi\int_0^{\pi}\frac{d\sigma}{d\Omega}\sin\theta\, d\theta = \sum_{l=0}^{\infty}\frac{4\pi(2l+1)}{k^2}\sin^2\delta_l \quad . \qquad (10.19)$$

This expression for the total cross section is only strictly valid for a system with a 'regular' potential. The infinite range of the Coulomb potential, besides affecting the form of the asymptotic radial wavefunction (Eqn. (10.8)), also prevents the description of the asymptotic wavefunction as having the two simple components of Eqn. (10.14). Instead a more complicated description is required and this, in turn, results in a much more complicated expression for the total cross section [52] which, at least in the case of a purely Coulombic potential, actually diverges to infinity.

Resonances

As mentioned briefly in the Introduction, the potential energy surface which is used to describe the elastic scattering of the two species, A and B, is equivalent to that which would be used to describe the dissociation of the molecule AB to form fragments A and B. Hence, the amount of the internal energy of any bound or quasi-bound vibrational state of AB, when introduced instead as the collision energy for the scattering of A by B, will result in the formation of orbiting complexes of A and B. These states will exist at energies within the potential well of the system and, dependent on the shape of the potential, can break down by travelling through the potential barrier (Figure 17).

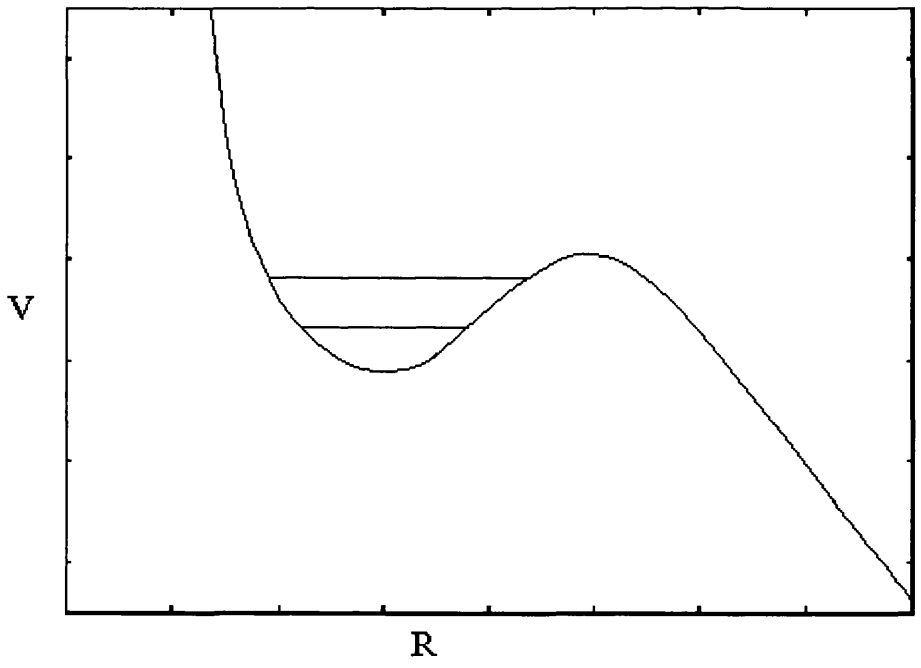

Figure 17 Example of potential surface supporting quasi-bound levels (horizontal lines) in potential well. The states may dissociate by tunnelling through the potential barrier.

Now, generally, the total flux of particles in a simple scattering interaction is conserved and this can be confirmed by evaluating the outgoing current destiny function, defined as:

$$j = \frac{-i\hbar}{2\mu}\left(\Psi^* \nabla\Psi - \Psi\nabla\Psi^*\right) \quad . \qquad (10.20)$$

Substituting the wavefunction, Eqn. (10.18), into Eqn. (10.20) gives

$$j^l = \frac{\hbar}{\mu}\left[S_l^2 - 1\right] \quad = \frac{\hbar}{\mu}\left[\left| e^{2i\delta_l}\right|^2 - 1\right] \quad = 0$$

as required. Thus, the radial wavefunction

$$\psi_l(R) = C\left(e^{-ik_k R} - (-1)^l S_l\, e^{ik_k R}\right) \qquad (10.21)$$

has incoming and outgoing components of the same magnitude.

At energies which correspond to quasi-bound states and orbiting complexes, however, the wavefunction must have a net incoming or net outgoing current density: for a system prepared as a quasi-bound state and allowed to dissociate, the radial wavefunction, Eqn. (10.21), will consist solely of an outgoing term, whereas the formation of an orbiting complex as a result of scattering would leave the radial wavefunction with a purely incoming term.

This lack of conservation of flux can be accounted for by introducing an imaginary component to the wavenumber, k [30]. Thus, if

$$k = k_1 + ik_2 \quad ,$$

the outgoing current density will become:

$$j_R^l = \frac{-i\hbar}{2\mu}\left(\psi_l^* \frac{d\psi_l}{dR} - \psi_l \frac{d\psi_l^*}{dR}\right)$$

$$= -\frac{i\hbar}{2\mu}\left(2(-1)^{(l+1)} k_2 \left(S_l\, e^{2ik_1 R} - S_l^*\, e^{-2ik_1 R}\right) - 2ik_1\left(e^{2k_2 R} - |S_l|^2 e^{-2k_2 R}\right)\right)$$

$$= \frac{\hbar}{2\mu}\left((-1)^{(l+1)}k_2\left(\sin(2k_1R - 2\delta_l)\right) - 2k_1\left(e^{2k_2R} - |S_l|^2 e^{-2k_2R}\right)\right) \quad .$$

As $R \to \infty$, the right-hand bracketed term will be dominant and so, the outgoing density will be negative (i.e. net incoming flux) if the product k_1k_2 is positive and positive (i.e. net outgoing flux) if the product k_1k_2 is negative.

The energy will then also be a complex number, since:

$$E = \frac{\hbar^2}{2\mu}k^2 = \frac{\hbar^2}{2\mu}\left(k_1^2 - k_2^2 + 2ik_1k_2\right)$$

and so, for the dissociation of a quasi-bound state the energy eigenvalue can be written as:

$$E_b = E_1 - iE_2 \qquad (10.22)$$

whilst, for the formation of an orbiting complex:

$$E_c = E_1 + iE_2 \qquad (10.23)$$

with $|E_b| = |E_c|$.

The quantity S_l is the ratio of the outgoing component of the radial wavefunction to the incoming component. Hence, S_l would be expected to become infinite as the energy tends towards the energy of the quasi-bound state and zero as the energy tends towards the energy of the orbiting complex. Thus, since for real energies $|S_l| = 1$, in the region of the quasi-bound/orbiting complex the S_l term can be written as:

$$S_l = e^{2i\delta_l} = \left[\frac{E - (E_1 + iE_2)}{E - (E_1 - iE_2)}\right]e^{2i\delta_l^{(0)}} \qquad (10.24)$$

and, recognising that, for

$$y = \tan x = -i\frac{\left(e^{ix} - e^{-ix}\right)}{\left(e^{ix} + e^{-ix}\right)} \quad ,$$

$$e^{2ix} = \left(\frac{1+iy}{1-iy}\right),$$

this gives the phase shift in terms of the Breit-Wigner [53] form:

$$\delta_l = \delta_l^{(0)} + \arctan\left(\frac{E_2}{E_1 - E}\right) \quad . \qquad (10.25)$$

As the energy of the system reaches E_1, therefore, the phase shift will increase by π at a rate determined by E_2. This results in the appearance of a resonance, of width $2E_2$ (usually written as Γ), in a plot of the total cross section as a function of collision energy, where:

$$\sigma_l = \frac{4\pi}{k^2}(2l+1)\sin^2\delta_l = \frac{4\pi}{k^2}(2l+1)\sin^2\left(\delta_l^{(0)} + \arctan\left(\frac{\Gamma}{2(E_1 - E)}\right)\right)$$

or, writing

$$\sin\delta_l = e^{-i\delta_l}(S_l - 1)$$

and using Eqn. (10.24) [54],

$$= \frac{4\pi}{k^2}(2l+1)\left[\sin^2\delta_l^{(0)} + \frac{\Gamma^2}{4(E-E_1)^2 + \Gamma^2} + 2\,\mathrm{Re}\left(e^{i\delta_l^{(0)}}\sin\delta_l^{(0)}\frac{\Gamma}{2(E_1 - E) - i\Gamma}\right)\right]. \qquad (10.26)$$

The lifetime of the quasi-bound state and orbiting complex can be determined by looking at the time-dependence of the wavefunction at the energy defined by Eqn. (10.22):

$$\Psi(t) = e^{-(iEt/\hbar)} = e^{-(iE_1 t/\hbar)}e^{-(\Gamma t/2\hbar)}.$$

The probability that the system remains intact is therefore:

$$|\Psi(t)|^2 = e^{-(\Gamma t/\hbar)}$$

and thus it decays exponentially with a lifetime, τ, where

$$\tau = \frac{\hbar}{\Gamma} \quad .$$

Potential Energy Surface

Bennett and McNab [50] have calculated *ab initio* the one-dimensional potential energy surface for the dissociation of HCl^{2+}, for the four lowest electronic states of HCl^{2+}. They used internally contracted multi-reference configuration interaction calculations, based on complete active space SCF wavefunctions. For this research, the points supplied [50] for the potential surface of the lowest electronic state, $X^3\Sigma^-$, have been fit to the potential function:

$$V(R) = a_1 \exp(-a_2 R)(1 + a_3 R + a_4 R^2 + a_5 R^3) + \frac{1}{R}.$$

and a section of the fitted surface is shown in Figure 18.

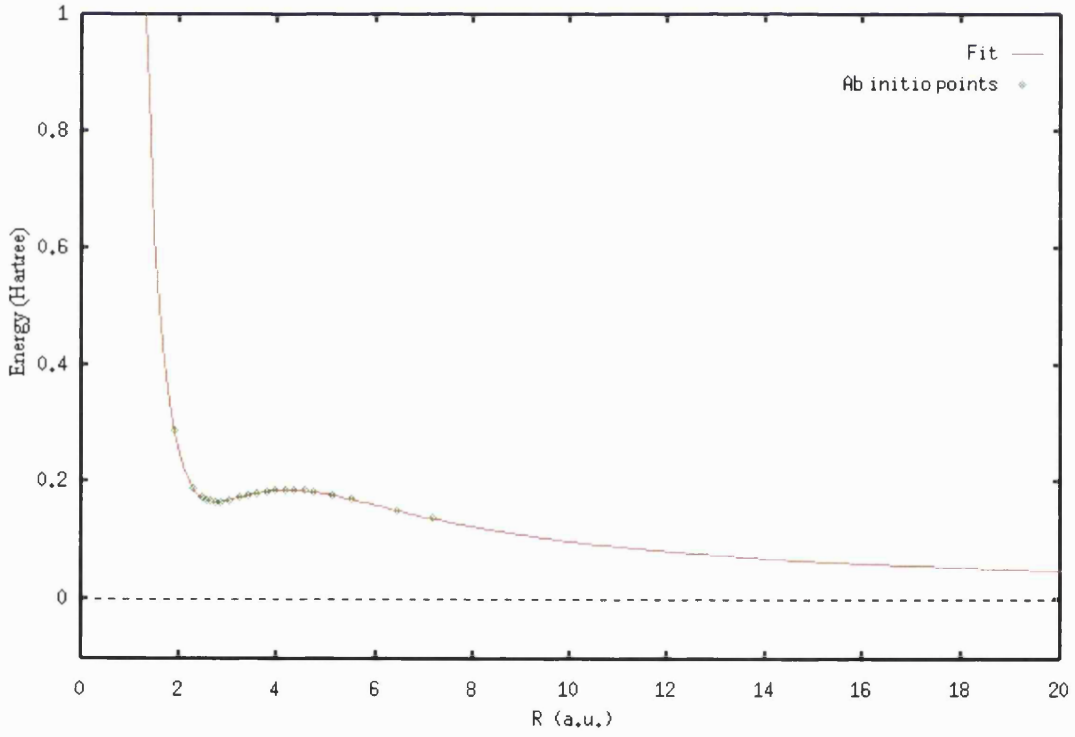

Figure 18 Potential energy surface for lowest electronic state of $HCl^{2+} \leftrightarrow H^+ + Cl^+$.

The $1/R$ term of the Coulombic potential results in the potential surface decaying at a much larger value of R than that for a non-Coulombic potential which would have repulsive terms only of order $1/R^2$ or less. This means that it will be necessary to propagate the wavefunction of a Coulombic system out to much large distances than are required for a system with a non-Coulombic potential, even when the correct asymptotic boundary conditions are applied.

It is worth noting, as Bennett and McNab point out, that, whereas the potentials of the three excited electronic states calculated in Ref. [50] exhibit some crossing between states, the lowest, $X^3\Sigma^-$, state is not crossed by any other. Therefore, whereas resonances found using the potentials of the excited states may be due to electronic predissociation as much as to tunnelling through the potential barrier, the ground electronic state of HCl^{2+} can only dissociate by tunnelling.

10.2 Results

The phase shift, δ_l, for the scattering of H^+ with Cl^+ has been calculated by the method of R-matrix propagation across the range of collision energies corresponding to the potential well in Figure 18, using both regular and Coulombic asymptotic boundary conditions (Eqns. (10.12) and (10.13)). Since the information about the quasi-bound levels published in Ref. [50] is only for zero angular momentum and moreover the aim of this study is just to compare the effects of the different boundary conditions, the calculations were carried out for $l = 0$ only.

As with the propagation of the inelastic scattering in Part 1, in order for the results to be meaningful it is necessary to find convergence in the results with respect to the width of the sectors into which the interaction space is divided and to the position at which the asymptotic boundary conditions are applied, R^∞. The phase shift can only be calculated modulo π and so it is easier to detect convergence in the total cross section, σ, as defined by Eqn. (10.19). Although, as discussed in the method, the definition of the total cross section used here is not strictly valid for scattering on a Coulombic potential and thus not consistent with the use of the Coulombic boundary conditions, it has nevertheless been used throughout in order to facilitate the comparison of the phase shifts evaluated using both forms of boundary conditions. This means that the values of the cross sections found here may not be comparable to experimentally observed cross sections, should such a study ever be made.

Figure 19 shows the results of a test of the convergence of the total cross section with respect to R^∞ using both forms of the boundary conditions. It can be seen that, whilst convergence was found when applying the Coulombic boundary conditions, albeit at a very large distance of R, such convergence was not observed at all when using regular boundary conditions.

These results reveal that it is necessary to use the Coulombic form of the boundary conditions when calculating theoretically the phase shifts and cross sections of an interaction with a Coulombic potential.

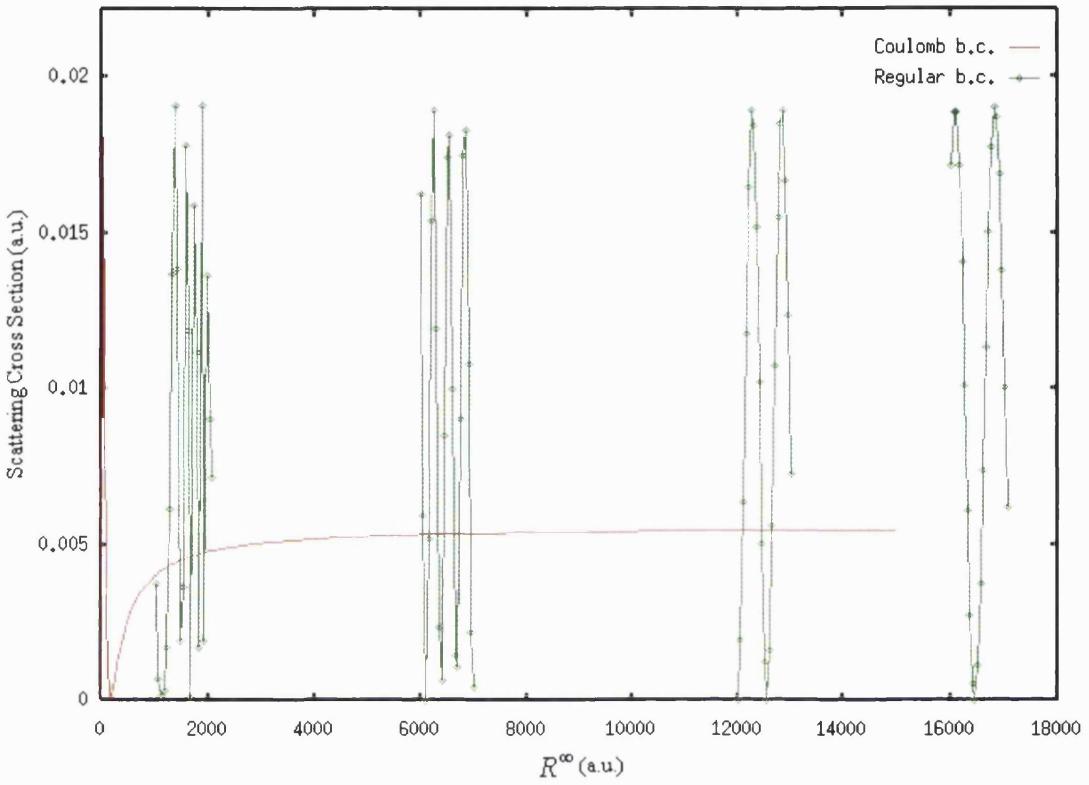

Figure 19 Comparison of convergence of total cross section for scattering of H^+ by Cl^+ with E_c = 5eV using regular and Coulombic boundary conditions. For clarity, only samples of the results using regular boundary conditions are shown.

Thus, in order to compare the effects of the alternative boundary conditions on the positions and widths of the resonances found in the scattering reaction, it has been necessary to choose an arbitrary value of R^{∞} when applying the regular boundary conditions. To ensure the validity of the conclusions made, two different values of R^{∞} have been used, both of which are considerably larger than that used for the Coulombic boundary conditions.

From Eqn. (10.25) it is seen that the presence of a resonance will result in a displacement of π in a plot of the curve of the phase shift as a function of collision energy. Therefore, since the phase shift is calculated modulo π, it is very possible that any resonance will be mistaken for a simple cyclic shift, particularly when the resonance is sharp. It is therefore a lot easier to locate resonances in a plot of the total cross section as a function of collision energy, which would have the shape defined by Eqn. (10.26).

However, it is still necessary to ensure that the grid of energy points at which the cross section is calculated is narrow enough to reveal any resonances present. Clearly, the longer the lifetime of the orbiting complex, the greater the resolution required in the cross section plot. A method of facilitating the detection of resonances has been used in this research which involves choosing three points along the curve of total cross section versus collision energy, E_c, and fitting them to a quadratic equation in E_c. This is repeated along the whole curve, keeping the first two points constant but varying the third. A plot of the coefficient of the squared term of the quadratic, as a function of E_c, will then be much more sensitive than the total cross section itself to the presence of a resonance. This is because, for small $(E-E_1)$, the second derivative with respect to E of Eqn. (10.26) shows greatly increased dependence on $(E-E_1)$.

Bennett and McNab [50] observe three resonances using the $X^3\Sigma^-$ potential surface and report their relative energies and the tunnelling lifetimes of the corresponding vibrational states. The longest lived state has a resonance width which is less than the rounding-error of the available computers and thus could not be located in this study. The other two resonances were located (Figure 20), using both forms of the boundary conditions, and fit to Eqn. (10.26) to give the values of Γ, E_1 and $\delta^{(0)}$ for each resonance. The results are shown in Table 4.

	Coulombic Boundary Conditions		Regular Boundary Conditions			
R^{∞} (a_0)	6000		10000		12500	
E_1 (eV)	4.8498227	5.0075245	4.8498227	5.00752369	4.8498227	5.00752695
Γ (eV)	8.0342 E-9	1.3718 E-4	7.9206 E-9	1.2673 E-4	7.9521 E-9	1.2129 E-4
τ (sec)	0.81 E-7	0.48 E-11	0.83 E-7	0.52 E-11	0.82 E-7	0.54 E-11
$\delta^{(0)}$	– 0.5046	– 0.71027	– 50.527	0.58421	– 68.285	0.78954

Table 4 Resonance parameters for the two highest orbiting complexes formed in the scattering of H^+ with Cl^+.

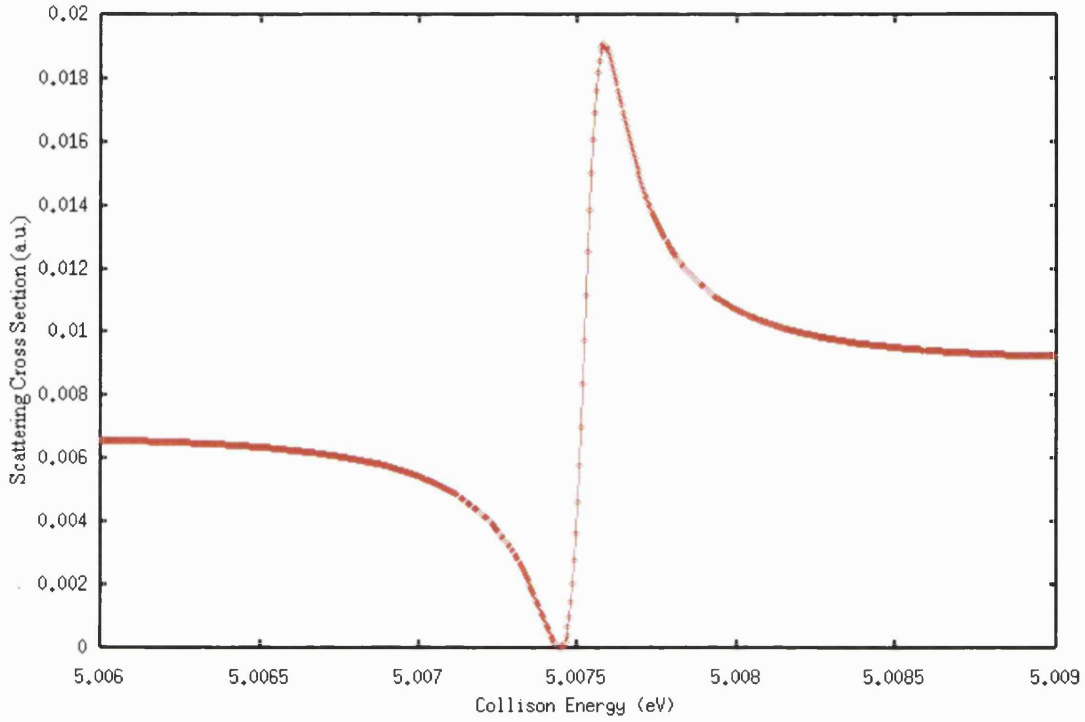

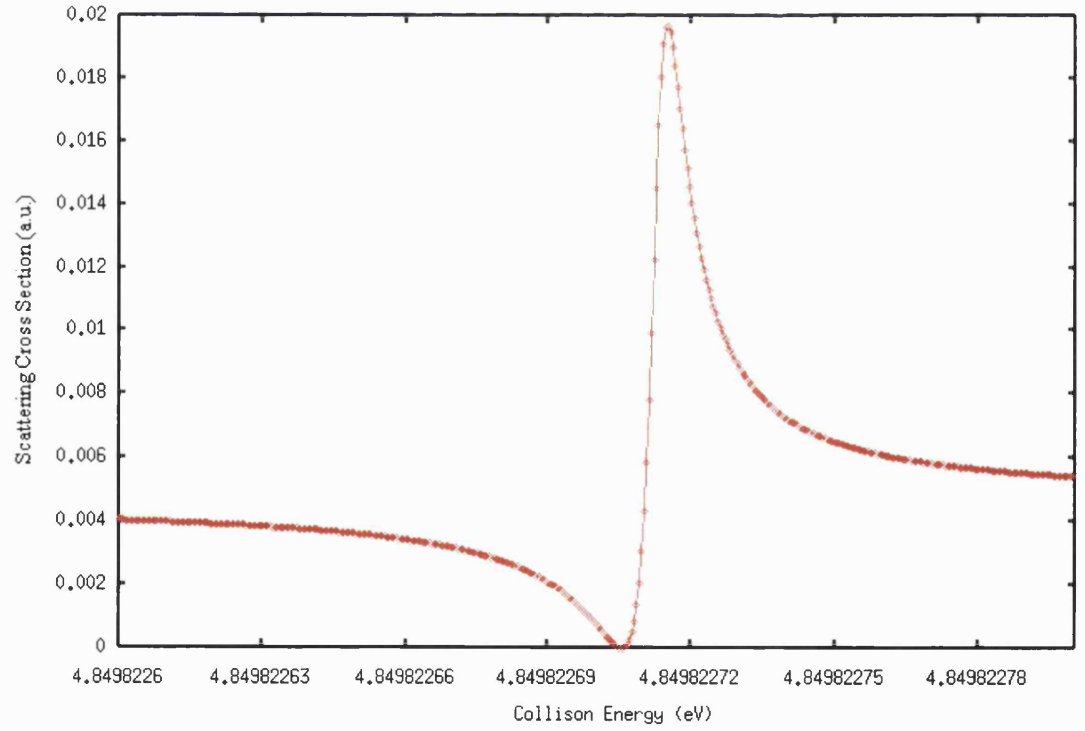

Figure 20 Resonances in the total cross section as a function of collision energy for the scattering of H^+ with Cl^+ using boundary conditions appropriate for a Coulombic potential.

As Table 4 shows, the energies and widths of the resonances found using the regular boundary conditions, at both values of R^{∞} tested, are well within the acceptable error range for the theoretical calculations, when compared to those found using the Coulombic boundary conditions. The only parameter which is significantly affected by the incorrect form of the asymptotic boundary conditions is $\delta^{(0)}$, the "background" phase-shift term of Eqn. (10.25), which is independent of the resonances. It appears, therefore, that all the information about a resonance is decided in the region of the potential barrier and no further propagation of the wavefunction would be necessary in order to ascertain the lifetime and energy of a quasi-bound state or orbiting complex. This is consistent with the results of a study made on the decay of HS^{2+} to $H^{+} + S^{+}$ by Parlant *et al* [55], where the lifetimes of quasi-bound states, calculated using the lifetime matrix theory of Smith [56], were found to be insignificantly affected by the Coulomb tail of the potential surface.

The conclusion of this study, then, is that it is necessary to consider the appropriate boundary conditions for a system with a Coulombic potential when calculating the phase shifts and cross sections of a scattering interaction, but not when ascertaining the energies or the widths of any resonances present. It remains to be seen, however, how the alternative boundary conditions would affect the internal product distribution of an event, such as the dissociation of O_3^{2+}, since this is only dependent on the relative probabilities of the different internal states rather than the absolute values.

11 Dissociation of the Ozone Dication: Method

The aim of the final investigation in this thesis is to find the relative probabilities of each of the internal energy states of the O_2^+ diatom being produced as a result of the double ionisation of the bound O_3 molecule. The double ionisation of the O_3 molecule can be considered as giving rise to a wavefunction which can be expressed as a linear combination of all possible wavefunctions of the system $O_3^{2+} \leftrightarrow O_2^+ + O^+$ that have outgoing components, in the asymptotic region, for only one internal state of the O_2^+ diatom [57]. There will be one such term of this expansion for each internal energy state of O_2^+ and the square of the coefficients of the expansion will therefore give the probabilities that the internal state associated with each coefficient will be produced.

It is possible to determine the value of these coefficients, and hence the product distribution of the O_2^+ fragment, by calculating the overlap of the wavefunction of the initial system with that of each of the possible final systems. Since the ionisation of the O_3 molecule in Ref. [47] is achieved through electron impact, a complete theoretical model of the experiment would have to involve describing the wavefunctions for the molecules together with the free electrons. However, such a calculation would be extremely complex and so, in this study, a Franck-Condon approximation has been made, such that just the transition of the molecules is considered.

Hence, since the objective is only to find the relative probabilities of the internal states of the O_2^+ product formed, the aim of the calculations is to evaluate the square of the overlaps of the molecular wavefunctions, namely:

$$P(f) \propto \left| \left\langle \Psi^f_{O_2^+ + O^+} \middle| \Psi_{O_3} \right\rangle \right|^2 \qquad (11.1)$$

for each f, where f labels the final state of the diatom.

As mentioned in the introduction, the wavefunction for the excited system is described here as a scattering wavefunction, even though the initial result of the

double ionisation of the neutral ozone molecule may well be a quasi-bound dication, O_3^{2+}. Nevertheless, since the primary purpose of these calculations is to determine the distribution of internal energies of the O_2^+ fragment at an ostensibly infinite distance from the position of the excitation, it is much more practicable to represent the excited system as a scattering interaction between O_2^+ and O^+ than as the dissociation of the bound molecule, O_3^{2+}. The internal energy of the O_3^{2+} dication is therefore to be associated with the total energy of the scattering system of $O_2^+ + O^+$.

Another noteworthy feature of the method outlined in this chapter relates to the form of the wavefunction for the bound O_3 molecule. Although it is possible to evaluate the required overlap of the scattering and bound wavefunctions using a description of the bound wavefunction calculated independently, the calculations can be simplified if the O_3 wavefunction is also described in terms of scattering coordinates and expanded using the same basis set as that of the $O_2^+ + O^+$ scattering wavefunction. As will be shown below, the precise value of the bound energy level of the O_3 molecule can actually be determined directly through a calculation of the overlap of the two wavefunctions and, as a result, this method has the additional advantage of providing a test for the computer code used in the calculations.

11.1 Close-Coupled Equations

Using the same notation as for Part 1, the Hamiltonian for the scattering wavefunction, $\Psi_{O_2^+ + O^+}$, in the body-fixed coordinate system is:

$$\hat{H}_{O_3^{2+}/O_2^+ + O^+} = -\frac{\hbar^2}{2\mu}\left[\left(\frac{\partial}{\partial R}+\frac{1}{R}\right)^2 - \frac{\left|\hat{J}-\hat{j}\right|^2}{R^2}\right] + \hat{H}_{O_2^+} + \hat{V}_{O_2^+ - O^+}(R,r,\gamma) \qquad (11.2)$$

where $\hat{H}_{O_2^+}$ is the Hamiltonian for the diatomic ion O_2^+, and the scattering wavefunction can be expressed as a partial wave expansion:

$$\Psi^{f}_{O_3^{2+}/O_2^+ + O^+} = \frac{1}{R}\sum_{v'j'}\phi_{j'}(r')\chi_{v'j'}(r)\psi^{O_2^+(f)+O^+}_{v'j'}(R) \quad . \qquad (11.3)$$

where, once again, f labels the internal state of the O_2^+ fragment. The basis set in this expansion consists, as in Part 1, of the solutions to the diatomic Schrödinger equation for O_2^+.

Since this basis set is complete, the bound wavefunction for O_3 can also be expanded in terms of the wavefunctions of O_2^+:

$$\Psi_{O_3} = \frac{1}{R}\sum_{v''j''}\phi_{j''}(r')\chi_{v''j''}(r)\psi^{O_3}_{v''j''}(R) \quad . \qquad (11.4)$$

Thus, the calculation of the overlap of the wavefunctions, Eqn. (11.1), becomes:

$$\mathbf{O} = \left\langle \frac{1}{R}\sum_{v'j'}\psi^{O_2^+(f)+O^+}_{v'j'}\chi_{v'j'}\phi_{j'} \middle| \frac{1}{R}\sum_{v''j''}\phi_{j''}\chi_{v''j''}\psi^{O_3}_{v''j''} \right\rangle$$

which, due to the orthonormal nature of the basis set, reduces to:

$$\mathbf{O} = \int_0^\infty \sum_{v'j'}\sum_{v''j''}\psi^{O_2^+(f)+O^+\,*}_{v'j'}\delta_{v'v''}\delta_{j'j''}\psi^{O_3}_{v''j''}\,dR \quad . \qquad (11.5)$$

Hence, the calculation of the product distribution can be achieved by solving close-coupled equations similar to those discussed in Part 1, for both the O_3 and the O_2^+ / O^+ systems, and evaluating the overlap of the solutions.

The calculations have only been carried out for zero total angular momentum, and so the close-coupled equations for the O_2^+/O^+ system can be written as:

$$\left[\frac{d^2}{dR^2}+k^2_{Sv''j''}-\frac{[j'''(j'''+1)]}{R^2}\right]\psi^{O_2^+(f)+O^+}_{v''j''}(R)=\frac{2\mu}{\hbar^2}\sum_{v'j'}\left\langle \phi_{j''}\chi_{v''j''}\left|\hat{V}_{O_2^+-O^+}\right|\phi_{j'}\chi_{v'j'}\right\rangle \psi^{O_2^+(f)+O^+}_{v'j'}(R) \tag{11.6}$$

where $\hat{V}_{O_2^+-O^+}$ is the interaction potential between the atom and diatom and:

$$k^2_{Sv''j''}=\frac{2\mu}{\hbar^2}\left(E^{O_3^{2+}}-\epsilon^{O_2^+}_{v''j''}\right) \quad .$$

There exists, at every value of the total energy for the scattering system, $E^{O_3^{2+}}$, a separate set of these coupled equations for each final internal state of O_2^+ and so, as with the coupled equations in Part 1, Eqns. (11.6) can be written in matrix form as:

$$\left[\frac{d^2}{dR^2}+k^2_{Sv''j''}-\frac{[j'''(j'''+1)]}{R^2}\right]\underline{\underline{\psi}}^{O_2^++O^+}=\underline{\underline{\hat{V}}}_{O_2^+-O^+}\underline{\underline{\psi}}^{O_2^++O^+} \quad . \tag{11.7}$$

The bound O_3 molecule would generally be expected to produce O_2+O were it to dissociate, as shown in Figure 16. Nevertheless, it is still entirely valid to write the nuclear Hamiltonian for O_3 in terms of the O_2^+ diatom as for the scattering system, Eqn. (11.2), since the kinetic operator terms are independent of the electronic charge, as long as the potential energy operator is adapted accordingly. Thus,

$$\hat{H}_{O_3}=-\frac{\hbar^2}{2\mu}\left[\left(\frac{\partial}{\partial R}+\frac{1}{R}\right)^2-\frac{\left|\hat{J}-\hat{j}\right|^2}{R^2}\right]+\left[\hat{T}_{O_2^+}(r)+\hat{V}_{O_2^+}(r,r')\right]+\hat{V}_{O_2^+-O^-}(R,r,\gamma)$$

or, describing the potential operator in terms of the potential surface of the bound O_3 molecule:

$$\hat{H}_{O_3}=-\frac{\hbar^2}{2\mu}\left[\left(\frac{\partial}{\partial R}+\frac{1}{R}\right)^2-\frac{\left|\hat{J}-\hat{j}\right|^2}{R^2}\right]+\hat{H}_{O_2^+}+\left[\hat{V}_{O_3}(R,r,\gamma)-\hat{V}_{O_2^+}(r,r')\right].$$

Substituting this Hamiltonian, along with the partial wave expansion in terms of O_2^+ eigenfunctions, Eqn. (11.4), into the Schrödinger equation for the bound O_3 molecule, leads to the close-coupled equations for the O_3 system:

$$\left[\frac{d^2}{dR^2} + k_{Bvj}^2 - \frac{[j(j+1)]}{R^2}\right]\psi_{vj}^{O_3}(R) = \frac{2\mu}{\hbar^2}\sum_{v'j'}\left\langle \phi_j \chi_{vj} \left| \hat{V}_{O_3} - \hat{V}_{O_2^+} \right| \phi_{j'} \chi_{v'j'} \right\rangle \psi_{v'j'}^{O_3}(R) \tag{11.8}$$

where $k_{Bvj}^2 = \frac{2\mu}{\hbar^2}\left(E^{O_3} - \epsilon_{vj}^{O_2^+}\right)$.

Unlike the coupled equations for the scattering reaction, at any given bound energy there exists only one possible linear combination of the basis set which fulfils the boundary conditions for the wavefunction of the bound molecule. Hence, the matrix form of the overlaps, Eqns. (11.5), would consist of the integration of a matrix multiplied by a vector:

$$\underline{\mathbf{O}}\left(E^{O_3^{2+}}, E^{O_3}\right) = \left\langle \underline{\underline{\psi}}^{O_2^+ + O^+}\left(E^{O_3^{2+}}\right) \middle| \underline{\psi}^{O_3}\left(E^{O_3}\right) \right\rangle \quad , \tag{11.9}$$

where the square of each element of the $\underline{\mathbf{O}}$ vector is the probability of a particular internal state of O_2^+ being detected as a result of the excitation of the O_3 neutral in the bound state with energy E^{O_3}, to the doubly ionised O_3^{2+} dication with total energy $E^{O_3^{2+}}$.

11.2 The Potential Energy Matrices

The elements of the potential energy matrix, $\langle \phi_{j'} \chi_{v'j'} | \hat{V} | \phi_j \chi_{vj} \rangle$, of both Eqn. (11.6) and Eqn. (11.8) involve the eigenfunction solutions to the Schrödinger equation for the diatomic ion O_2^+. The diatomic rotation wavefunctions, ϕ_j, are the normalised spherical harmonic wavefunctions, $Y_{j0}(r')$, and the ro-vibrational terms, $\chi_{vj}(r)$, are calculated using the PO-DVR method described in Part 1, Section 3.4.

11.2.1 The Potential Matrix Elements for O_3^{2+}

The *ab initio* potential energy surface for process (3) has been calculated by Champkin *et al* [48] using the state averaged CASSCF/MRCI method implemented in the program MOLPRO. The lowest potential surface is that of the triplet state of O_3^{2+} and that surface has been used in the present analysis. The grid of potential energy points, provided by Champkin, has been incorporated into these calculations using the same method as that of the Σ treatment described in Part 1, Section 3.2.2.

The potential matrix elements of Eqn. (11.6) can therefore be expressed in a similar form as that derived in Section 3.3.1, namely:

$$\langle \phi_{j''} \chi_{v''j''} | \hat{V}_{O_2^+ - O^+} | \phi_{j'} \chi_{v'j'} \rangle = (2j'+1)^{1/2}(2j'''+1)^{1/2} \sum_{l}^{\infty} \int dr\, \chi^*_{v''j''}(r)\, V_{l0}(R,r) \chi_{v'j'}(r) \begin{pmatrix} j' & l & j''' \\ 0 & 0 & 0 \end{pmatrix} \begin{pmatrix} j' & l & j''' \\ 0 & 0 & 0 \end{pmatrix} \quad (11.10)$$

and, as in Part 1, for the homonuclear $^{16}O_2^+$ diatom, j takes only even values.

11.2.2 The Potential Matrix Elements for O_3

The potential energy surface for the bound O_3 molecule used in this analysis is based upon the potential function developed by Barbe, Secroun and Jouve [49] to fit with spectroscopic data for $^{16}O_3$. For simplicity, the expansion of the potential in terms of the internal coordinates of O_3 has been truncated to the quadratic terms. Thus, the potential function is written as:

$$\hat{V}_{O_3} = \tfrac{1}{2} f_r\left(\Delta r_1^2 + \Delta r_2^2\right) + f_{rr}\left(\Delta r_1 \Delta r_2\right) + f_{r\theta}\left(\Delta r_1 + \Delta r_2\right) r_e \Delta\theta + \tfrac{1}{2} f_\theta r_e^2 \Delta\theta^2 \qquad (11.11)$$

where $\Delta r_1 = r_1 - r_{1e}$

$\Delta r_2 = r_2 - r_{2e}$

$\Delta\theta = \theta - \theta_e$

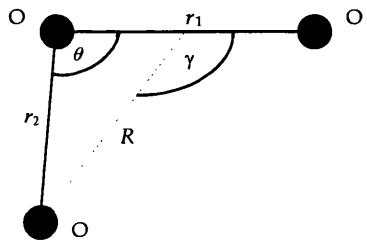

and the subscript e refers to the equilibrium values, which are:

$$r_e = r_{1e} = r_{2e} = 1.2717 \text{ Å} \quad ; \quad \theta_e = 116.783^\circ \quad .$$

The quadratic force constants are taken as [49]:

$$f_r = 6.163 \text{ mdynes Å}^{-1} \quad ; \quad f_{rr} = 1.602 \text{ mdynes Å}^{-1}$$

$$f_{r\theta} = 0.402 \text{ mdynes Å}^{-1} \quad ; \quad f_\theta = 1.300 \text{ mdynes Å}^{-1} \quad .$$

For the purposes of these calculations, the coordinates in the potential function are transformed to those used for the scattering system, such that:

$$r_1 = r \quad ; \quad r_2 = \left[R^2 + \left(r/2\right)^2 - rR\cos\left(\pi - \gamma\right) \right]^{1/2} \quad ; \quad \theta = \cos^{-1}\left(\frac{\left(r/2\right)^2 + r_2^2 - R^2}{r \times r_2} \right).$$

The potential matrix elements of Eqn. (11.8) are then integrated over the angular coordinate directly:

$$\left\langle \phi_j \middle| \hat{V}_{O_2^+ - O^-} \middle| \phi_{j'} \right\rangle$$

$$= \int_0^\pi \tfrac{1}{2}(2j+1)^{1/2}(2j''+1)^{1/2} P_j(\cos\gamma) \left[\hat{V}_{O_3}(R, r, (\cos\gamma)) - \hat{V}_{O_2^+} \right] P_{j'}(\cos\gamma) \sin\gamma \, d\gamma \, .$$

11.3 Calculating the Overlap Matrix

The solution of the coupled equations, Eqn. (11.6) and Eqn. (11.8), can be simplified, as explained in Chapter 4, by dividing the interaction space into sectors within each of which the potential surface is considered to be constant with respect to the translational coordinate, R. However, the integration which must be carried out to obtain the vector of overlaps, Eqn. (11.9), requires a knowledge of the actual translational wavefunctions, $\psi(R)$, across the entire interaction space, not just the asymptotic R-matrix as in Part 1. Rather than propagating the bound and scattering wavefunctions individually across the whole interaction space before determining the total overlap, Light and co-workers [58–61] have developed the R-matrix theory of Ref. [45] to enable the calculation of the overlap for each sector, followed by the propagation of the overlap itself. The precise details used in this research have been taken from Heather and Light, Ref. [60].

The method devised by Heather and Light has only ever been described for systems where the scattering wavefunction is assumed to tend to non-Coulombic boundary conditions in the asymptotic region. The scattering process, $O_2^+ + O^+$, analysed in this research, however, has a Coulombic potential and it is therefore necessary to adapt the theory to be applicable here, if the correct boundary conditions are to be taken into account.

Since one of the aims of this research is to compare the effects of the use of the Coulombic boundary conditions with those of the 'regular' boundary conditions, the theory will initially be presented here treating the scattering system as one which displays 'regular' behaviour in the asymptotic region, before discussing the necessary modifications of the theory to accommodate Coulombic systems.

The method of Heather and Light [60] is predicated on the ability to formulate the actual translational wavefunctions, at every point, in terms of the local solutions to the coupled equations of any small sector of the interaction space which can be easily propagated across the interaction coordinate. Thus, the overlaps of the actual translational wavefunctions can be calculated within each sector as the functions are propagated from one sector to the next, and the sum of the overlaps of all the sectors will be the total overlap of the wavefunctions.

11.3.1 Scattering System Component of Sector Overlap

For every sector, i, the coupled equations for the scattering system, Eqns. (11.6), are decoupled by the diagonalisation of the matrix $\underline{\underline{W}}$, consisting of the potential matrix elements (calculated using the value of R at the centre of the i^{th} sector) added to a diagonal matrix containing the values of

$$\frac{j'''(j'''+1)}{R^{(i)2}} + \epsilon^{O_2^+}_{v'''j'''} \quad ,$$

so that

$$\underline{\underline{\bar{T}}}^{(i)} \underline{\underline{W}}(R^{(i)}) \underline{\underline{T}}^{(i)} = \underline{\underline{e}}^{(i)} \quad ,$$

where $\underline{\underline{T}}^{(i)}$ is the transformation matrix for sector i, which is made up of the orthonormal eigenvectors of $\underline{\underline{W}}(R_i)$, and $\underline{\underline{e}}^{(i)}$ is the diagonal matrix of eigenvalues, $e_l^{(i)}$. Thus, if

$$\underline{\underline{F}}^{(i)} = \underline{\underline{\bar{T}}}^{(i)} \underline{\underline{\Psi}}^{O_2^+ + O^+} \quad ,$$

the uncoupled equations can be written as:

$$\frac{d^2}{dR^2} F_{lm}^{(i)}(R) = -\frac{2\mu}{\hbar^2}(E - e_l^{(i)}) F_{lm}^{(i)}(R) = -\lambda_l^{2(i)} F_{lm}^{(i)}(R) \quad . \qquad (11.12)$$

Since the function ψ and its derivative must both be continuous at the boundaries between sectors,

$$\underline{\underline{T}}^{(i-1)}\,\underline{\underline{F}}^{(i-1)}\left(R_{b^{(i-1)}}\right)=\underline{\underline{T}}^{(i)}\,\underline{\underline{F}}^{(i)}\left(R_{a^{(i)}}\right) \quad ; \quad \underline{\underline{T}}^{(i-1)}\,\underline{\underline{F}}'^{(i-1)}\left(R_{b^{(i-1)}}\right)=\underline{\underline{T}}^{(i)}\,\underline{\underline{F}}'^{(i)}\left(R_{a^{(i)}}\right)$$

where R_a and R_b are the values of R at the left-hand (i.e. closer to $R = 0$) and right-hand boundaries of a sector, respectively. Hence, if

$$\underline{\underline{Q}}^{(i)}=\overline{\underline{\underline{T}}}^{(i-1)}\,\underline{\underline{T}}^{(i)} \quad ,$$

then

$$\underline{\underline{F}}^{(i-1)}\left(R_{b^{(i-1)}}\right)=\underline{\underline{Q}}^{(i)}\,\underline{\underline{F}}^{(i)}\left(R_{a^{(i)}}\right) \quad ; \quad \underline{\underline{F}}'^{(i-1)}\left(R_{b^{(i-1)}}\right)=\underline{\underline{Q}}^{(i)}\,\underline{\underline{F}}'^{(i)}\left(R_{a^{(i)}}\right) .$$

The method of Heather and Light involves expressing the solutions to Eqn. (11.12) in the form:

$$F_{lm}^{(i)}=\sin\left(\lambda_l^{(i)}\left(R-R_{a^{(i)}}\right)\right)A_{lm}^{(i)}+\cos\left(\lambda_l^{(i)}\left(R-R_{a^{(i)}}\right)\right)B_{lm}^{(i)} \quad , \qquad (11.13)$$

and the derivative will therefore be:

$$F_{lm}'^{(i)}=\lambda_l^{(i)}\cos\left(\lambda_l^{(i)}\left(R-R_{a^{(i)}}\right)\right)A_{lm}^{(i)}-\lambda_l^{(i)}\sin\left(\lambda_l^{(i)}\left(R-R_{a^{(i)}}\right)\right)B_{lm}^{(i)} \quad .$$

Hence, at the border between sectors i and $(i-1)$:

$$\underline{\underline{F}}^{(i)}\left(R_{a^{(i)}}\right)=\underline{\underline{B}}^{(i)}=[\underline{\underline{Q}}^{(i)}]^{-1}\,\underline{\underline{F}}^{(i-1)}\left(R_{b^{(i-1)}}\right)$$

and

$$\underline{\underline{F}}'^{(i)}\left(R_{a^{(i)}}\right)=\underline{\underline{\lambda}}^{(i)}\,\underline{\underline{A}}^{(i)}=[\underline{\underline{Q}}^{(i)}]^{-1}\,\underline{\underline{F}}'^{(i-1)}\left(R_{b^{(i-1)}}\right)$$

and so:

$$\underline{\underline{F}}^{(i)}=[\underline{\underline{\lambda}}^{(i)}]^{-1}\,\underline{\underline{S}}^{(i)}\,[\underline{\underline{Q}}^{(i)}]^{-1}\,\underline{\underline{F}}'^{(i-1)}\left(R_{b^{(i-1)}}\right)+\underline{\underline{C}}^{(i)}\,[\underline{\underline{Q}}^{(i)}]^{-1}\,\underline{\underline{F}}^{(i-1)}\left(R_{b^{(i-1)}}\right)$$

or:

$$\underline{\underline{F}}^{(i)}=\left[[\underline{\underline{\lambda}}^{(i)}]^{-1}\,\underline{\underline{S}}^{(i)}+\underline{\underline{C}}^{(i)}\,\underline{\underline{R}}\left(R_{b^{(i-1)}}\right)\right][\underline{\underline{Q}}^{(i)}]^{-1}\,\underline{\underline{F}}'^{(i-1)}\left(R_{b^{(i-1)}}\right) \qquad (11.14)$$

where $\underline{\underline{\lambda}}^{(i)}$, $\underline{\underline{S}}^{(i)}$ and $\underline{\underline{C}}^{(i)}$ are the diagonal matrices with elements $\lambda_l^{(i)}$, $\sin\left(\lambda_l^{(i)}\left(R-R_{a^{(i)}}\right)\right)$ and $\cos\left(\lambda_l^{(i)}\left(R-R_{a^{(i)}}\right)\right)$, respectively, and

$$\underline{\underline{R}}\left(R_{b^{(i-1)}}\right)=[\underline{\underline{Q}}^{(i)}]^{-1}\underline{\underline{F}}^{(i-1)}\left(R_{b^{(i-1)}}\right)\left[\underline{\underline{F}}'^{(i-1)}\left(R_{b^{(i-1)}}\right)\right]^{-1}\underline{\underline{Q}}^{(i)} \ .$$

Eqn. (11.14) provides a simple means of calculating the translational wavefunction in one sector given the wavefunction in the preceding sector.

In order for this propagated wavefunction to correctly describe the scattering system, it must fulfil the asymptotic boundary conditions for the actual translational wavefunction of the system. For a non-Coulombic system, these boundary conditions are similar to those formulated in Chapter 4 except that, whereas in Part 1 the inelastic scattering was described by a single incoming channel, the wavefunction for dissociation will be described by a single outgoing channel [57]. Thus, in the asymptotic region the translational wavefunction can be written in the form:

$$\underline{\underline{\Psi}}(R) \xrightarrow[R\to\infty]{} \left(\underline{\underline{k}}^{-1/2}\underline{\underline{O}}(R)+\underline{\underline{k}}^{-1/2}\underline{\underline{I}}(R)\underline{\underline{\mathbf{S}}}\right) \qquad (11.15)$$

where $\underline{\underline{I}}$ is a diagonal matrix of incoming waves of momentum $-k_{v_j}\hbar$, with elements:

$$I_{nn} = \exp\left(-i\left(k_n R-\frac{(J+j)\pi}{2}\right)\right)$$

and $\underline{\underline{O}}$ is a diagonal matrix of outgoing waves of momentum $k_{v_j}\hbar$, with elements:

$$O_{nn} = \exp\left(i\left(k_n R-\frac{(J+j)\pi}{2}\right)\right) \ .$$

$\underline{\underline{k}}$ is the diagonal matrix of k_n, where:

$$k_n^2 = \frac{2\mu}{\hbar^2}\left(E-\epsilon_n^{diatom}\right)$$

and n labels internal diatomic state (v, j). Each column of the wavefunction matrix thus consists of incoming wave components for all internal states of the diatom but an outgoing wave component for only one internal state.

The S-matrix in Eqn. (11.15) is comparable to that used in Part 1 and is a unitary matrix. For any value of R at the asymptotic limit (written as $\bar{R}$ from now on), the R-matrix, defined as:

$$\underline{\underline{\mathfrak{R}}} = \left[\underline{\underline{\Psi}}\right]\left[\frac{d\underline{\underline{\Psi}}}{dR}\right]^{-1}$$

will be:

$$\underline{\underline{\mathfrak{R}}}(\bar{R}) = \left[\underline{\underline{k}}^{-1/2}\underline{\underline{Q}}(\bar{R}) + \underline{\underline{k}}^{-1/2}\underline{\underline{I}}(\bar{R})\underline{\underline{\mathbf{S}}}\right]\left[i\underline{\underline{k}}^{1/2}\underline{\underline{Q}}(\bar{R}) - i\underline{\underline{k}}^{1/2}\underline{\underline{I}}(\bar{R})\underline{\underline{\mathbf{S}}}\right]^{-1}$$

and hence the asymptotic S-matrix can be written as:

$$\underline{\underline{\mathbf{S}}} = \left[\underline{\underline{\mathfrak{R}}}(\bar{R})\, i\underline{\underline{k}}^{1/2}\,\underline{\underline{I}}(\bar{R}) + \underline{\underline{k}}^{-1/2}\underline{\underline{I}}(\bar{R})\right]^{-1}\left[\underline{\underline{\mathfrak{R}}}(\bar{R})\, i\underline{\underline{k}}^{1/2}\,\underline{\underline{Q}}(\bar{R}) - \underline{\underline{k}}^{-1/2}\underline{\underline{Q}}(\bar{R})\right] .$$

Since the S-matrix must be unitary and the R-matrix is real symmetric,

$$\underline{\underline{\mathbf{S}}} = \left[\underline{\underline{\mathbf{S}}}^{*T}\right]^{-1} = \left[\underline{\underline{\mathfrak{R}}}(\bar{R})\, i\underline{\underline{k}}^{1/2}\,\underline{\underline{I}}(\bar{R}) + \underline{\underline{k}}^{-1/2}\underline{\underline{I}}(\bar{R})\right]^{*T}\left[\underline{\underline{\mathfrak{R}}}(\bar{R}) i\underline{\underline{k}}^{1/2}\underline{\underline{Q}}(\bar{R}) - \underline{\underline{k}}^{-1/2}\underline{\underline{Q}}(\bar{R})\right]^{*T\,-1}$$

$$= \left[i\underline{\underline{k}}^{1/2}\underline{\underline{Q}}(\bar{R})\underline{\underline{\mathfrak{R}}}(\bar{R}) - \underline{\underline{k}}^{-1/2}\underline{\underline{Q}}(\bar{R})\right]\left[i\underline{\underline{k}}^{1/2}\underline{\underline{I}}(\bar{R})\underline{\underline{\mathfrak{R}}}(\bar{R}) + \underline{\underline{k}}^{-1/2}\underline{\underline{I}}(\bar{R})\right]^{-1} .$$

If the propagated wavefunction is multiplied by a constant it would still be a solution to the coupled equations, so the asymptotic boundary conditions are met by first multiplying the whole translational wavefunction on the right by:

$$\left[\underline{\underline{F}}'^{(N)}\left(R_{b^{(N)}}\right)\right]^{-1}\underline{\underline{Q}}^{(N+1)}$$

where N labels the sector in the asymptotic region. This means that the solutions to the uncoupled equations for every sector, i, up to and including sector N will become:

$$\underline{\underline{G}}^{(i)}(R)\prod_{n=i}^{N}\left[\underline{\underline{G}}'^{(n)}\left(R_{b^{(n)}}\right)\right]^{-1}\underline{\underline{Q}}^{(n+1)} \qquad (11.16)$$

where:

$$\underline{\underline{G}}^{(i)}(R) = \left[\left[\underline{\underline{\lambda}}^{(i)}\right]^{-1}\underline{\underline{\mathrm{S}}}^{(i)}(R) + \underline{\underline{\mathrm{C}}}^{(i)}(R)\,\underline{\underline{R}}\left(R_{b^{(i-1)}}\right)\right] ,$$

whilst the solution in sector $(N+1)$ will be simply:

$$\underline{\underline{F}}^{(N+1)}\left[\underline{\underline{F}}'^{(N)}\left(R_{b^{(N)}}\right)\right]^{-1}[\underline{\underline{Q}}^{(N+1)}] = \left[[\underline{\underline{\lambda}}^{(N+1)}]^{-1}\,\underline{\underline{S}}^{(N+1)} + \underline{\underline{C}}^{(N+1)}\,\underline{\underline{R}}\left(R_{b^{(N)}}\right)\right] \quad . \qquad (11.17)$$

However, at the asymptotic limit, $\underline{\underline{Q}}^{(N+1)} \approx \mathrm{I}$ and $\underline{\underline{\lambda}}^{(N+1)} \approx \underline{\underline{k}}$, so:

$$\underline{\underline{R}}\left(R_{b^{(N)}}\right) = \underline{\underline{\mathfrak{R}}}\left(\overline{R}\right) \quad .$$

Writing the matrices $\underline{\underline{S}}$ and $\underline{\underline{C}}$ in sector $(N+1)$ in terms of $\underline{\underline{I}}$ and $\underline{\underline{O}}$ gives:

$$\underline{\underline{S}} = \frac{1}{2i}\left(\underline{\underline{O}}(R)\,\underline{\underline{I}}\left(\overline{R}\right) - \underline{\underline{I}}(R)\,\underline{\underline{O}}\left(\overline{R}\right)\right)$$

$$\underline{\underline{C}} = \frac{1}{2}\left(\underline{\underline{O}}(R)\,\underline{\underline{I}}\left(\overline{R}\right) + \underline{\underline{I}}(R)\,\underline{\underline{O}}\left(\overline{R}\right)\right)$$

and thus the wavefunction at the asymptotic limit, Eqn. (11.17), becomes:

$$\underline{\underline{F}}^{(N+1)}\left[\underline{\underline{F}}'^{(N)}\left(R_{b^{(N)}}\right)\right]^{-1}[\underline{\underline{Q}}^{(N+1)}] =$$

$$\frac{1}{2i}\left[\underline{\underline{k}}\right]^{-1}\left(\underline{\underline{O}}(R)\left[\underline{\underline{I}}\left(\overline{R}\right) + i\underline{\underline{k}}\,\underline{\underline{I}}\left(\overline{R}\right)\underline{\underline{\mathfrak{R}}}\left(\overline{R}\right)\right] + \underline{\underline{I}}(R)\left[i\underline{\underline{k}}\,\underline{\underline{O}}\left(\overline{R}\right)\underline{\underline{\mathfrak{R}}}\left(\overline{R}\right) - \underline{\underline{O}}\left(\overline{R}\right)\right]\right).$$

Since this can be written as:

$$= \frac{1}{2i}\left[\underline{\underline{k}}^{-\frac{1}{2}}\right]\left(\underline{\underline{O}}(R) + \underline{\underline{I}}(R)\,\underline{\underline{k}}^{-\frac{1}{2}}\left[i\underline{\underline{k}}\,\underline{\underline{O}}\left(\overline{R}\right)\underline{\underline{\mathfrak{R}}}\left(\overline{R}\right) - \underline{\underline{O}}\left(\overline{R}\right)\right]\left[\underline{\underline{I}}\left(\overline{R}\right) + i\underline{\underline{k}}\,\underline{\underline{I}}\left(\overline{R}\right)\underline{\underline{\mathfrak{R}}}\left(\overline{R}\right)\right]^{-1}\underline{\underline{k}}^{\frac{1}{2}}\right)$$

$$\times\, \underline{\underline{k}}^{-\frac{1}{2}}\left[\underline{\underline{I}}\left(\overline{R}\right) + i\underline{\underline{k}}\,\underline{\underline{I}}\left(\overline{R}\right)\underline{\underline{\mathfrak{R}}}\left(\overline{R}\right)\right]$$

$$= \frac{1}{2i}\left[\underline{\underline{k}}^{-\frac{1}{2}}\underline{\underline{O}}(R) + \underline{\underline{k}}^{-\frac{1}{2}}\underline{\underline{I}}(R)\,\underline{\underline{\mathbf{S}}}\right]\underline{\underline{k}}^{-\frac{1}{2}}\left[\underline{\underline{I}}\left(\overline{R}\right) + i\underline{\underline{k}}\,\underline{\underline{I}}\left(\overline{R}\right)\underline{\underline{\mathfrak{R}}}\left(\overline{R}\right)\right] \quad ,$$

the whole translational wavefunction can now easily be transformed to meet the requirements of Eqn. (11.15), by multiplying it on the right by $\underline{\underline{D}}$ where:

$$\underline{\underline{D}} = 2i\left[\underline{\underline{I}}\left(\overline{R}\right) + i\underline{\underline{k}}\,\underline{\underline{I}}\left(\overline{R}\right)\underline{\underline{\mathfrak{R}}}\left(\overline{R}\right)\right]^{-1}\underline{\underline{k}}^{\frac{1}{2}}$$

$$= \left[\frac{1}{2}\underline{\underline{k}}^{\frac{1}{2}}\,\underline{\underline{\mathfrak{R}}}\left(\overline{R}\right) - \frac{i}{2}\underline{\underline{k}}^{-\frac{1}{2}}\right]^{-1}\underline{\underline{O}}\left(\overline{R}\right) \quad .$$

11.3.2 Bound System Component of Sector Overlap

The above formulation of the solutions to the coupled equations within each sector, Eqn. (11.16), can equally be applied to describe the translational wavefunction for the bound molecule. Expressing both the wavefunctions of an overlap in this fashion has previously been done for the calculation of perturbation integrals [61, 62].

The boundary conditions for the bound wavefunction are that it and its derivative be zero at the two ends of the potential well. This requirement is only met at certain discrete values of the energy E^{O_3} and so, in order to obtain the overlap of the bound wavefunction for O_3 with the scattering wavefunction of $O_2^+ + O^+$, it is first necessary to determine the specific value of the energy of the bound state.

Gordon [63] has developed a method for obtaining the energy levels of a bound wavefunction via the propagation of the wavefunction and its derivative over the interaction coordinate and Danby [64] has proposed a similar method for propagation of the R-matrix, as in Part 1 of this thesis. The first step is to expand the bound translational wavefunction vector, $\underline{\psi}^{O_3}$, as a linear combination of orthogonal functions each of which are solutions to the coupled equations for the bound system, but which, individually, do not satisfy the necessary boundary conditions for the bound molecule. These solutions can therefore be written as a matrix, similar to that for the scattering wavefunction, $\underline{\underline{\psi}}^{O_2^+ + O^+}$, and this assures the stability of the wavefunction as it is propagated from sector to sector. The boundary conditions appropriate to the bound wavefunction at the two edges of the potential well are then taken as starting points for a simultaneous propagation of the R-matrix from both sides of the potential well. The energy at which the R-matrices from both propagations are found to be identical at the position where they coincide will then be an eigenvalue of the Schrödinger equation for the bound molecule.

However, when finding the overlap of the bound wavefunction with another wavefunction, as is done in this research, locating the bound energy level

through simultaneous propagation from both sides is not necessary. This is due to consideration of the fact that the square of the overlap elements can be understood as the probability of measuring the amount that one wavefunction is found to be 'present' in the other. Hence, at values of E^{O_3} for which the solutions to the Schrödinger equation do not meet the required boundary conditions for a bound molecule and therefore are not allowed to exist in reality, the overlap will be negligible. Only at the correct bound energy levels will the overlap be significant. Therefore, the energy of a bound state of the O_3 molecule, with the potential surface described in Section 11.2.2, can be calculated by simply locating a resonance in the spectrum of the overlaps, $\underline{\underline{\mathbf{O}}}$, with respect to variation in the bound energy, E^{O_3}.

The first step in the propagation of the bound wavefunction is to express the coupled equations for the O_3 system, Eqns. (11.8), in matrix form:

$$\left[\frac{d^2}{dR^2} + k^2_{Bvj} - \frac{[j(j+1)]}{R^2}\right] \underline{\underline{\psi}}^{O_3} = \underline{\underline{\hat{V}}}_{O_2^+ - O^-} \underline{\underline{\psi}}^{O_3} \quad . \tag{11.18}$$

where the columns of the wavefunction matrix, $\underline{\underline{\psi}}^{O_3}$, will be orthogonal solutions to the translational Schrödinger equation for the bound system, but which do not necessarily satisfy the correct boundary conditions for the bound wavefunction. The overlap function to be calculated now becomes the matrix:

$$\underline{\underline{\mathbf{O}}}\left(E^{O_3^{2+}}, E^{O_3}\right) = \left\langle \underline{\underline{\psi}}^{O_2^+ + O^+}\left(E^{O_3^{2+}}\right) \middle| \underline{\underline{\psi}}^{O_3}\left(E^{O_3}\right) \right\rangle \quad . \tag{11.19}$$

The coupled equations for the bound system, Eqns. (11.18), are decoupled in the same way as those for the scattering system, namely by adding the potential matrix elements for each sector, at $R^{(i)}$, to the diagonal matrix of elements

$$\frac{j(j+1)}{R^{(i)2}} + \epsilon^{O_2^+}_{vj}$$

and diagonalising the resulting matrix. The solutions within each sector are taken to be of the same form as Eqn. (11.14) but with the $\underline{\underline{\lambda}}$ defined by the uncoupled equations for the bound system.

11.3.3 Propagation of the Overlap

Thus, the total overlap matrix is calculated by evaluating the matrix of integrals:

$$\underline{\underline{X}}^{(i)} = \int_{R_a(i)}^{R_b(i)} dR \left[\underline{\underline{G}}^{(i)}_{O_2^+ + O^+}(R)\right]^{*T} \left[\underline{\underline{T}}^{(i)}_{O_2^+ + O^+}\right]^{*T} \underline{\underline{T}}^{(i)}_{O_3}\, \underline{\underline{G}}^{(i)}_{O_3}(R) \qquad (11.20)$$

for each sector, i. These sector integrals only need be calculated for the sectors which fall within the Franck-Condon region for the excitation, since the bound wavefunction will be zero outside of that area [60]. Hence, $\underline{\underline{X}}^{(i)} = 0$ for all i at which $R_{b(i)}$ is greater than the boundary of the potential well for O_3.

The sum of the contributions to the overlap matrix integral from all sectors up to sector i is then taken as:

$$\underline{\underline{Y}}^{(i)} = [\,\underline{\underline{Q}}^{(i+1)}_{O_2^+ + O^+}\,]^T \left\{\left[\,\underline{\underline{G'}}^{(i)}_{O_2^+ + O^+}\left(R_{b(i)}\right)\right]^{-1}\right\}^{*T} \left[\underline{\underline{Y}}^{(i-1)} + \underline{\underline{X}}^{(i)}\right], \qquad (11.21)$$

which is expressed in the $(i+1)$ uncoupled basis, and the total overlap matrix will therefore be:

$$\underline{\underline{\mathbf{O}}} = \underline{\underline{D}}^T \underline{\underline{T}}^{(N+1)} \underline{\underline{Y}}^{(N)} \quad . \qquad (11.22)$$

For a basis set of size M, each of the M rows of the total overlap matrix represents the contribution from the scattering wavefunction for a different final state of the O_2^+ diatom. Each of the M columns represents the contribution from a different solution to the translational Schrödinger equation for the O_3 molecule at energy E^{O_3}.

Since, when E^{O_3} is one of the discrete bound state energy levels for O_3, these orthogonal solutions will span the entire Hilbert space occupied by the true bound wavefunction (i.e. the solution to the Schrödinger equation for the O_3 molecule which meets the required boundary conditions), it can be expressed as a linear combination of them. The coefficients of this expansion, however, are not known.

Nevertheless, it should still be possible to obtain the product distribution of O_2^+ from the overlap matrix, even without explicit knowledge of the bound O_3 wavefunction. For, at the bound energy level, each of the columns of the $\underline{\underline{\psi}}^{O_3}$ matrix, being a solution to the translational Schrödinger equation for the bound system, can itself be expressed as an expansion in terms of the actual bound wavefunction and the $M-1$ functions which are orthogonal to *it*, as they too span the same Hilbert space. Since, as explained above, the overlap will be negligible for all wavefunctions that do not exist in reality, the only significant contribution to the elements of the overlap matrix made by each column of the $\underline{\underline{\psi}}^{O_3}$ matrix will therefore be from the 'true' bound wavefunction component of such an expansion. The product distribution of internal energy states of the O_2^+ fragment, defined as the relative probability of each state being observed, can therefore be obtained by simply taking the squares of the elements in any of the columns of the overlap matrix and dividing them by the sum of the squares of the elements in that one column.

If this theory is correct, the results of such an operation should be near identical for each column of the final overlap matrix that is used or, indeed, for the sum of the squares of the elements of each row from any number of the columns, as long as the appropriate 'total' is chosen as the denominator. The validity of this hypothesis will be tested in this study.

The Sector Integrals

The matrix of integrals within each sector, Eqn. (11.20), are calculated analytically using the formulation derived as follows:

$$X_{jn}^{(i)} = \int_{R_a(i)}^{R_b(i)} dR \left[\underline{\underline{G}}_{O_2^+ + O^+}^{(i)\,*T} \; \underline{\underline{T}}_{O_2^+ + O^+}^{(i)\,*T} \; \underline{\underline{T}}_{O_3}^{(i)} \; \underline{\underline{G}}_{O_3}^{(i)} \right]_{jn}$$

$$= \int_{R_a(i)}^{R_b(i)} dR \sum_k \sum_m \sum_l \left[\underline{\underline{G}}_{O_2^+ + O^+}^{(i)\,*T} \right]_{jk} \left[\underline{\underline{T}}_{O_2^+ + O^+}^{(i)\,*T} \right]_{kl} \left[\underline{\underline{T}}_{O_3}^{(i)} \right]_{lm} \left[\underline{\underline{G}}_{O_3}^{(i)} \right]_{mn}$$

$$= \int_{R_a(i)}^{R_b(i)} dR \sum_k \sum_m \sum_l \left[\underline{\underline{T}}_{O_2^+ + O^+}^{(i)\,*} \right]_{lk} \left[\underline{\underline{T}}_{O_3}^{(i)} \right]_{lm} \left[\underline{\underline{G}}_{O_2^+ + O^+}^{(i)\,*} \right]_{kj} \left[\underline{\underline{G}}_{O_3}^{(i)} \right]_{mn}$$

$$= \int_{R_a(i)}^{R_b(i)} dR \sum_k \sum_m \sum_l \left[\underline{\underline{T}}_{O_2^+ + O^+}^{(i)\,*} \right]_{lk} \left[\underline{\underline{T}}_{O_3}^{(i)} \right]_{lm} \left[[\underline{\underline{\lambda}}_{O_2^+ + O^+}^{(i)}]^{-1} \underline{\underline{S}}_{O_2^+ + O^+}^{(i)} + \underline{\underline{C}}_{O_2^+ + O^+}^{(i)} \underline{\underline{R}}_{O_2^+ + O^+} \left(R_{b^{(i-1)}} \right) \right]_{kj}^{*}$$

$$\times \left[[\underline{\underline{\lambda}}_{O_3}^{(i)}]^{-1} \underline{\underline{S}}_{O_3}^{(i)} + \underline{\underline{C}}_{O_3}^{(i)} \underline{\underline{R}}_{O_3} \left(R_{b^{(i-1)}} \right) \right]_{mn}$$

so that, for every sector, dropping the i index for convenience,

$$X_{jn} = \int_{R_a}^{R_b} dR \sum_k \sum_m \sum_l \left[\underline{\underline{T}}_{O_2^+ + O^+}^{*} \right]_{lk} \left[\underline{\underline{T}}_{O_3} \right]_{lm} \times$$

$$\left(\left[\sin\left(\lambda_k^{O_2^+ + O^+} \left(R - R_a \right) \right) \Big/ \lambda_k^{O_2^+ + O^+} \right]^{*} \delta_{kj} + \sum_q \left[\cos\left(\lambda_k^{O_2^+ + O^+} \left(R - R_a \right) \right) \right]_{kq} \delta_{kq} \left[\underline{\underline{R}}_{O_2^+ + O^+} \right]_{qj} \right)$$

$$\times \left(\left[\sin\left(\lambda_m^{O_3} \left(R - R_a \right) \right) \Big/ \lambda_m^{O_3} \right] \delta_{mn} + \sum_p \left[\cos\left(\lambda_m^{O_3} \left(R - R_a \right) \right) \right]_{mp} \delta_{mp} \left[\underline{\underline{R}}_{O_3} \right]_{pn} \right)$$

which becomes:

$$X_{jn} = \sum_{l} \left[\underline{\underline{T}}^{*}_{O_2^+ + O^+} \right]_{lj} \left[\underline{\underline{T}}_{O_3} \right]_{ln} \int_{R_a}^{R_b} \left[\sin\left(\lambda_j^{O_2^+ + O^+} (R - R_a) \right) \Big/ \lambda_j^{O_2^+ + O^+} \right]^{*} \times \left[\sin\left(\lambda_n^{O_3} (R - R_a) \right) \Big/ \lambda_n^{O_3} \right] dR$$

$$+ \sum_{m} \sum_{l} \left[\underline{\underline{T}}^{*}_{O_2^+ + O^+} \right]_{lj} \left[\underline{\underline{T}}_{O_3} \right]_{lm} \int_{R_a}^{R_b} \left[\sin\left(\lambda_j^{O_2^+ + O^+} (R - R_a) \right) \Big/ \lambda_j^{O_2^+ + O^+} \right]^{*} \times \sum_{p} \left[\cos\left(\lambda_m^{O_3} (R - R_a) \right) \right]_{mp} \delta_{mp} \left[\underline{\underline{R}}_{O_3} \right]_{pn} dR$$

$$+ \sum_{k} \sum_{l} \left[\underline{\underline{T}}^{*}_{O_2^+ + O^+} \right]_{lk} \left[\underline{\underline{T}}_{O_3} \right]_{ln} \int_{R_a}^{R_b} \left[\sum_{q} \left[\cos\left(\lambda_k^{O_2^+ + O^+} (R - R_a) \right) \right]_{kq} \delta_{kq} \left[\underline{\underline{R}}_{O_2^+ + O^+} \right]_{qj} \right]^{*} \times \left[\sin\left(\lambda_n^{O_3} (R - R_a) \right) \Big/ \lambda_n^{O_3} \right] dR$$

$$+ \sum_{k} \sum_{m} \sum_{l} \left[\underline{\underline{T}}^{*}_{O_2^+ + O^+} \right]_{lk} \left[\underline{\underline{T}}_{O_3} \right]_{lm} \int_{R_a}^{R_b} \left[\sum_{q} \left[\cos\left(\lambda_k^{O_2^+ + O^+} (R - R_a) \right) \right]_{kq} \delta_{kq} \left[\underline{\underline{R}}_{O_2^+ + O^+} \right]_{qj} \right]^{*} \times \sum_{p} \left[\cos\left(\lambda_m^{O_3} (R - R_a) \right) \right]_{mp} \delta_{mp} \left[\underline{\underline{R}}_{O_3} \right]_{pn} dR$$

It should be noted that the λ terms are not restricted to being real numbers and that therefore, for $\lambda^2 < 1$, the trigonometric functions will become their hyperbolic function equivalent.

Defining the sector distance, ($R_b - R_a$), as h and carrying out the integration gives:

$$X_{jn} = \sum_l \left[\underline{\underline{T}}^{*}_{O_3^{2+}}\right]_{lj} \left[\underline{\underline{T}}_{O_3}\right]_{ln} \times \frac{1}{\lambda_j^{O_3^{2+}*} \lambda_n^{O_3}} \left(\frac{1}{\left(\lambda_j^{O_3^{2+}*} - \lambda_n^{O_3}\right)} \left[\sin\left(\left(\lambda_j^{O_3^{2+}*} - \lambda_n^{O_3}\right)h\right)\right] - \frac{1}{\left(\lambda_j^{O_3^{2+}*} + \lambda_n^{O_3}\right)} \left[\sin\left(\left(\lambda_j^{O_3^{2+}*} + \lambda_n^{O_3}\right)h\right)\right] \right)$$

$$+ \sum_m \sum_l \left[\underline{\underline{T}}^{*}_{O_3^{2+}}\right]_{lj} \left[\underline{\underline{T}}_{O_3}\right]_{lm} \times \frac{\left[\underline{\underline{R}}_{O_3}\right]_{mn}}{\lambda_j^{O_3^{2+}*}} \left(\frac{1}{\left(\lambda_m^{O_3} - \lambda_j^{O_3^{2+}*}\right)} \left[\cos\left(\left(\lambda_m^{O_3} - \lambda_j^{O_3^{2+}*}\right)h\right) - 1\right] - \frac{1}{\left(\lambda_m^{O_3} + \lambda_j^{O_3^{2+}*}\right)} \left[\cos\left(\left(\lambda_m^{O_3} + \lambda_j^{O_3^{2+}*}\right)h\right) - 1\right] \right)$$

$$+ \sum_k \sum_l \left[\underline{\underline{T}}^{*}_{O_3^{2+}}\right]_{lk} \left[\underline{\underline{T}}_{O_3}\right]_{ln} \times \frac{\left[\underline{\underline{R}}_{O_3^{2+}}\right]_{kj}}{\lambda_n^{O_3}} \left(\frac{1}{\left(\lambda_k^{O_3^{2+}*} - \lambda_n^{O_3}\right)} \left[\cos\left(\left(\lambda_k^{O_3^{2+}*} - \lambda_n^{O_3}\right)h\right) - 1\right] - \frac{1}{\left(\lambda_k^{O_3^{2+}*} + \lambda_n^{O_3}\right)} \left[\cos\left(\left(\lambda_k^{O_3^{2+}*} + \lambda_n^{O_3}\right)h\right) - 1\right] \right)$$

$$+ \sum_k \sum_m \sum_l \left[\underline{\underline{T}}^{*}_{O_3^{2+}}\right]_{lk} \left[\underline{\underline{T}}_{O_3}\right]_{lm} \times \left[\underline{\underline{R}}_{O_3^{2+}}\right]_{kj} \left[\underline{\underline{R}}_{O_3}\right]_{mn} \left(\frac{1}{\left(\lambda_k^{O_3^{2+}*} - \lambda_m^{O_3}\right)} \left[\sin\left(\left(\lambda_k^{O_3^{2+}*} - \lambda_n^{O_3}\right)h\right)\right] + \frac{1}{\left(\lambda_k^{O_3^{2+}*} + \lambda_m^{O_3}\right)} \left[\sin\left(\left(\lambda_k^{O_3^{2+}*} + \lambda_m^{O_3}\right)h\right)\right] \right) \tag{11.23}$$

unless $\lambda^{O_3^{2+}*} = \pm \lambda^{O_3}$, in which case the

$$\frac{1}{\left(\lambda^{O_3^{2+}*} \pm \lambda^{O_3}\right)} \left[\sin\left(\left(\lambda^{O_3^{2+}*} \pm \lambda^{O_3}\right)h\right)\right]$$

terms are replaced by h, whilst the

$$\left[\cos\left(\left(\lambda^{O_3} \pm \lambda^{O_3^{2+}*}\right)h\right) - 1\right]$$

terms become zero.

11.4 Modifications for Coulombic Potential

The description given above for the propagation of the overlap matrix is only accurate for a scattering system with a potential function that tends to zero as $1/R^2$ or faster. As explained in Chapter 10 in the context of elastic scattering, the wavefunction for a system with a Coulombic potential, such as $O_2^+ + O^+$, takes a different form in the asymptotic region than that of a system with a 'regular' potential, due to the infinite range of the Coulombic potential.

Thus, as an extension of the theory for the elastic scattering case, for dissociation, the asymptotic form of the translational wavefunction of the $O_2^+ + O^+$ scattering system is actually:

$$\underline{\underline{\Psi}}(R) \xrightarrow[R\to\infty]{} \left(\left[\underline{\underline{k^C}}\right]^{-1/2} \underline{\underline{O^C}}(R) + \left[\underline{\underline{k^C}}\right]^{-1/2} \underline{\underline{I^C}}(R) \underline{\underline{\mathbf{S}}} \right) \qquad (11.24)$$

where $\underline{\underline{I^C}}$ is the diagonal matrix consisting of terms:

$$I_{nn}^C = \exp\left(-i\left(k_n R - \frac{(J+j)\pi}{2} - \gamma_n \ln 2k_n R\right)\right)$$

and $\underline{\underline{O^C}}$ is the diagonal matrix of terms:

$$O_{nn}^C = \exp\left(i\left(k_n R - \frac{(J+j)\pi}{2} - \gamma_n \ln 2k_n R\right)\right) \quad .$$

$\underline{\underline{k^C}}$ is the diagonal matrix of elements

$$k_{nn}^C = \left(k_n - \gamma_n / R\right),$$

where n labels internal diatomic state (v, j), and:

$$k_n^2 = \frac{2\mu}{\hbar^2}\left(E - \epsilon_n^{diatom}\right) \quad .$$

In an analogous fashion to the elastic scattering case of Chapter 10,

$$\gamma_n = \frac{\mu}{k_n}$$

since the product of the charges of the scattering species (in atomic units) for $O_2^+ + O^+$ is: $Z_A Z_B = 1$.

At the asymptotic limit, therefore, the R-matrix for the Coulombic wavefunction is:

$$\underline{\underline{\mathfrak{R}}}(\bar{R}) = \left[\left[\underline{\underline{k^C}}\right]^{-\frac{1}{2}} \underline{\underline{O^C}}(\bar{R}) + \left[\underline{\underline{k^C}}\right]^{-\frac{1}{2}} \underline{\underline{I^C}}(\bar{R}) \underline{\underline{\mathbf{S}}} \right] \left[i\left[\underline{\underline{k^C}}\right]^{\frac{1}{2}} \underline{\underline{O^C}}(\bar{R}) - i\left[\underline{\underline{k^C}}\right]^{\frac{1}{2}} \underline{\underline{I^C}}(\bar{R}) \underline{\underline{\mathbf{S}}} \right]^{-1} \quad (11.25)$$

and the S-matrix can be written as:

$$\underline{\underline{\mathbf{S}}} = \left[\underline{\underline{\mathfrak{R}}}(\bar{R})\, i\left[\underline{\underline{k^C}}\right]^{\frac{1}{2}} \underline{\underline{I^C}}(\bar{R}) + \left[\underline{\underline{k^C}}\right]^{-\frac{1}{2}} \underline{\underline{I^C}}(\bar{R})\right]^{-1} \left[\underline{\underline{\mathfrak{R}}}(\bar{R})\, i\left[\underline{\underline{k^C}}\right]^{\frac{1}{2}} \underline{\underline{O^C}}(\bar{R}) - \left[\underline{\underline{k^C}}\right]^{-\frac{1}{2}} \underline{\underline{O^C}}(\bar{R})\right]$$

$$= \left[i\left[\underline{\underline{k^C}}\right]^{\frac{1}{2}} \underline{\underline{O^C}}(\bar{R})\, \underline{\underline{\mathfrak{R}}}(\bar{R}) - \left[\underline{\underline{k^C}}\right]^{-\frac{1}{2}} \underline{\underline{O^C}}(\bar{R}) \right] \left[i\left[\underline{\underline{k^C}}\right]^{\frac{1}{2}} \underline{\underline{I^C}}(\bar{R})\, \underline{\underline{\mathfrak{R}}}(\bar{R}) + \left[\underline{\underline{k^C}}\right]^{-\frac{1}{2}} \underline{\underline{I^C}}(\bar{R}) \right]^{-1}.$$

In order to use the method of Heather and Light [60] accurately for a Coulombic system, it is necessary to express the sector solutions to the uncoupled equations of Eqn. (11.12) in a form which can be readily transformed to meet the asymptotic boundary conditions of Eqn. (11.24). However, this cannot be achieved by simply adjusting the form of the solutions within every sector, Eqn. (11.13), so that they include the required logarithmic term, since, within each sector, the potential is considered to be constant with respect to R and therefore functions of the type:

$$\exp\left(i\left(\lambda_n R - \gamma_n \ln 2\lambda_n R\right)\right)$$

cannot be solutions to the uncoupled equations (11.12).

Nevertheless, in sector N, the sector at the asymptotic limit, it *is* possible to introduce the desired form of the solutions since, there, the Coulombic potential energy term, $\frac{2\mu}{\hbar^2}\hat{V}_{O_2^+-O^+}(R)$ of Eqn. (11.6), is small enough to be considered as zero, which is therefore equivalent to saying that, there:

$$\frac{2\mu}{\hbar^2}\frac{1}{R} \to 0.$$

Consequently, it would be necessary to consider that the solution to the uncoupled equations of sector N:

$$\frac{d^2}{dR^2}F_{lm}^{(N)}(R) = -\frac{2\mu}{\hbar^2}(E - e_l^{(N)})F_{lm}^{(N)}(R) = -\lambda_l^{2(N)}F_{lm}^{(N)}(R)$$

could be of the form:

$$F_{lm}^{(N)}(R) = \exp\left(i\left(\lambda_l^{(N)}R - \gamma_l \ln 2\lambda_l^{(N)}R\right)\right)$$

since then:

$$\frac{d^2}{dR^2}F_{lm}^{(N)}(R) = -\left(\lambda_l^{(N)} - \frac{\gamma_l}{R}\right)^2 F_{lm}^{(N)}(R) + \frac{i\gamma_l}{R^2}\left(\lambda_l^{(N)} - \frac{\gamma_l}{R}\right)F_{lm}^{(N)}(R)$$

$$= -\left(\lambda_l^{2(N)} - \frac{2\gamma_l\lambda_l^{(N)}}{R} + \frac{\gamma_l^2}{R^2}\right)F_{lm}^{(N)}(R) + \frac{i\gamma_l}{R^2}\left(\lambda_l^{(N)} - \frac{\gamma_l}{R}\right)F_{lm}^{(N)}(R)$$

which, for $\frac{2\mu}{\hbar^2}\frac{1}{R} \to 0$ (and $\lambda_l \to k_l$), becomes:

$$\frac{d^2}{dR^2}F_{lm}^{(N)}(R) = -\lambda_l^{2(N)}F_{lm}^{(N)}(R) \quad .$$

Therefore, the method of Heather and Light is adapted to be applicable to a scattering system with a Coulombic potential by altering the solution to the uncoupled equations in sector N (and $N+1$), such that:

$$F_{lm}^{(i)} = \sin\left(\lambda_l^{(i)}\left(R - R_{a^{(i)}}\right) - \gamma_l \ln\frac{R}{R_{a^{(i)}}}\right)A_{lm}^{(i)} + \cos\left(\lambda_l^{(i)}\left(R - R_{a^{(i)}}\right) - \gamma_l \ln\frac{R}{R_{a^{(i)}}}\right)B_{lm}^{(i)}$$

for all $i \geq N$. Hence, at the border between sectors i and $(i-1)$, for sectors $i \geq N$,

$$\underline{\underline{F}}^{(i)}\left(R_{a^{(i)}}\right) = \underline{\underline{B}}^{(i)} = [\underline{\underline{Q}}^{(i)}]^{-1}\underline{\underline{F}}^{(i-1)}\left(R_{b^{(i-1)}}\right)$$

and

$$\underline{\underline{F}}'^{(i)}\left(R_{a^{(i)}}\right) = \left[\underline{\underline{\lambda}}^{(i)} - \frac{1}{R_{a^{(i)}}}\underline{\underline{\gamma}}\right]\underline{\underline{A}}^{(i)} = [\underline{\underline{Q}}^{(i)}]^{-1}\underline{\underline{F}}'^{(i-1)}\left(R_{b^{(i-1)}}\right)$$

so that:

$$\underline{\underline{F}}^{(i)} = \left[\left[\underline{\underline{\lambda}}^{(i)} - \frac{1}{R_{a^{(i)}}} \underline{\underline{\gamma}} \right]^{-1} \underline{\underline{S}}^{C^{(i)}} + \underline{\underline{C}}^{C^{(i)}} \; \underline{\underline{R}}\left(R_{b^{(i-1)}}\right) \right] [\underline{\underline{Q}}^{(i)}]^{-1} \underline{\underline{F}}'^{(i-1)}\left(R_{b^{(i-1)}}\right)$$

where $\underline{\underline{S}}^{C^{(i)}}$ is the diagonal matrix with elements:

$$S_{nn}^{C(i)} = \sin\left(\lambda_n^{(i)}\left(R - R_{a^{(i)}}\right) - \gamma_n \ln \frac{R}{R_{a^{(i)}}} \right)$$

and $\underline{\underline{C}}^{C^{(i)}}$ the diagonal matrix with elements:

$$C_{nn}^{C(i)} = \cos\left(\lambda_n^{(i)}\left(R - R_{a^{(i)}}\right) - \gamma_n \ln \frac{R}{R_{a^{(i)}}} \right).$$

The whole wavefunction is then multiplied on the right by this Coulombic version of

$$\left[\underline{\underline{F}}'^{(N)}\left(R_{b^{(N)}}\right)\right]^{-1} \underline{\underline{Q}}^{(N+1)}$$

and the solution to Eqns. (11.12) within each sector, i, up to and including sector N becomes, once again

$$\underline{\underline{G}}^{(i)}(R) \prod_{n=i}^{N} \left[\underline{\underline{G}}'^{(n)}\left(R_{b^{(n)}}\right)\right]^{-1} \underline{\underline{Q}}^{(n+1)}$$

but with

$$\underline{\underline{G}}^{(N)}(R) = \left[\left[\underline{\underline{\lambda}}^{(N)} - \frac{1}{R_{a^{(N)}}} \underline{\underline{\gamma}} \right]^{-1} \underline{\underline{S}}^{C^{(N)}} + \underline{\underline{C}}^{C^{(N)}} \; \underline{\underline{R}}\left(R_{b^{(N-1)}}\right) \right]$$

whereas:

$$\underline{\underline{G}}^{(i)}(R) = \left[[\underline{\underline{\lambda}}^{(i)}]^{-1} \underline{\underline{S}}^{(i)}(R) + \underline{\underline{C}}^{(i)}(R) \; \underline{\underline{R}}\left(R_{b^{(i-1)}}\right) \right] \quad ,$$

for all sectors $i < N$.

The solution in sector $(N+1)$ will now become:

$$\underline{\underline{F}}^{(N+1)}\left[\underline{\underline{F}}'^{(N)}\left(R_{b^{(N)}}\right)\right]^{-1}[\underline{\underline{Q}}^{(N+1)}] = \left[\left[\underline{\underline{k}}^{C}\right]^{-1}\underline{\underline{S}}^{C(N+1)} + \underline{\underline{C}}^{C(N+1)}\,\underline{\underline{\mathfrak{R}}}(\overline{R})\right] .$$

where the R-matrix is defined as in Eqn. (11.25). Writing matrices $\underline{\underline{S}}^{C}$ and $\underline{\underline{C}}^{C}$ in terms of $\underline{\underline{I}}^{C}$ and $\underline{\underline{O}}^{C}$ and rearranging the wavefunction at the asymptotic limit, gives the analogous result to that for the non-Coulombic system:

$$\underline{\underline{F}}^{(N+1)}\left[\underline{\underline{F}}'^{(N)}\left(R_{b^{(N)}}\right)\right]^{-1}[\underline{\underline{Q}}^{(N+1)}] =$$

$$\frac{1}{2i}\left[\underline{\underline{k}}^{C}\right]^{-\frac{1}{2}}\left(\underline{\underline{O}}^{C}(R)+\underline{\underline{I}}^{C}(R)\left[\underline{\underline{k}}^{C}\right]^{-\frac{1}{2}}\left[i\underline{\underline{k}}^{C}\,\underline{\underline{O}}^{C}(\overline{R})\,\underline{\underline{\mathfrak{R}}}(\overline{R})-\underline{\underline{O}}^{C}(\overline{R})\right]\left[\underline{\underline{I}}^{C}(\overline{R})+i\underline{\underline{k}}^{C}\,\underline{\underline{I}}^{C}(\overline{R})\,\underline{\underline{\mathfrak{R}}}(\overline{R})\right]^{-1}\left[\underline{\underline{k}}^{C}\right]^{\frac{1}{2}}\right)$$
$$\times\left[\underline{\underline{k}}^{C}\right]^{-\frac{1}{2}}\left[\underline{\underline{I}}^{C}(\overline{R})+i\underline{\underline{k}}^{C}\,\underline{\underline{I}}^{C}(\overline{R})\,\underline{\underline{\mathfrak{R}}}(\overline{R})\right]$$

$$=\frac{1}{2i}\left(\left[\underline{\underline{k}}^{C}\right]^{-\frac{1}{2}}\underline{\underline{O}}^{C}(R)+\left[\underline{\underline{k}}^{C}\right]^{-\frac{1}{2}}\underline{\underline{I}}^{C}(R)\,\underline{\underline{\mathbf{S}}}\right)\left[\underline{\underline{k}}^{C}\right]^{-\frac{1}{2}}\left[\underline{\underline{I}}^{C}(\overline{R})+i\underline{\underline{k}}^{C}\,\underline{\underline{I}}^{C}(\overline{R})\,\underline{\underline{\mathfrak{R}}}(\overline{R})\right] .$$

The whole translational wavefunction is then transformed to meet the requirements of Eqn. (11.24), by multiplying it on the right by $\underline{\underline{D}}^{C}$ where:

$$\underline{\underline{D}}^{C} = 2i\left[\underline{\underline{I}}^{C}(\overline{R})+i\underline{\underline{k}}^{C}\,\underline{\underline{I}}^{C}(\overline{R})\,\underline{\underline{\mathfrak{R}}}(\overline{R})\right]^{-1}\left[\underline{\underline{k}}^{C}\right]^{\frac{1}{2}}$$

$$=\left[\frac{1}{2}\left[\underline{\underline{k}}^{C}\right]^{\frac{1}{2}}\underline{\underline{\mathfrak{R}}}(\overline{R})-\frac{i}{2}\left[\underline{\underline{k}}^{C}\right]^{-\frac{1}{2}}\right]^{-1}\underline{\underline{O}}^{C}(\overline{R}) .$$

Since the only changes made for the Coulombic potential involve the sectors in the asymptotic region, which is outside of the Franck-Condon region, the sector integrals, Eqn. (11.23), will all remain unaffected. The total overlap matrix is then calculated using Eqn. (11.21) as before and applying the Coulombic form of the asymptotic transformation, so that:

$$\underline{\underline{\mathbf{O}}} = \left[\underline{\underline{D}}^{C}\right]^{T}\underline{\underline{T}}^{(N+1)}\,\underline{\underline{Y}}^{(N)} .$$

12 Results of Calculations on Dissociation of O_3^{2+}

12.1 Potential Fit

The points supplied by Champkin for the *ab initio* potential surface for the process:

$$O_2^+ + O^+ \leftrightarrow O_3^{2+}$$

were fitted as an expansion in Legendre polynomials using the method described at the end of Section 3.2.2 and taking the values of r_m of Eqn. (3.14) to be:

$$r_m = 1.82\ a_0,\ 2.02\ a_0, 2.12\ a_0, 2.42\ a_0$$

and the values of γ_k as:

$$\gamma_k = 0°, 30°, 60°, 75°, 90° \quad ,$$

with $L = 5$ and $N = 4$.

Some cross-sections of the fitted potential surfaces are shown in Figure 21 and Figure 22, at values of r and γ which were used in the matrices of Eqn. (3.14) to create the potential energy functions. The Coulomb term in the potential function dominates at large R and results in the asymptotic limit, where the potential can be considered as having zero magnitude, being much further out than for a non-Coulombic potential.

The potential well, in the region of $R \approx 3a_0$, has a minimum at $V_e^{O_3^{2+}} \approx 5.4$ eV.

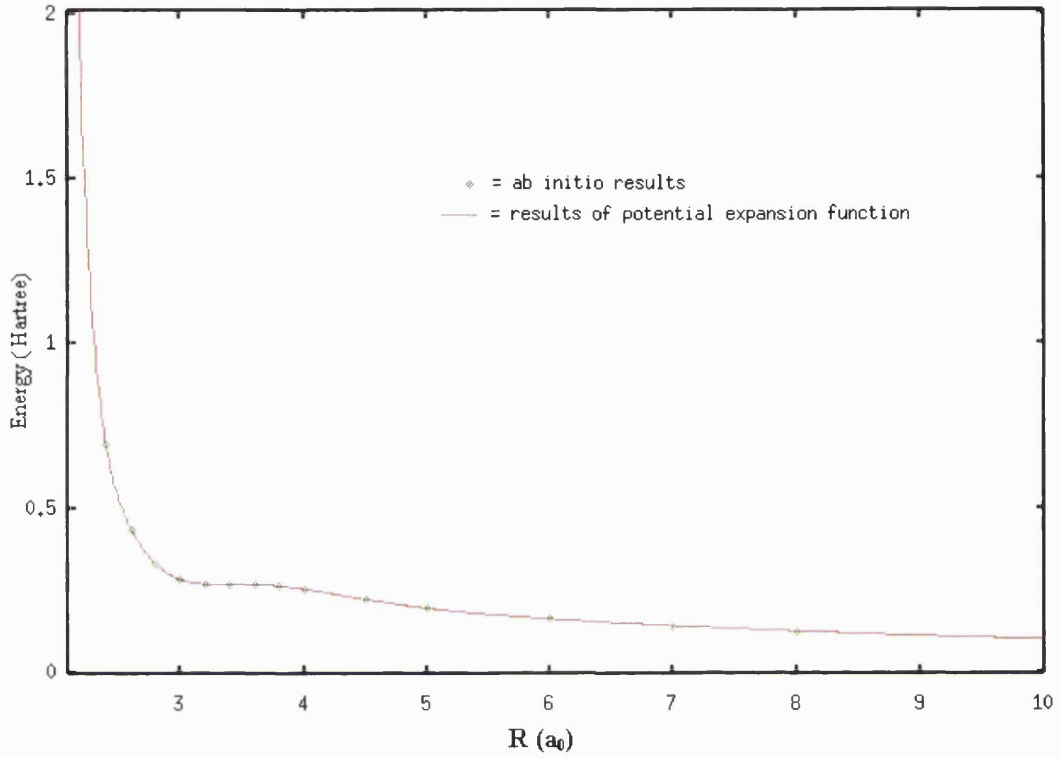

Figure 21 Cut of potential energy surface for $O_2^+ + O^+$ at r =2.02 a_0 ; $\gamma = 30°$.

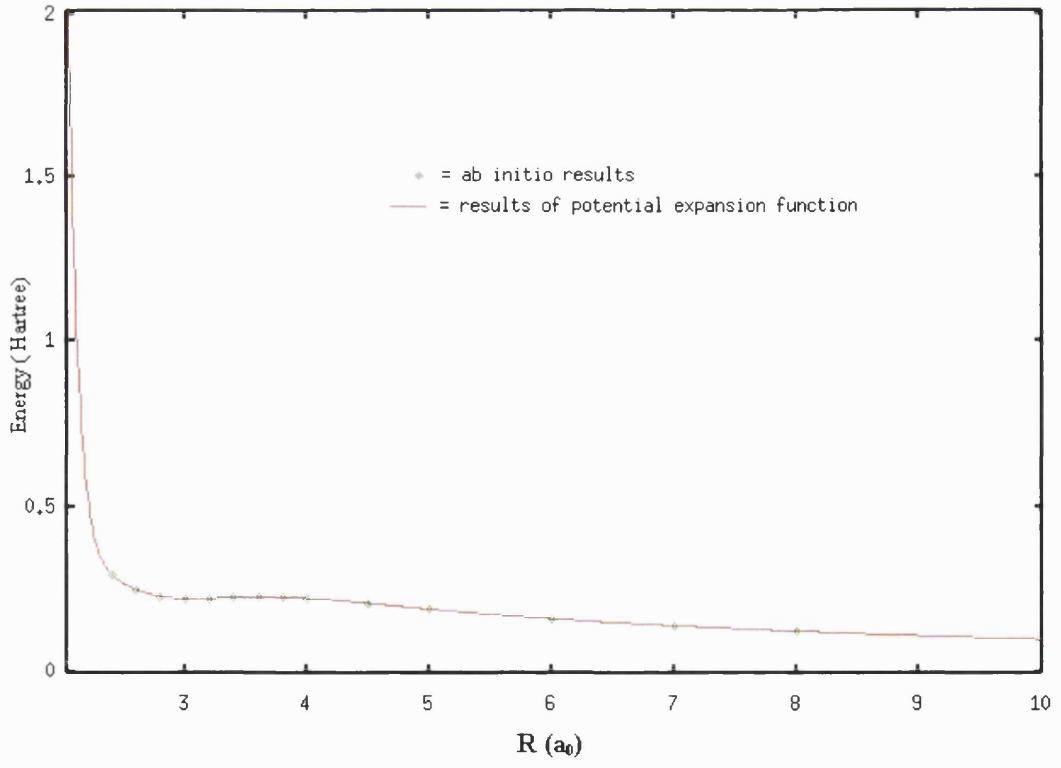

Figure 22 Cut of potential energy surface for $O_2^+ + O^+$ at $r = 2.42$ a_0 ; $\gamma = 60°$.

The potential surface fit was tested by comparing the values of the potential generated by the expansion functions to those provided by Champkin for values of r and γ other than those included in the fitting procedure. Figure 23 shows results of a test of the fitted potential expansion function at a value of γ which was used in the fitting procedure, but at a value of r which was not. Figure 24 shows results of a test of the fitted potential expansion function at a value of r which was used in the fitting procedure, but at a value of γ which was not. Finally, Figure 25 shows results of a test of the fitted potential expansion function at a value of r and a value of γ which were both not used in the fitting procedure.

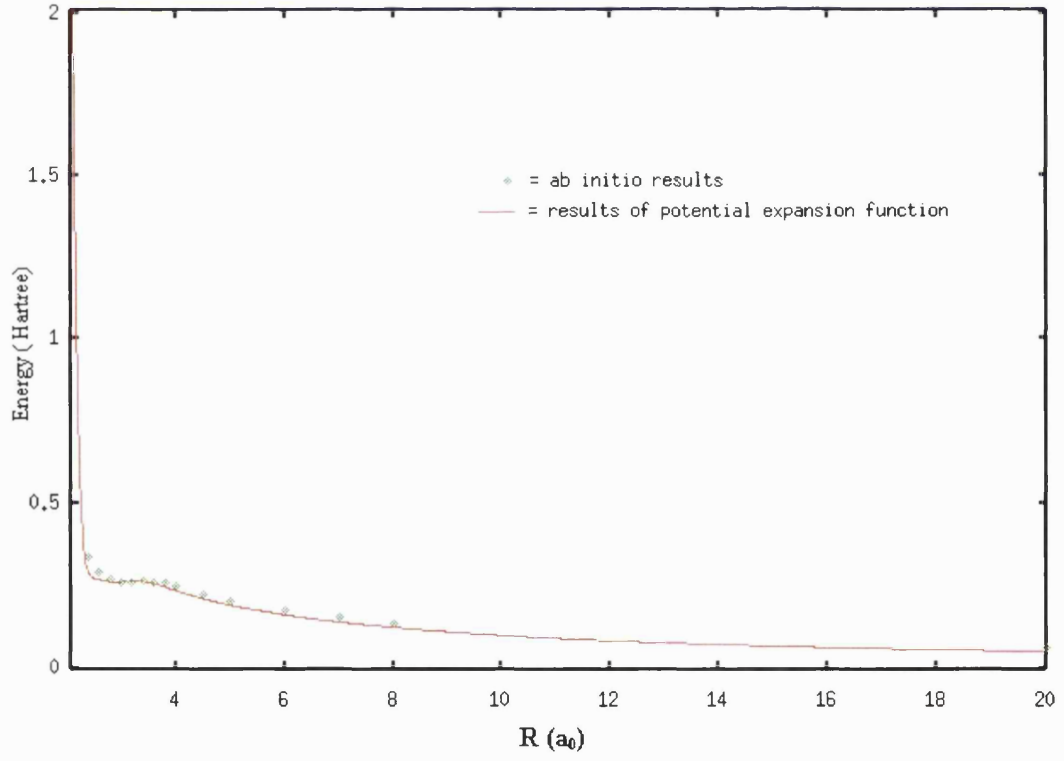

Figure 23 Cut of potential energy surface for $O_2^+ + O^+$ at $r = 2.22\ a_0$; $\gamma = 75°$.

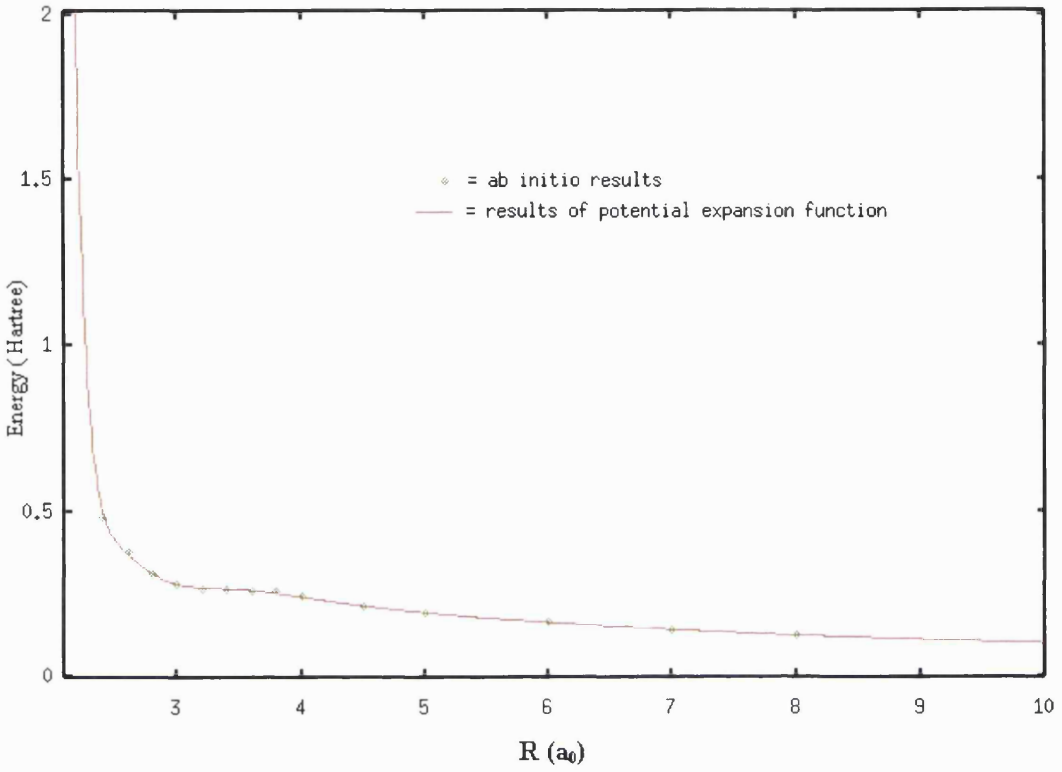

Figure 24 Cut of potential energy surface for $O_2^+ + O^+$ at $r = 2.12\ a_0$; $\gamma = 45°$.

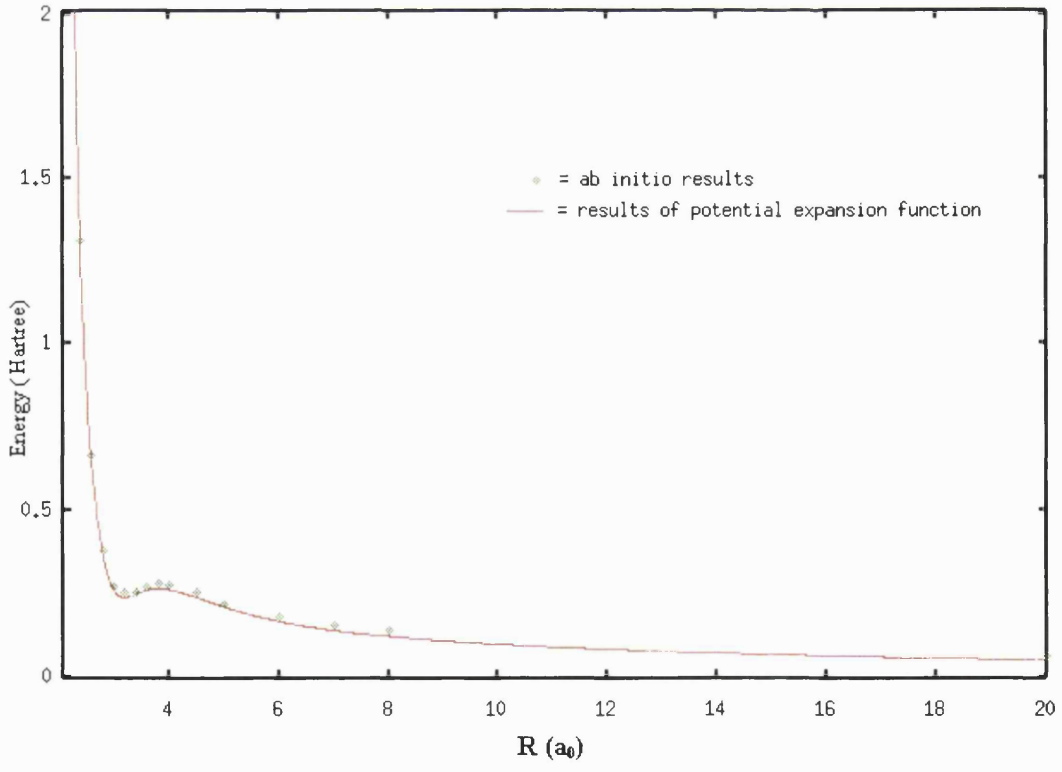

Figure 25 Cut of potential energy surface for $O_2^+ + O^+$ at $r = 2.22\ a_0$; $\gamma = 15°$.

12.2 Overlap Matrix

The method described in Chapter 11 for calculating the overlap matrix

$$\underline{\underline{\mathbf{O}}}\left(E^{O_3^{2+}}, E^{O_3}\right) = \left\langle \underline{\underline{\psi}}^{O_2^+ + O^+}\left(E^{O_3^{2+}}\right) \middle| \underline{\underline{\psi}}^{O_3}\left(E^{O_3}\right) \right\rangle \quad , \tag{12.1}$$

where $E^{O_3^{2+}}$ is the total energy of the scattering system:

$$O_2^+ + O^+ \leftrightarrow O_3^{2+}$$

and E^{O_3} is the energy of the bound ozone molecule, was implemented to explore the reaction:

$$O_3 \xrightarrow{e^-} O_3^{2+} \rightarrow O_2^+ + O^+ + \text{K.E.} \tag{2}$$

The purpose of this study was to provide a theoretical analysis of the process (2), which had previously been investigated experimentally by Newson and Price [47] to determine the energy and lifetime of the ozone dication produced from the double ionisation of O_3 in its ground state.

The final aim of these calculations has been to evaluate the product distribution of the internal energy states of the O_2^+ diatom formed in process (2). However, the Franck-Condon excitation of O_3 to O_3^{2+} will be most efficient for a particular range of the total energy of the excited system, $E^{O_3^{2+}}$, and this will decide the amount of energy imparted by the impacting electron to the ozone molecule. Hence, in order to calculate the product distribution observed in reality, the overlap matrix must be calculated at the value of $E^{O_3^{2+}}$ found to be most efficient for the excitation. This will be determined by the range of values of $E^{O_3^{2+}}$ at which the overlap between the wavefunction for O_3 and that for the scattering system of $O_3^{2+} \leftrightarrow O_2^+ + O^+$ is maximised.

Thus, the analysis of process (2) involves three steps:

(a) To determine the bound energy of the O_3 molecule.

(b) To determine the energy of the O_3^{2+} dication formed by the Franck-Condon excitation of the O_3 molecule through electron impact.

(c) To evaluate the product distribution of the internal energy levels of the O_2^+ diatomic cation produced by the subsequent fragmentation of the O_3^{2+} triatomic dication.

Each of these three steps can be achieved through the propagation of the overlap of the scattering and the bound wavefunctions, Eqn. (12.1), at appropriate values of E^{O_3} and $E^{O_3^{2+}}$.

An additional aim of this study has been to assess the effects of the use of the correct boundary conditions for a Coulombic potential when calculating the overlap matrix, in comparison with the boundary conditions generally used, which are only strictly valid for a non-Coulombic system. From the conclusions of the study made on the elastic scattering of $H^+ + Cl^+$, Chapter 10 of this thesis, it can be predicted that the use of the alternative boundary conditions will only affect step (c) of the calculations, since the earlier steps involve simply locating the energy of a resonance which is not dependent on the long-range part of the scattering potential.

Parameters

As with the coupled-states calculations in Part 1, the results of the propagation of the overlap matrix need to converge with respect to the parameters used in the calculations, such as the size of the basis set and the sector width, before any meaningful conclusions can be made.

Generally, the larger the total energy, the greater the size of basis set required. Since step (b) requires the calculation of the overlap matrix over a range of values of the energy of the scattering system in order to locate the most efficient energy for the ionisation, a basis set suitable for the largest value of $E^{O_3^{2+}}$ studied must be used if a re-examination of the convergence at each value of $E^{O_3^{2+}}$ is to be avoided. Thus, for $E^{O_3^{2+}} \leq 8\,\text{eV}$ the basis set used was:

$$v = 0-7\,,\ j = 0-58$$
$$v = 8,\ j = 0-46$$
$$v = 9,\ j = 0-22$$

where v is the vibrational quantum number and j is the rotational quantum number of the O_2^+ diatom. As mentioned in the method, only even values of j were employed.

The requirement to use such a large basis set (276 states), as a result of the considerable total energies of the scattering system that were to be studied, meant that the calculations were very costly. This is particularly true due to the fact that the method used for the calculation of the overlap, described in Chapter 11, involved using the same basis set for both the bound and scattering systems. Furthermore, the Coulomb term of the potential for the scattering system means that the asymptotic boundary conditions are only valid at extremely large values of R. It was therefore important to find ways of economising the amount of computer time and power that was required for the calculations and these involved optimising the values of the other parameters of the propagation, so that no unnecessary sectors were included in the propagation.

Consequently, for convergence with respect to the sector width, the interaction space was divided into three areas, based on the different sensitivity of the overlap matrix to the potential surface in each area, and convergence tests were carried out in each area independently. The area and sector widths for which convergence was found were:

R (a_0)	Sector width (a_0)
2.38 – 4.48	0.0075 (280 sectors)
4.48 – 100.48	0.05 (1920 sectors)
100.48 – R^{∞}	0.1

For small R, the sector width used must be very thin in order to adequately consider the presence of the shallow well in the potential surface which is found in that area.

Optimisation of the distance over which the overlap matrix is propagated could severely reduce the amount of computer time required, given the large size of the basis set being used. The value of R out to which the matrix need be propagated is different for each of the three steps involved in the calculation and will therefore be discussed along with the results for each step presented below.

12.2.1 Determining the Energy of the Bound State

The conditions of the experiment of Newson and Price [47], which this theoretical analysis is attempting to recreate, had the bound O_3 molecule in its ground state prior to ionisation to O_3^{2+}. The potential surface of Barbe, Secroun and Jouve [49] for the O_3 molecule, which has been used in this research, was developed based on the three spectroscopically observed harmonic frequencies of $^{16}O_3$:

$$\hbar\omega_1 = 1134.9 \text{ cm}^{-1}$$

$$\hbar\omega_2 = 716.0 \text{ cm}^{-1}$$

$$\hbar\omega_3 = 1089.2 \text{ cm}^{-1}.$$

The ground energy of the O_3 molecule should therefore be:

$$E^{O_3} = \sum_i \tfrac{1}{2}\hbar\omega_i = 1470.05 \text{ cm}^{-1} = 0.18226 \text{ eV}.$$

As explained in section 11.3.2, the precise value of the bound energy levels for the potential surface used in the present calculations can be ascertained by locating a sudden increase in the magnitude of the overlap matrix. Hence, a search for a resonance in the sum of the squares of all the elements of the overlap matrix as a function of E^{O_3} was made, for a fixed value of $E^{O_3^{2+}}$, in the region of $E^{O_3} \approx 0.18$ eV.

Since the wavefunction for the bound molecule will tend to zero for large values of R, the overlap matrix need not be propagated much further than the outer wall of the well in order to locate the bound energy. It is not necessary for the scattering wavefunction to reach the asymptotic region, since the actual product distribution is not required in this step of the calculations. Consequently, the propagation was halted at R = 3.64 a_0, at which point the minimum value of $\hat{V}_{O_3}$ is much greater than 0.18 eV.

The bound state was found, as shown in Figure 26, at:

$$E^{O_3} = 0.182408 \text{ eV}.$$

The small difference between this value and the harmonic value of 0.18226 eV is most likely due to the truncation of the potential function of Ref. [49] to just the quadratic terms, as described in Section 11.2.2. The success in finding the bound energy of the ground state of O_3 is a good test for the proficiency of the computer code being used and this provides some reassurance as to the validity of the rest of the calculations.

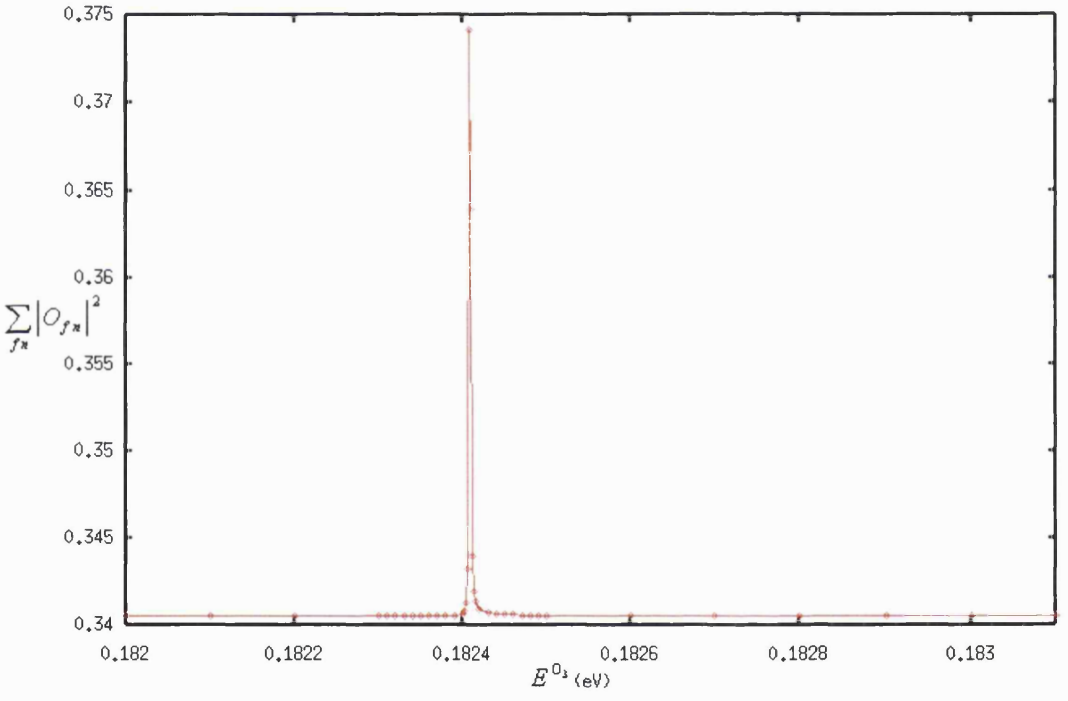

Figure 26 Resonance in plot of the sum of the squares of the elements of the overlap matrix as a function of the total energy of the bound system. The energy of the resonance denotes the ground energy level of the O_3 moelcule.

12.2.2 Determining the Energy of the Ozone Dication Formed

The second step of the calculations is to ascertain the energy of the O_3^{2+} dication formed from the double ionisation of O_3 in its ground energy state, which is equivalent to finding the total energy of the excited scattering system, $O_3^{2+} \leftrightarrow O_2^+ + O^+$, for which the ionisation is most efficient. This Franck-Condon zone can be determined by setting the energy of the bound system, E^{O_3}, to the value of the ground energy level of O_3 found in the previous stage and then calculating the overlap matrix, $\underline{\underline{\mathbf{O}}}\left(E^{O_3^{2+}}, E^{O_3}\right)$, over a range of values of $E^{O_3^{2+}}$, until a resonance in the sum of the squares of the elements of the matrix is observed.

The task of locating the resonance in the curve of the sum of the squares of the overlap matrix elements as a function of the energy of the scattering system, $E^{O_3^{2+}}$, was facilitated by applying the method described in section 10.2, which involves repeatedly fitting to a quadratic in $E^{O_3^{2+}}$ two fixed points of the curve together with every subsequent point. A plot of the coefficients of the squared term of the quadratic (c_3) as a function of $E^{O_3^{2+}}$ will then exhibit much greater sensitivity to the presence of a resonance.

Since the probability density of the wavefunction for the scattering system is generally concentrated in the area where R is small, it should not be necessary to propagate the overlap matrix too far in order to observe the resonance in the plot of the overlap matrix versus $E^{O_3^{2+}}$. As discussed earlier, keeping the distance over which the propagation was performed to a minimum was crucial in this analysis, due to the sizeable basis set being used. This was especially true for this step of the calculations, since the overlap matrix had to be calculated over a large range of energies in order to find the resonance with respect to the energy of the scattering system. Thus, the propagation was halted at $R = 5.38\ a_0$.

However, the further out that the overlap matrix is propagated, the greater the amount of the scattering wavefunction that would be considered in the overlap

and, as a result, the exact energy of the resonance was found to change slightly when the distance of the propagation was increased, until about $R = 200\ a_0$. Furthermore, it was found that, for values of R a lot less than R^{∞}, many resonances were observed in the plot of the sum of the squared elements of the overlap matrix as a function of $E^{O_3^{2+}}$ (Figure 27), rather than just the single resonance representing the Franck-Condon zone. This was attributed to the fact that the nullification of the overlap of the scattering wavefunction at values of $E^{O_3^{2+}}$ other than those in the Franck-Condon range would be incomplete, as a result of the truncation of the propagation. Most of these 'false' resonances were able to be discounted through the use of the method mentioned above for facilitating the detection of resonances by fitting the overlap matrix to a series of quadratic equations (Figure 28). The single resonance representing the actual Franck-Condon region for the excitation could then be identified by propagating the overlap matrix to a greater value of R, since only the 'true' resonance would be observed consistently at all propagation distances (Figure 29).

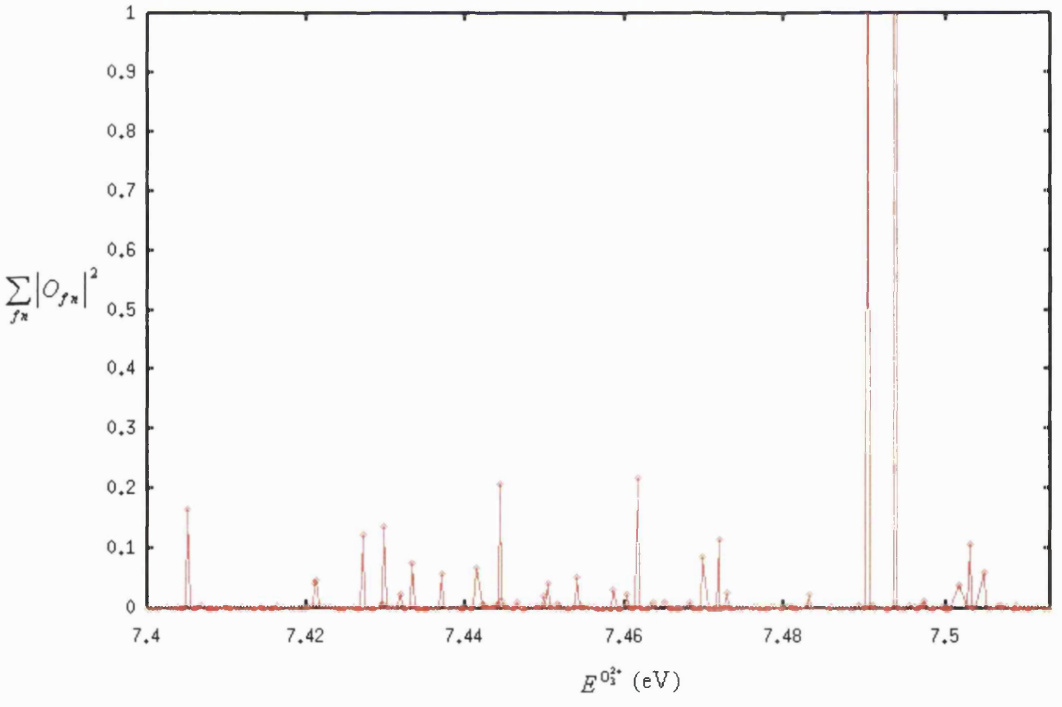

Figure 27 Plot of the sum of the squares of the elements of the overlap matrix as a function of the total energy of the scattering system. The overlap matrix has only been propagated out to $R = 5.38\ a_0$ and, as a result, many resonances are observed.

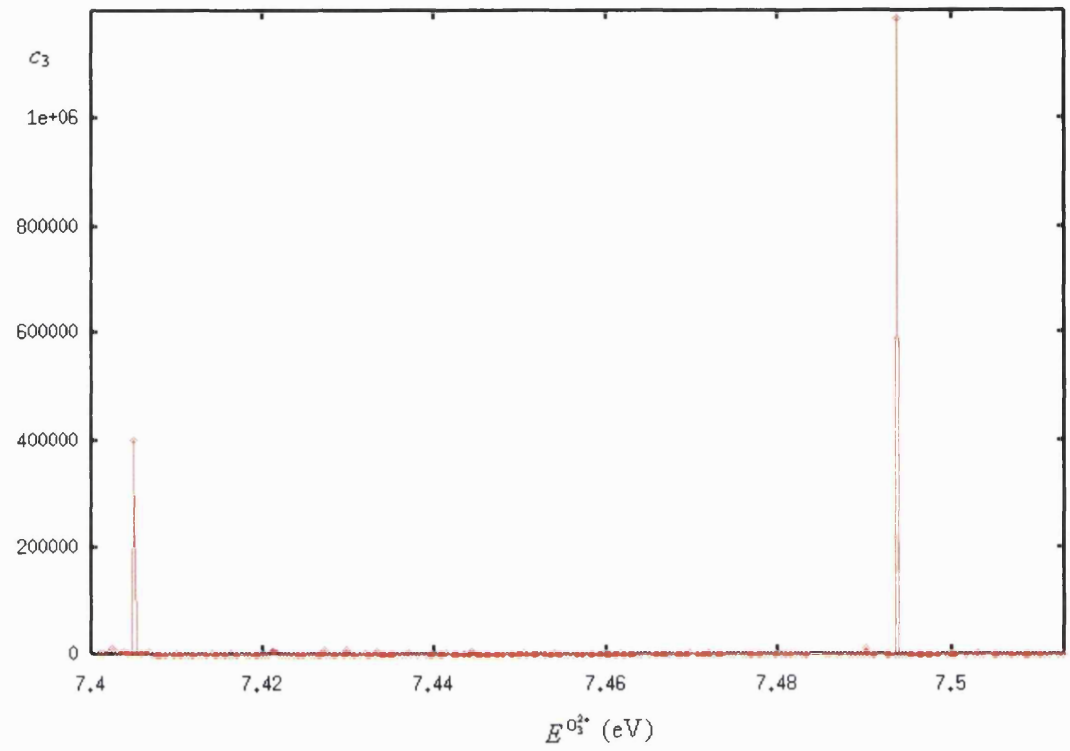

Figure 28 Plot of the coefficient of the squared term of a quadratic-equation fit to Figure 27, as a function of the total energy of the scattering system. The resonance for the Franck-Condon excitation was later identified as being the one on the left.

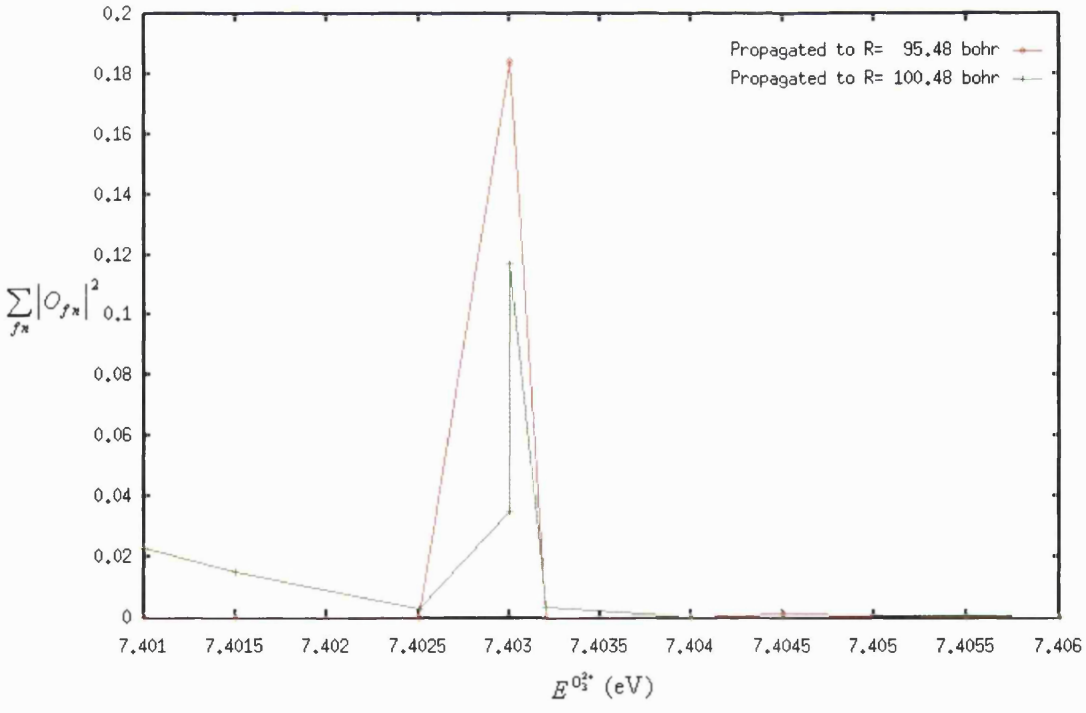

Figure 29 Plot of the sum of the squares of the elements of the overlap matrix as a function of the total energy of the scattering system, with the matrix propagated out to two different values of R.

Thus, the total energy of the scattering system of $O_2^+ + O^+ \leftrightarrow O_3^{2+}$ for which the double ionisation of the ground state O_3 molecule was found to be most efficient was:

$$E^{O_3^{2+}} = 7.403 \text{ eV}.$$

The lifetime of the O_3^{2+} dication formed from the double ionisation can be evaluated by measuring Γ, the width at half-height of the resonance, which, from Figure 30, is seen to be $\Gamma = 1.1 \times 10^{-6}$ eV. The lifetime of the dication before it dissociates to $O_2^+ + O^+$ is therefore:

$$\tau = \frac{\hbar}{\Gamma} = 5.98 \times 10^{-10} \text{ s}.$$

The position and the lifetime of the resonance were found to be independent of the form of the asymptotic boundary conditions.

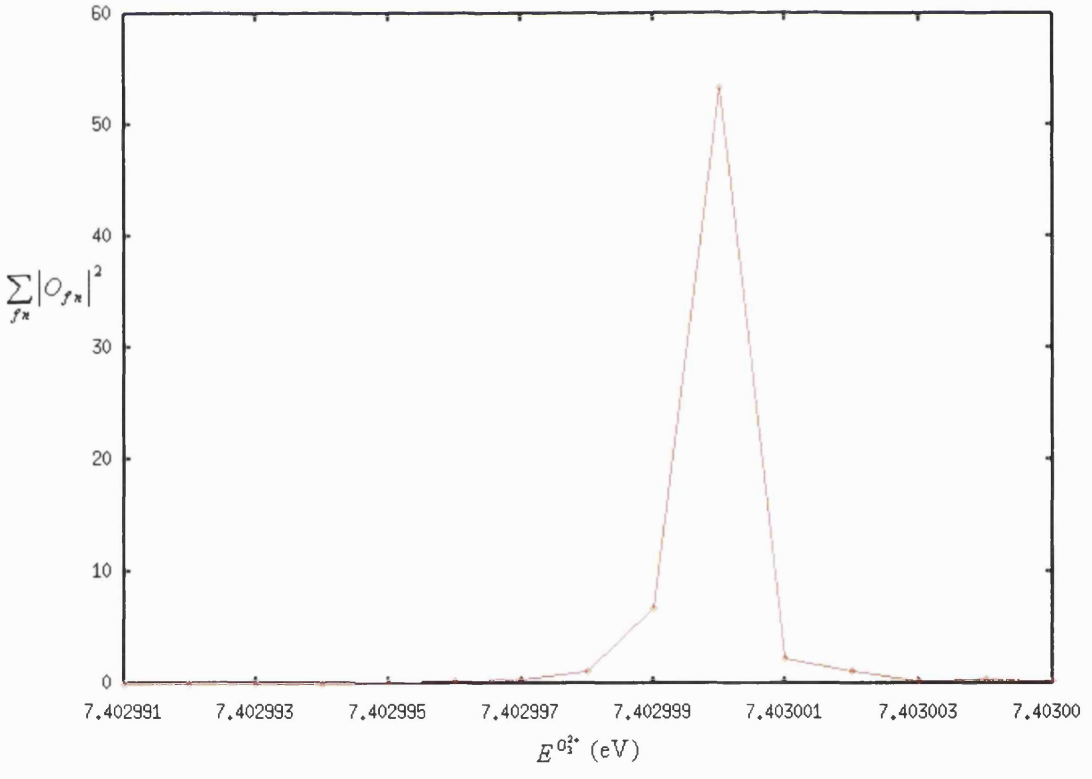

Figure 30 Plot of the sum of the squares of the elements of the overlap matrix as a function of the total energy of the scattering system, with the matrix propagated out to $R = 100.48$ a_0.

12.2.3 Evaluating the Product Distribution of O_2^+

After having obtained the values of the ground energy state of the ozone molecule and the most efficient total energy of the scattering system for its double ionisation, the product distribution of the O_2^+ diatomic ion produced from the dissociation of the O_3^{2+} dication could then be calculated. This required propagating the overlap matrix, Eqn. (12.1), out to the asymptotic region, using the values of E^{O_3} and $E^{O_3^{2+}}$ determined from the two previous steps of the calculations.

The probability of each internal energy state of O_2^+ being produced from the reaction:

$$O_3 \xrightarrow{e^-} O_3^{2+} \longrightarrow O_2^+ + O^+$$

is:

$$P(f) \propto \left| \left\langle \Psi^f_{O_2^+ + O^+} \middle| \Psi_{O_3} \right\rangle \right|^2 ,$$

where f labels the final state of the diatom. As discussed in section 11.3.3, each row of the total overlap matrix corresponds to one product state of the O_2^+ diatom. So, to determine the product distribution of the internal energy states of the O_2^+ fragment, the elements of the total overlap matrix were squared and the sum of the squared elements of each row were then divided by the sum of the squares of all the elements of the matrix.

It was proposed in section 11.3.3 that an equivalent result for the product distribution should be obtained were the squared elements within a single column to be divided by the total of the squared elements within that one column, independent of which column of the overlap matrix was chosen. This supposition was tested by comparing the relative values of the squared elements of three different, arbitrarily chosen columns (1, 2 and 87) of the overlap matrix, with the relative values of the sums of the squares of all the columns of the matrix. The propagation of the matrix was halted at 17.7 a_0 for the purposes of this test. Figure 31 shows that a plot of these relative values, $P(n)$, as a function of each row, n, of the overlap matrix does indeed prove the hypothesis.

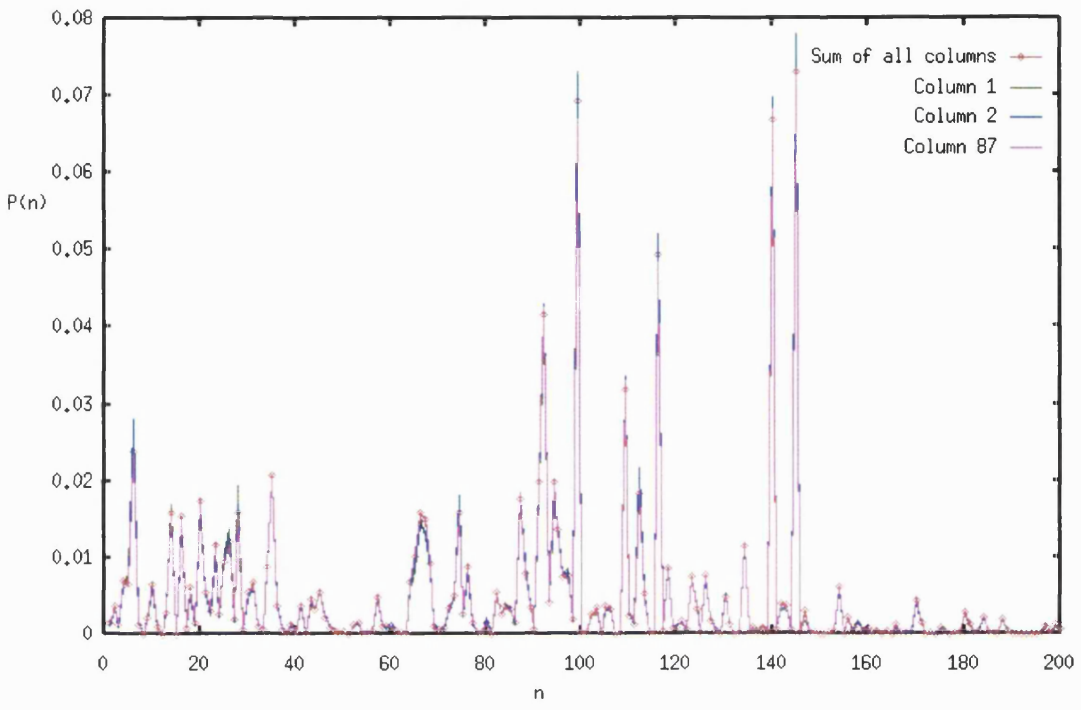

Figure 31 Comparison of the square of the elements of each of the n rows of the overlap matrix divided by the sum of the squared elements, for different columns of the matrix.

The total overlap matrix, $\underline{\underline{\mathbf{O}}}\left(E^{O_3^{2+}}, E^{O_3}\right)$, at energies $E^{O_3} = 0.182408$ eV and $E^{O_3^{2+}} = 7.403$ eV, when propagated out to R^{∞}, should predict the outcome of the dissociation of the O_3^{2+} dication formed from the double ionisation of O_3 in the ground state and, for this step of the calculations, the requirement of the use of the correct boundary conditions for a Coulombic system was tested. In order to accurately predict the product distribution of the O_2^{+} fragment formed, $\underline{\underline{\mathbf{O}}}$ must be converged with respect to the value of R at which the asymptotic boundary conditions are applied. Thus, both the Coulombic and the 'regular' asymptotic transformations described in Chapter 11 were applied to the propagated overlap matrix at regular intervals and the results were tested for convergence.

Generally, rotational product distributions are very sensitive to slight changes in R and so, rather than try to find convergence in the distribution over rotational states, the probabilities for all the rotational states within each vibrational state were added together to give the product distribution over the vibrational states of the diatomic ion.

As with the elastic scattering of Chapter 10, the Coulomb tail of the potential for the $O_3^{2+} \leftrightarrow O_2^+ + O^+$ process means that the value of R at which the asymptotic boundary conditions can be applied is much larger than would be usual for a non-Coulombic system. Consequently, the propagation of the overlap matrix in this study took several weeks of computer time before any convergence of the product distribution with respect to R^∞ was observed.

Even so, convergence was only found when the Coulombic boundary conditions were used (Figures 32 and 33). As predicted, the energy of the Franck-Condon excitation and the width of the resonance shown in Figure 30 were found to be independent of the form of the asymptotic transformation that was employed. However, the distribution of the final internal states of the diatom was discovered to be very different for the two types of boundary conditions, at every value of R^∞ tested.

Due to the sensitivity of the product distribution to R, even the convergence obtained using the Coulombic boundary conditions is imperfect. However, it is sufficient to reveal that some vibrational excitation in the O_2^+ diatomic ion produced from the fragmentation of the doubly ionised O_3 molecule would be expected, with vibrational quantum number $v = 5$ being observed most strongly. This is equivalent to an internal energy of the product O_2^+ diatom in the region of $1.2 - 1.4$ eV.

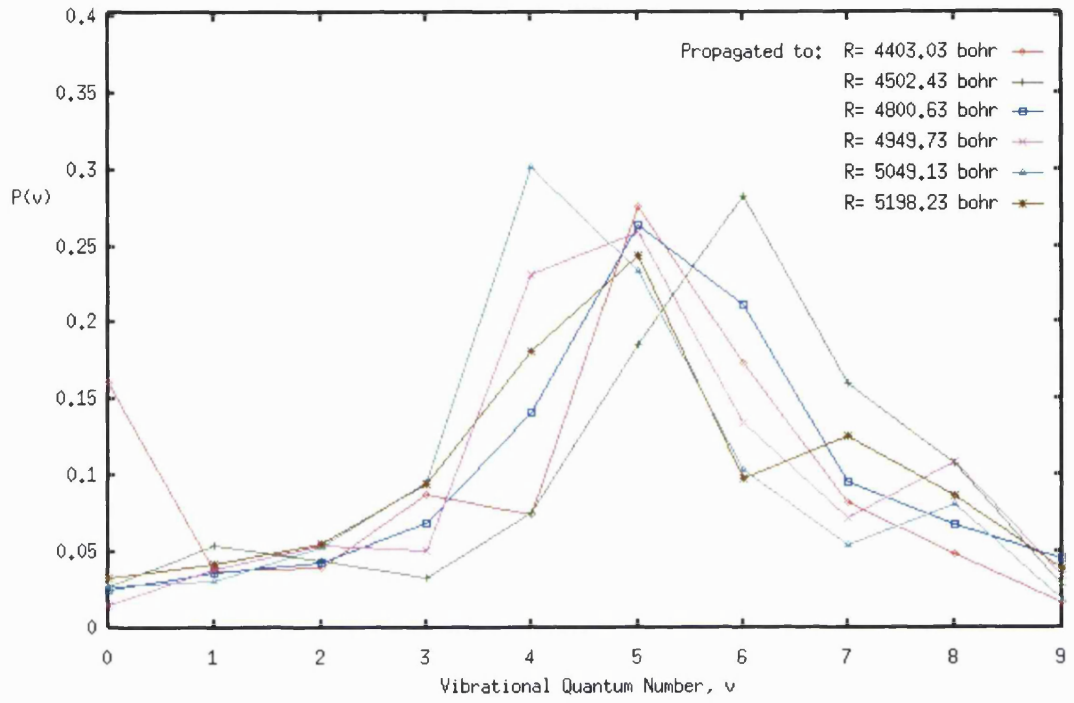

Figure 32 Product distribution over vibrational states of O_2^+ formed from the double ionisation of O_3, using the Coulombic form of the asymptotic boundary conditions.

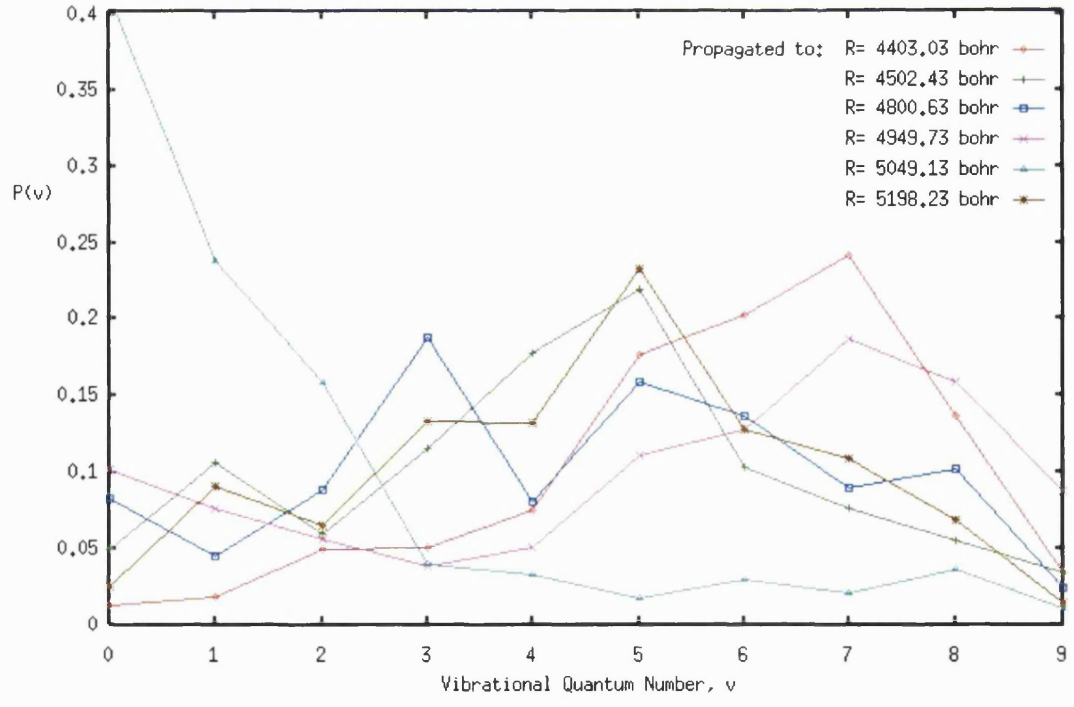

Figure 33 Product distribution over vibrational states of O_2^+ formed from the double ionisation of O_3, using the 'regular' form of the asymptotic boundary conditions.

13 Discussion and Conclusions of Analysis of O_3^{2+}

The aim of this part of the research has been to recreate theoretically the experimental study of Newson and Price [49] and provide some interpretation of their results. Before discussing the findings of this analysis, therefore, it would be advantageous to summarise their investigation and the conclusions that they drew from it.

The experiments of Newson and Price [49] attempted to measure, using time-of-flight mass spectrometry, the lifetime of the O_3^{2+} dication formed from the double ionisation via electron impact of O_3 in its ground state and to determine its energy. Only ions with lifetimes in the order of microseconds or more can be detected by mass spectrometry and they did not observe the presence of any O_3^{2+} ions with such a lifetime. They thus concluded that it was unlikely that any stable quasi-bound state of the O_3^{2+} dication was formed as a result of the double ionisation and that therefore only repulsive regions of the potential energy surface of the dication could be accessed by a vertical transition from the neutral ozone molecule.

In order to determine the energy of the Franck-Condon zone for the excitation, they measured the kinetic energy released from the dissociation of O_3^{2+} to $O_2^+ + O^+$ and obtained a value of 7.5 ± 0.3 eV. They then added this result to the asymptotic energy for forming $O_2^+ + O^+$ in their ground state, relative to the ground state of the neutral ozone molecule, which was evaluated using thermodynamical tables [65] to be 26.8 eV. They therefore concluded that, assuming that the $O_2^+ + O^+$ fragments of the dissociation were indeed produced in their ground state, the excitation energy of O_3^{2+} from O_3 in its ground state was 34.3 ± 0.3 eV.

They then carried out a further test of the lowest energy state of O_3^{2+} to decay to $O_2^+ + O^+$ by monitoring the yield of the products of the dissociation as a function of the energy of the electron beam used to excite the ozone neutral molecule. This test provided a state energy of 34 ± 2 eV.

There has been little previous theoretical work done on O_3^{2+}. However, there have been two studies of 22 electron triatomics, investigating symmetric geometries [66, 67]. They concluded that the ground state of O_3^{2+} was weakly bound and that the vertical double ionisation potential energy should lie at around 35 – 36 eV.

Turning now to the results of the present study, it should first be noted that the potential surface for the scattering system, $O_2^+ + O^+ \leftrightarrow O_3^{2+}$, that was employed in these calculations had not previously been rigorously tested. Nevertheless, the total energy of the scattering system for which the double ionisation was found to be most efficient was calculated to be 7.403 eV which, when added to the asymptotic energy for forming $O_2^+ + O^+$ in their ground state, gives a value for the double ionisation potential energy of O_3^{2+} of 34.203 eV. This result is in good agreement with both the theoretical prediction [66, 67] and the experimental observations [47].

The product distribution of the internal energy states of the O_2^+ diatom, formed from the dissociation of the doubly ionised ozone molecule, was found to be concentrated around the $v = 5$ level, corresponding to an internal energy of about 1.2 – 1.4 eV. Consequently, these calculations would predict that the kinetic energy released from the fragmentation of the O_3^{2+} ion would be expected to be in the region of 6 – 6.2 eV. Although this is somewhat different to the kinetic energy release of 7.5 ± 0.3 eV found experimentally by Newson and Price [47], it is worth noting that their experiments actually measured a kinetic energy release distribution with a half-width of 4.6 eV.

Due to the multi-dimensional nature of the scattering system, a thorough investigation as to whether the O_3^{2+} dication formed from the double ionisation of the ground state ozone molecule exists in a quasi-bound state prior to its dissociation is a complex task. However, the lifetime of 5.98×10^{-10} seconds, which was observed for the resonance in the overlap of the bound and scattering wavefunctions, is sufficiently large to indicate that the vertical transition does result in the formation of a weakly bound dication, in accord with the prediction of the theoretical studies [66, 67]. This lifetime would still

be too small to be detected by the apparatus used in the experiment of Newson and Price [47].

The equilibrium position of O_3 in its ground state, determined from the potential energy function of Eqn. 11.11, is:

$$R = 3.356\ a_0\ ,\ r = 2.403\ a_0\ ,\ \gamma = 140.27°\ .$$

An examination of the fitted potential energy surface for the O_2^+ / O^+ scattering system at these coordinates (Figure 34) reveals that a vertical transition from ground-state ozone would result in the O_2^+ / O^+ system being accessed at a configuration for which the interaction potential energy operator has a value of 6.19 eV, an energy which falls within the potential well of the surface.

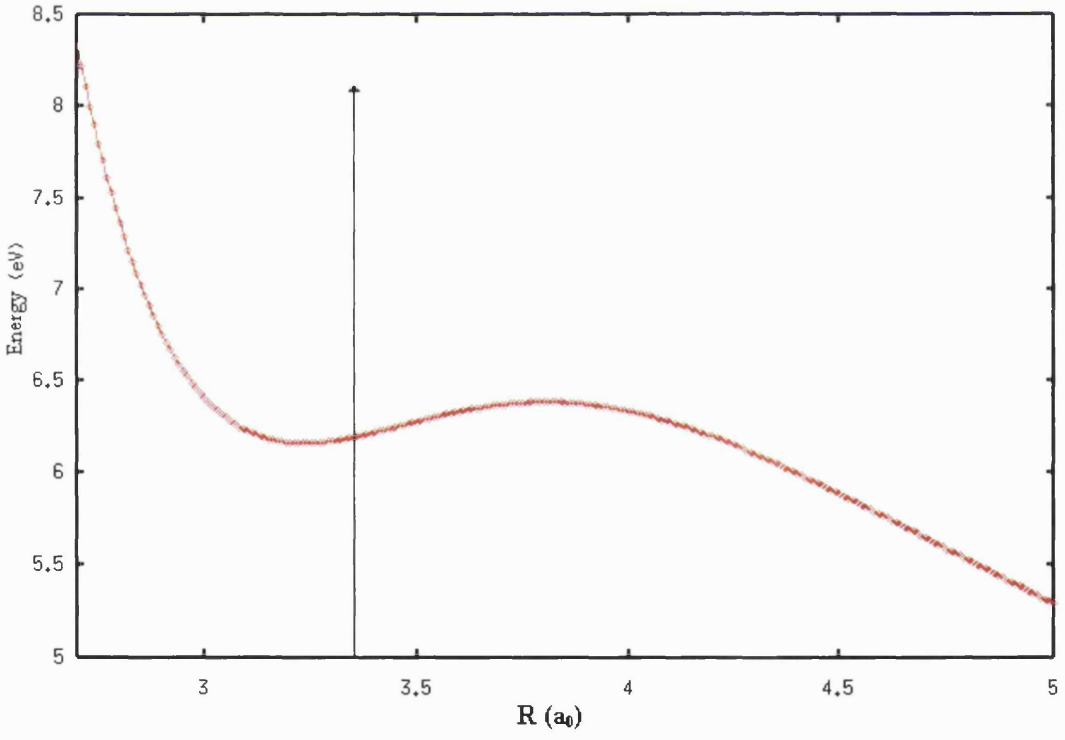

Figure 34 Cut of potential energy surface for $O_2^+ + O^+$ at $r = 2.403\ a_0$; $\gamma = 140.27°$. The vertical arrow at $R = 3.356\ a_0$ indicates the position of the vertical transition from the ground state O_3 molecule.

It is of interest to note that the energy difference between the Franck-Condon region determined from the calculations and this value of the interaction potential is $7.403 - 6.19 = 1.213$ eV, which is similar to the amount of internal energy found to be most common in the O_2^+ fragment formed from the dissociation of the doubly ionised ozone molecule. The interaction potential surface of the atom/diatom scattering system is a measure of the amount of energy required for the system were the energy in the diatom to remain constantly in the ground state throughout the interaction. This observation therefore suggests that the source of the 1.2 – 1.4 eV internal energy of the product O_2^+ fragment may be as a result of the Franck-Condon overlap of the neutral and excited systems being greatest for a configuration of the O_3^{2+} dication within which the diatomic bond is vibrationally (or rotationally) active and remains so, with little transference of this internal energy to translational energy, throughout the subsequent dissociation.

A support for such a hypothesis can be found from an examination of the 'adiabats' of the scattering system. The adiabats are the eigenvectors, $e_l(R)$, of the effective potential energy matrix, which has elements:

$$\left\langle \phi_n \chi_n \left| \hat{V}_{O_2^+ - O^+}(R,r,\gamma) \right| \phi_m \chi_m \right\rangle + \delta_{mn}\left[\frac{j_m(j_m+1)}{R^2} + \epsilon_m^{O_2^+} \right]$$

from Eqn. (11.6), and they are evaluated during the calculation of the overlap matrix, as described in Chapter 11, for every sector of the propagation. The adiabats are so called because they are a diagonalised form of the effective potential matrix, with one adiabat for each final internal state of the diatom, which do not cross with each other when plotted as a function of the interaction distance, R. They can be understood as a measure of the effective potential felt by the diatom with a particular final internal state as it dissociates from the atom, averaged over the r and γ coordinates of the system. An analysis of the adiabats of the $O_2^+ + O^+$ system therefore provides some information as to the shape of the effective potential for each final state of the O_2^+ product.

Figure 35 is a plot of the adiabats of the $O_3^{2+} \leftrightarrow O_2^+ + O^+$ scattering system. For the sake of clarity, only the adiabats corresponding to the $j = 0$ states of the diatom are shown.

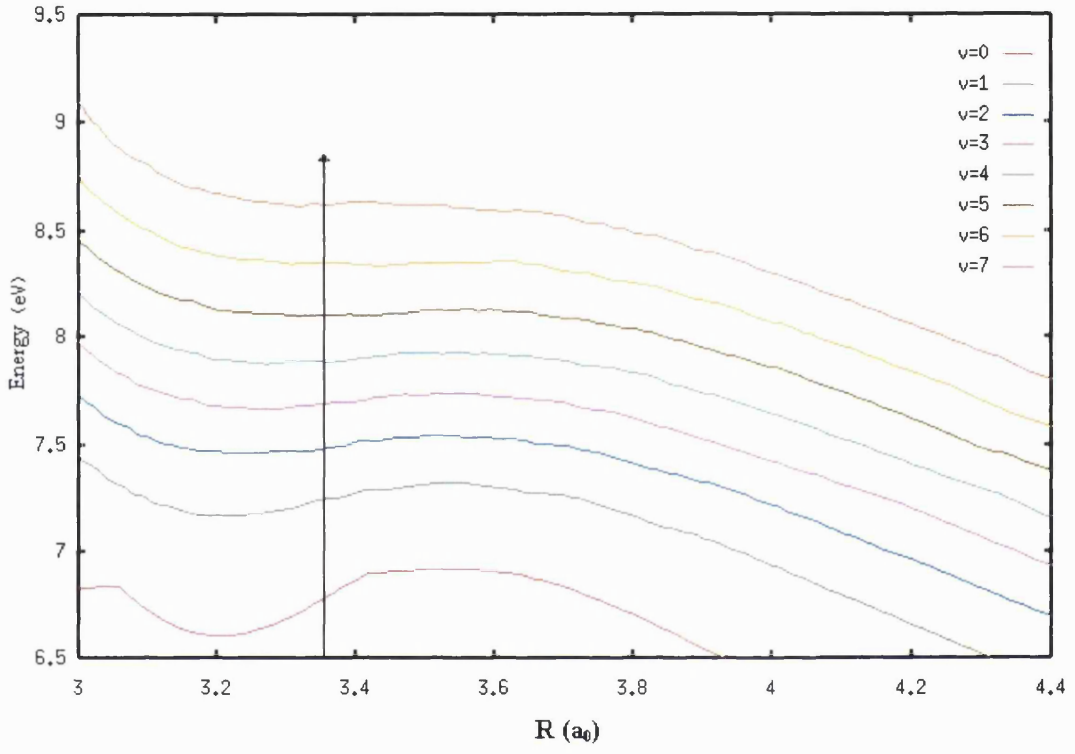

Figure 35 The first 8 vibrational adiabats of the $O_2^+ + O^+$ system. The vertical arrow at $R = 3.356\,a_0$ indicates the position of the vertical transition from the ground state O_3 molecule.

Figure 35 reveals that the potential well of the adiabats corresponding to the product states $v = 4 - 6$ of the O_2^+ diatom is centred closer to the position of the vertical transition from the ground state O_3 molecule than it is for the adiabats of lower (and higher) diatomic vibrational states. This means that there could exist a quasi-bound ground state of the O_3^{2+} dication with an equilibrium position close to that of the ground state of the ozone molecule and that, were this state to be accessed by a vertical transition from the neutral ozone, the subsequent dissociation of the dication would be expected to lead to the formation of O_2^+ which favoured the vibrationally excited states $v = 4 - 6$.

The suggestion that there exists a quasi-bound state of O_3^{2+}, with total energy 7.403 eV relative to the asymptotic energy of ground state $O_2^+ + O^+$, would therefore explain both the relatively small width (large lifetime) of the resonance observed in the overlap of the O_3 and O_3^{2+} wavefunctions and the concentration of the product distribution around an internal energy of ~ 1.3 eV in the O_2^+ fragment. This research therefore conforms with the results of the theoretical analysis of Refs. [66, 67] which predicts the existence of a weakly bound metastable state of the O_3^{2+} dication.

As discussed earlier, the implementation of the theory described in this research to the particular reaction under analysis was encumbered by several factors. These included the necessity of using a large basis set in order to adequately describe the scattering wavefunction at high total energies. Moreover, the same basis was simultaneously used for the wavefunction of the bound system. The calculations had then to be repeated for a large number of energies in order to detect resonances as a function of both the bound energy and the energy of the scattering system. Finally, the propagation had to be performed over an extremely large distance, due to the Coulombic nature of the potential for the scattering system.

However, in addition to providing some insight into the specifics of the double ionisation of ozone, the method that was used in this research has resulted in a number of important general observations regarding the calculation of the Franck-Condon overlap between a bound and scattering system. This study shows that, when calculating the overlap of the wavefunction of a molecule in a bound state with the wavefunction of another system, the energy of the bound state can be calculated without having to resort to a simultaneous propagation from both sides of the potential well of the bound molecule. The ground energy of ozone was accurately determined in these calculations by simply searching for a sudden increase in the value of the overlap obtained through a one-way propagation. As discussed in the method, this is attributed to the fact that the solution to the Schrödinger equation of the

bound system at any other energy will not exist as a wavefunction in reality, since it fails to fulfils the necessary boundary conditions of the bound molecule, and it will therefore have a negligible overlap with any other wavefunction.

Another outcome of this study relates to the extraction of the product distribution from the overlap. For a bound molecule at a bound energy, there can be only one possible expansion of the wavefunction in terms of any orthonormal basis set and, as a result, the overlap of its wavefunction with that of a scattering system, both expressed as expansions of that same basis set, would be simply a column vector. However, as asserted by Danby [64], in order to propagate a bound wavefunction it is first necessary to expand it as a linear combination of all possible solutions to the Schrödinger equation at that energy. Consequently, the overlap would become an $n \times n$ square matrix, where n is the size of the basis set. Nevertheless, it has been successfully shown in this research that, to obtain the product distribution from the matrix of the overlap of a bound wavefunction with a scattering wavefunction, it is only necessary to know the elements of a single column of the matrix and that all columns will yield the same result.

Perhaps most importantly, the final observation which comes out of these calculations involves the choice of boundary conditions. One of the aims of this research was to compare the effects of applying different asymptotic boundary conditions to the wavefunction of a scattering system which has a Coulomb term in its potential energy function. The results show that, just as for the elastic scattering case in Chapter 10, the energy and width of the resonances investigated were not dependent on using the boundary conditions appropriate to a Coulombic system. This was true despite the fact that the position of the resonance in the overlap of the wavefunctions as a function of the total energy of the scattering system was affected by increased propagation of the scattering wavefunction to large distances. The energy of the resonance was not wholly defined by the shape of the wavefunctions at small interaction distances and

yet, nevertheless, the choice of asymptotic boundary conditions had no effect upon it.

However, the product distribution that was evaluated when using regular boundary conditions was found to be drastically different to that found using the Coulombic boundary conditions. Furthermore, only when the Coulombic boundary conditions were applied was there seen to be any convergence in the product distribution with respect to the value of the interaction distance at which the asymptotic boundary conditions were applied.

Hence, the conclusion of this study is that it is necessary to consider the Coulombic nature of a system such as $O_2^+ + O^+$ if one wishes to obtain information about the state of that system in the asymptotic region.

Conclusion

This thesis has discussed research involving the application of quantum dynamical calculations to different chemical systems. All of the processes studied relate to the collisions of molecular ions and the different calculations share much of the same theory and concepts of quantum dynamics.

The first part of the thesis shows that the use of the centrifugal sudden approximation is justified for studying vibrational relaxation of a diatomic ion, even when the quencher employed is a heavy atom, such as Kr. It is valid even when the potential surface involved in the reaction is highly anisotropic and contains a deep potential well.

The theory for incorporating potential surfaces of two different symmetries has been implemented, for the first time, to study the vibrational relaxation of a diatom with Π electronic ground state using quantum dynamical methods. The validity of approximating such a system as one where the diatom is in a Σ state is shown to be untenable in a quantum dynamical analysis, since the resulting cross sections and rate constants obtained using such an approximation may be drastically different to those found without it. Consequently, it would seem advisable to include the potential surfaces of all the various symmetries present when evaluating the cross sections and rate constants of an inelastic scattering process. An analysis of the effects of the inclusion of the potential energy surfaces of both symmetries of the O_2^+ / Kr system appears to support the suggestion that the presence of the unfilled electron shell of the O_2^+ diatom is the major cause of the unusually efficient vibrational quenching observed experimentally in that system.

The study of the vibrational relaxation of a molecular ion, O_2^+, through collision with an atom, Kr, that is presented here also provides some support for the suggested mechanism of such an interaction. The negative temperature-dependence of the rate constant for the reaction at low temperatures is accompanied by the presence of a pronounced resonance structure in a plot of the total cross section as a function of total angular momentum and this could

be a result of the formation of an orbiting complex. Such resonances are absent at higher temperatures, where the positive dependence on temperature of the rate constant implies that a more direct mechanism is dominant.

The second part of this thesis reveals that the results of difficult quantum dynamical calculations on the dissociation of doubly ionised ozone leads to the suggestion that the molecular dication O_3^{2+} exists in a weakly bound state, with energy 34.203 eV relative to the ground state ozone molecule, prior to its decay. In addition, the O_2^+ fragment of the dissociation is predicted to have an internal energy distribution concentrated around an energy of 1.2 – 1.4 eV.

A method of calculating the Franck-Condon overlap between a bound and a scattering system without prior knowledge of the precise energy or wavefunction of the bound system has been discussed and developed. The procedure does not require a simultaneous propagation of the overlap in two opposite directions.

Finally, an investigation has been made into the necessity of using the asymptotic boundary conditions appropriate to a system with a Coulomb term in its potential. This required the development of existing theory which had previously only considered non-Coulombic systems. The study concludes that it does not appear necessary to include Coulombic boundary conditions in quantum calculations of resonances and bound states. It is necessary, however, to apply the Coulombic boundary conditions when extracting information pertaining to the state of the system in the asymptotic region.

All of the studies undertaken in this thesis involve the investigation of processes which have recently been studied experimentally. The research therefore attests to the ability of quantum dynamics to theoretically model a range of different types of experiments and to successfully determine many of the observable quantities of a collision process.

REFERENCES

[1] E.E. Ferguson *J. Phys. Chem.* **90**(1986)731

[2] E.E. Ferguson *Comments At. Mol. Phys.* **24**(1990)327

[3] L.D. Landau, E. Teller *Phys. Z. Sowjetunion* **10**(1936)34

[4] D.J. Miller, R.C. Millikan *J. Chem. Phys.* **53**(1970)3384

[5] H. Böhringer, M. Durup-Ferguson, D.W. Fahey, F.C. Fehsenfeld, E.E. Ferguson *J. Chem. Phys.* **79**(1983)4201

[6] W. Federer, W. Dobler, F. Howorka, W. Lindinger, M. Durup-Ferguson, E.E. Ferguson *J. Chem. Phys.* **83**(1985)1032

[7] M. Kriegl, R. Richter, P. Tosi, W. Federer, W. Lindinger, E.E. Ferguson *Chem. Phys. Lett.* **124**(1986)583

[8] J.F. Bott, N. Cohen *J. Chem. Phys.* **58**(1973)934

[9] P.F. Zittel, C.B. Moore *J. Chem. Phys.* **59**(1973)6636

[10] J.T. Yardley *Introduction to molecular energy transfer* (Academic Press, New York, 1980)

[11] P. Tosi, M. Ronchetti, A. Lagana *J. Chem. Phys.* **88**(1988)4814

[12] G. Ramachandran, G.S. Ezra *J. Chem. Phys.* **97**(1992)6322

[13] J.D. Lambert *Vibrational and Rotational Relaxation in Gases* (Clarendon Press, Oxford, 1977)

[14] P. Tosi, M. Ronchetti, A. Lagana *Chem. Phys. Lett.* **136**(1987)398

[15] V. Zenevich, W. Lindinger, G.D. Billing *Chem. Phys. Lett.* **197**(1992)99

[16] E. Goldfield *J. Chem. Phys.* **97**(1992)1773

[17] F.A. Gianturco, S. Serna, A. Palma, G.D. Billing, V. Zenevich *J. Phys. B: At. Mol. Opt. Phys.* **26**(1993)1839

[18] A.S. Dickinson *Comput. Phys. Commun.* **17**(1979)51

[19] B. Ramiro Diaz, P. Wahnon, V. Sidis *Chem. Phys. Lett.* **212**(1993)218

[20] B. Ramiro Diaz, P. Wahnon, V. Sidis *J. Chem. Phys.* **104**(1996)191

[21] M.F. Jarrold, L. Misev, M.T. Bowers *J. Chem. Phys.* **81**(1984)4369

[22] R.T Pack *J. Chem. Phys.* **60**(1974)633 and refs. therein

[23] P. McGuire, D.J. Kouri *J. Chem. Phys.* **60**(1974)2488

[24] S.K. Pogrebnya, D.C. Clary *Chem. Phys. Lett.* **219**(1994)366

[25] S.K. Pogrebnya, A. Kliesch, D.C. Clary, M. Cacciatore *International J. Mass Spec. and Ion Proc.* **149**(1995)207

[26] M. Jacob, G.C. Wick *Ann. Phys.* 7(1959)404

[27] K.P. Lawley, J. Ross *J. Chem. Phys.* **43** (1965)2930

[28] D.M. Brink, G.R. Satchler *Angular momentum*, 2nd Ed. (Oxford Univ. Press, London, 1975)

[29] R.N. Zare *Angular Momentum* (Wiley-Interscience Publication, USA, 1987)

[30] M.S. Child *Molecular Collision Theory* (Academic Press, London, 1974)

[31] G.S. Schatz, A. Kuppermann *J. Chem. Phys.* **65**(1976)4642

[32] H. Klar *J.Phys. B:At. Mol. Phys.* **6**(1973)2139

[33] D. Poppe *Chem. Phys. Lett.* **19**(1973)63; *Chem. Phys.* **25**(1977)29

[34] S. Green, R.N. Zare *Chem. Phys.* 7(1975)6

[35] R.N. Dixon, D. Field *Proc. R. Soc. Lond Ser. A* **368**(1979)99

[36] M.H. Alexander *Chem.Phys.* **92**(1985)337

[37] C.G. Gray *Can. J. Phys.* **54** (1976) 505

[38] M. Larsson *Physica Scripta* **23**(1981)835

[39] H.-J. Werner, B. Follmeg, M.H. Alexander *J. Chem. Phys.* **89**(1988)3139

[40] P. Huxley, J.N. Murrell *J. Chem. Soc., Faraday Trans.* 2 **79**(1983)323

[41] D.O. Harris, G.G. Engerholm, W.D. Gwinn *J. Chem. Phys.* **43**(1965)1515

[42] J.C. Light, I.P. Hamilton, J.V. Lill *J. Chem. Phys.* **82**(1985)1401

[43] J. Echave, D.C. Clary *Chem. Phys. Lett.* **190**(1992)225

[44] J.N. Murrell, S.D. Bosanac *Theory of Atomic and Molecular Collisions* (John Wiley & Sons, England, 1989)

[45] E.B. Stechel, R.B. Walker, J.C. Light *J. Chem. Phys.* **69**(1978)3518

[46] P.W. Atkins *Molecular Quantum Mechanics*, 2nd Edition (Oxford University Press, Oxford, 1983)

[47] K.A. Newson, S.D. Price *Int. J. Mass Spec. & Ion Processes* **153**(1996)151

[48] P. Champkin, N. Kaltsoyannis, S.D. Price *J. Elect. Spec. & Relat. Phenom.* **105**(1999)21

[49] A. Barbe, C. Secroun, P. Jouve *J. Molec. Spec.* **49**(1974)171

[50] F.R. Bennett, I.R. McNab *Chemical Physics Letters* **251**(1996)405

[51] J.W. Cooley *Math Comput* **15**(1961)363

[52] N.F. Mott, H.S. Massey *The Theory of Atomic Collisions*, 3rd Edition (Oxford Science Publications, Oxford, 1965)

[53] G. Breit, E.P. Wigner *Phys. Rev.* **51**(1937)593

[54] C.J. Joachain *Quantum Collision Theory* (North-Holland Publishing Co., Oxford, 1975)

[55] G. Parlant, J. Senekowitsch, S.V. O'Neil, D.R. Yarkony *J. Chem. Phys.* **94**(1991)7208

[56] F.T. Smith *Phys. Rev.* **118**(1960)349

[57] R. Schinke *Photodissociation Dynamics*, 1st Edition (Cambridge University Press, 1993)

[58] G.A. Parker, T.G. Schmalz, J.C. Light *J. Chem. Phys.* **73**(1980)1757

[59] K.C. Kulander, J.C. Light *J. Chem. Phys.* **73**(1980)4337

[60] R.W. Heather, J.C. Light *J. Chem. Phys.* **78**(1983)5513

[61] K.B. Whaley, J.C. Light *J. Chem. Phys.* **81**(1984)3334

[62] D.C. Clary *J. Chem. Phys.* **83**(1985)4470

[63] R.G. Gordon *J. Chem. Phys.* **51**(1969)14

[64] G. Danby *J. Phys. B* **16**(1983)3393

[65] H.M. Rosenstock, K. Draxl, B.W. Steiner, J.T. Herron *J. Phys. Chem. Ref. Data* **6**(1977) Suppl.1

[66] P. Pyykkö *Chem. Phys. Lett.* **156**(1989)337

[67] P. Pyykkö, Y. Zhao *J. Phys. Chem.* **94**(1990)7753

The following publication resulted from this research:

M. Craimer, S.K. Pogrebnya, D.C. Clary *J. Chem. Phys.* **111**(1999)1972